Department of Spatial Sciences

School of Earth and Planetary Sciences

Assessing and Predicting the Impact of Land Use and Land Cover Change on Groundwater Using Geospatial Techniques: A Case Study of Tabuk, Saudi Arabia

Eman Albalawi

This thesis is presented for of the Degree of Doctor of Philosophy of Curtin University

December 2020

Declaration

To the best of my knowledge and belief this thesis contains no material previously published by any other person except where due acknowledgment has been made.

This thesis contains no material which has been accepted for the award of any other degree or diploma in any university.

Signature:

Date

14/12/2020

Abstract

Assessing land use and land cover (LULC) change is important for planning limited natural resources and the sustainable management of ecosystems. Agricultural and urban land expansion is a result of an ongoing complex interaction between policy settings, the physical environment, and socio-economic factors. Determinants driving agricultural and urban expansion contribute to the analysis of the main causes of land use change. This can assist policymakers to understand the importance of a wide range of depleting resources (e.g., groundwater) on the associated agricultural and urban land use change, particularly in the arid regions of Saudi Arabia.

Substantial oil revenue and rapid growth in urban population have exerted immense pressure on groundwater resources in Saudi Arabia. Among regional cities, Tabuk in the northwest of Saudi Arabia, is an epicentre of agriculture which relies on fossil-based groundwater for irrigation and domestic use.

The purpose of this study was to test the hypothesis that in the Tabuk Region the conversion of natural land ecosystems to an agricultural ecosystem impacts the hydrological cycle by changing groundwater levels. However, the unavailability of groundwater monitoring data for the region made it difficult to evaluate the impact of LULC change on water resources. Therefore, in this work a mathematical model was developed to assess the groundwater requirements for crop cultivation and water requirements for urban use over the last 30-years (1985-2015) in Tabuk city, Saudi Arabia.

The hypothesis was examined through aerial multi-temporal remote sensing imagery, urban groundwater monitoring records, historical climatic variables, and field surveys, together with geospatial techniques investigating the effects of LULC change on groundwater. An object-based image analysis (OBIA) and post-classification comparison were performed to determine the spatio-temporal change in LULC. The prediction of land use and land cover was carried out through an integration of Markov chain and cellular automata (MCCA) methods.

Agricultural crop water requirements (CWR) were estimated using an evapotranspiration (ET) based hydrological model, from which the CWR net irrigation requirements (NIR) were computed. Abstraction data from urban tube wells were utilized to determine urban water demand.

The results revealed that, over the past three decades (1985-2015), 731 km^2 of barren land in Tabuk was converted to agriculture (464 km^2) and urban (266 km^2) with an obvious increase since 1985. Accuracy of LULC change detection indicated an overall accuracy about 93% with corresponding kappa statistics about 0.90. The LULC prediction exercise showed substantial expansion of agricultural and urban lands, driven mainly by population growth in 2025 and 2035. These land conversions could accelerate land degradation which may put more pressure on meagre natural resources.

Hydrological model indicated that agricultural water consumption increased approximately 4.2 x 10^{10} m^3 during 1985-2015. Analysis of CWR suggested that maize has the highest water demand whilst wheat has the lowest water demand among the agricultural crops examined. Further, the study showed that water abstraction by urban wells increased substantially by more than 8 times in 2015 compared to 1995.

The study provided a clear indication that the unsustainable use of groundwater puts Tabuk at high risk of groundwater depletion. Further changes in land use and land cover and current irrigation practices could increase soil salinity, which may result in the loss of ecosystem services and enhance land degradation. This work calls for the prudent use of resources via policy shifts and a better accounting of water usage.

Related publications

Albalawi, E., Dewan, A., & Corner, R. (2018). Spatio-temporal analysis of land use and land cover changes in arid region of Saudi Arabia. International Journal of Geomate, 14(44), 73-81.

Albalawi, E., Dewan, A., & Corner, R. (2018). Predicting spatio-temporal urban growth in Tabuk, Saudi Arabia using a Cellular Automata-Markov Model. Proceedings of 156th IASTEM International Conference, Auckland, New Zealand, 5th-6th December 2018.

Acknowledgements

I thank God (Allah) for helping me to finish this thesis and giving me the grace to endure until the end.

I would like to express my sincere gratitude to my supervision panel namely, Dr Ashraf Dewan, Dr Sri Adiyanti, and Dr Robert Corner for their constant guidance, encouragement, and support during my research. I also extend a thank you to the thesis committee chairperson Dr Ivana Ivánová for her valuable advice during crucial stages of my research. I would like to thank my fellow graduate students and staff members at Curtin University in Perth, Australia, who helped me directly and indirectly with their suggestions and encouragement. I would especially like to acknowledge my colleague and friend Dr Claudia De Los Rios Perez, for her valuable time and advice.

A very special thanks to my husband Ali and my children (Tala, Tameem, and Bader) for their great encouragement, support, and patience especially when I was heavily pre-occupied with my research. I would also like to express my deepest gratitude to my parents and siblings for their continuous prayers and support. I would especially like to acknowledge my brothers, Bader, and Mohamed, for their help during my fieldwork in Tabuk, Saudi Arabia.

I am very thankful to Dr Kerri Clarke for her enormous support and encouragement and for all of the things she taught me in both my personal and academic life. I would also like to thank Dr Tauseef Gulrez for the technical support provided, and for his patience and generous contribution of time and knowledge.

I greatly appreciate the support of the General Authority for Meteorology and Environmental Protection (GAMEP) of Tabuk for providing me with key climate data that I used in my research. I would like also to thank engineers, Hassan Al-Ali and Ahamed Alsarhani, from the Tabuk Water Ministry for providing me with groundwater data. Finally, I express my gratitude to the Department of Geography, Umm Al-Qura University in Makkah, Saudi Arabia for financing my PhD.

Table of contents

List of figures

List of tables

List of acronyms

AHP	Analytical hierarchy process
ANN	Artificial neural network
APR	Aquifer pumping and artificial recharge
ASL	Above sea level
ASR	Aquifer storage and recovery
BIM	Boolean intersection method
CA	Cellular automata
CDSI	Central Department of Statistics and Information (Saudi Arabia)
CLUE	Conversion of Land Use and its Effects at Small regional extent
CR	Consistency ratio
CWR	Crop water requirements
DEM	Digital elevation model
DOS	Dark object subtraction
DT	Decision tree
EM	Error matrix
ETc	Crop evapotranspiration
ETM+	Enhanced Thematic Mapper Plus
ET	Evapotranspiration
FAO	Food and Agriculture Organization
FMF	Fuzzy membership function
GASTAT	General Authority for Statistics (Saudi Arabia)
GAMEP	General Authority for Meteorology and Environmental Protection
GCP	Ground control points
GCS	General Commission for Survey
GDP	Gross Domestic Product
GIS	Geographical information system
GPS	Geographical positioning system
JOG	Joint operations graphic
KACST	King Abdulaziz City for Science and Technology
KIA	Kappa index of agreement
KNN	K-nearest neighbour
LULC	Land use and land cover

MAW	Ministry of Agriculture and Water (Saudi Arabia)
MC	Markov chain
MCCA	Markov chain and cellular automata
MCE	Multi-criteria evaluation
MDC	Minimum distance classification
MEWA	Ministry of Environment, Water and Agriculture (Saudi Arabia)
ML	Merge level
MLC	Maximum likelihood classification
MLC	Maximum likelihood classification
MOLA	Multi-objective land allocation
MPMR	Ministry of Petroleum and Mineral Resources (Saudi Arabia)
NDVI	Normalised difference vegetation index
NIR	Net irrigation requirement
NSMA	Near spectral mixture analysis
OBIA	Object-based image analysis
OLI	Operational land imager
PET	Potential evapotranspiration
RF	Rainfall
RH	Relative humidity
RMSE	Root mean square error
RS	Remote Sensing
SL	Scale level
SVM	Support vector machine
TLM	Topographic line map
TM	Thematic mapper
TOA	Top of atmosphere
TST	Tasseled cap transformation
UGAT	Urban growth analysis tool
UN	United Nations
USGS	United States Geological Survey
UTM	Universal transverse mercator
WLC	Weighted linear combination
WS	Wind speed

1 Introduction

1. 1 Background

Land use and land cover (LULC) change is a dynamic process that may have serious consequences for urban and agricultural land and groundwater. Assessing the change in LULC is important in quantifying the impact on the environment and socio-economic development. The dependency of Arid regions on limited groundwater resources are particularly vulnerable (Zhou et al. 2015). Mismanagement of fragile land in arid areas often seen in the practice of intensive agriculture can lead to land degradation, (including an increase in soil salinity), water and air pollution, and biodiversity loss (Youssef and Maerz 2013). Land resource management and policy development for arid areas requires a regular and accurate assessment of LULC to improve land use efficiency and reduce environmental impacts when responding to the demands of an increasing population. Many cities are expanding rapidly in terms of population growth and economic activity leading to urban territorial expansion, which is a significant factor in land use change. Urbanisation increases worldwide, and by 2050, the world's population is estimated to rise to about 10 billion with 66% of the population is predicted to live in urban settings (Leeson 2018). The increase in urbanisation is a result of the combined effects of population growth and anthropogenic activities operating at both regional and global scales (Wubie et al. 2016). Population growth is most significant in developing countries worldwide (Tewolde and Cabral 2011; Halmy et al. 2015) and is problematic for semi-arid and arid regions where the environment is fragile. Economic activity has an important role in the process of urban development including creating new jobs, increasing employment opportunities, improving living standards and increasing production and demand. However, without proper planning urban growth can lead to resource scarcity e.g., water and land degradation, increased air pollution, emergence of random and unplanned housing, and desertification (Youssef and Maerz 2013; Deep and Saklani 2014; Hegazy and Kaloop 2015; Zheng et al. 2015; MacLachlan et al. 2017; Du and Huang 2017).

Assessing LULC change can deliver spatial and temporal land use which is essential information to understand the process, causes and implications for better land use management and sustainable development policies (Batty 2008). This may require a thorough study utilising remote sensing to understand the current trends and pattern of land uses especially in arid and semi-arid areas where expansion often encroaches on fragile desert environments occur (Mubako et al. 2018).

The dynamics of LULC and settlement expansion require a powerful system to detect the changes (Lillesand et al. 2014). Remote sensing (RS) data, combined with ancillary data in geographical information systems (GIS), are valuable tools for detecting changes in LULC (Rozenstein and Karnieli 2011; Joshi et al. 2016). GIS tools are powerful for analysing, integrating, interpreting, and visualising reference datasets via map overlays. The temporal and spatial observation of changes over a specific time can provide reliable information for mapping and analysing LULC change at local, regional, and global scales (Campbell and Wynne 2011). Numerous studies have been conducted to understand LULC dynamics in arid and semi-arid environments around the world e.g., Mexico (Mendoza-Ponce et al. 2018), China (Yanli et al. 2012), Nepal (Rimal 2011), Eritrea (Tewolde and Cabral 2011), Tanzania (Eckert 2011), Turkey (Erener et al. 2012), Egypt (El-Kawy et al. 2011), Morocco (Barakat et al. 2019), Benin Republic (Guidigan et al. 2019), and Jordan (Al-Bakri et al. 2013). The environmental problems associated with urban expansion have also been identified in many studies. Urbanisation due to population growth creates a high demand for domestic food, water, and space, placing pressure on resources (such as groundwater) that can lead to severe land degradations and other environmental issues including land overuse and pollution (Jakeman et al. 2016; Quesada and Rayfuse 2019).

Saudi Arabia has undergone major changes in LULC over the last decades largely due to the high value of national oil revenues leading to an ambitious government program of national development, resulting in a rapid growth in urban population (Mubarak 2004).

The overall increase in the rate of urbanisation has taken place in all regions of Saudi Arabia. The 2018 population growth rate of 1.8% (World Bank 2018) with an uneven distribution across the country has influenced the LULC patterns in Saudi Arabia.

According to the General Authority for Statistics (GASTAT), Saudi Arabia's population in 2019 was 34.22 million, a 24% increase from 27.56 million in 2010, with 80% living in urban areas. This percentage is estimated to reach approximately 97.6 % by 2030, placing an urban planning and management to the top priority for the future of Saudi Arabia. Urban area expansion continues to increase with the population increases which will, in turn, increase the demand for space, food, and water, which are of critical concern to all countries but particularly so in arid environments such as Saudi Arabia.

In the past decades, agricultural lands and ecosystems have become of prime importance in Saudi Arabia as they account for ecological balance and replenishment of resources (including groundwater resources) essential for human inhabitants (Al-Shayaa et al. 2012). An expansion of agricultural areas in Saudi Arabia in the late 1980s, especially in the north-western Tabuk region, have posed a threat to the groundwater resources serving the urban areas of Tabuk. Such imbalances led to less productivity of the ecosystem. As a result, the local government had to take action to avoid the scarcity of groundwater resources (Ouda 2014; Alzahrani et al. 2017), which resulted in agricultural land expansion ceased, yet constant groundwater monitoring is still required to assess the impact of alterations on the agricultural landscape (Fiaz et al. 2018).

1.1.1 Policy drivers of land-use change in Saudi Arabia

1.1.1.1 Agricultural policies

A major land use change from under-developed land to agricultural land is seen in most regions of Saudi Arabia, including Tabuk. This is a result of urbanisation pressures resulting from rapid population growth and increased economic activity (Carley and Christie 2017). Land for agricultural production has increased from 1.62 million ha in the 1960s to 86.170 million ha in 1992, and 173.619 million hectares in 2016 (FAO 2016; Elhadj 2004). As a result, increased pressure on fragile land areas and valuable water resources have been observed (Abderrahman 2003; Al-Shayaa et al. 2012). In 2015, the agriculture sector consumed 82% of a total 24.8 billion m^3 waters in the country. The primary (90%) groundwater source for agriculture is water extracted from fossil aquifers which are a non-renewable blue water (Elhadj 2004). In 2015, a total of 164,324 wells were used for irrigation in the country with the majority (69.6%) using axial sprinklers for extracting water from artesian sources (SSYB 2015). With almost no surface water available, agricultural expansion draws upon groundwater from both shallow and deep aquifers (Al-Ahmadi 2009). This practice has its own implications for water shortages and sustainability.

Several development plans behind the agricultural expansion in Saudi Arabia over the last few decades since the first comprehensive agricultural renaissance in the mid-1970s is illustrated in Figure 1.1. Since 1970s, the country focused on accelerating agricultural production. The policy of freely distributing undeveloped land to farmers and citizens for agricultural development was one of the first main policies to boost agriculture (Al-Shayaa et al. 2012). From 1970 to 1974, there was also an increase in the consumption of various agricultural products due to increased population and improved standards of living post oil boom era.

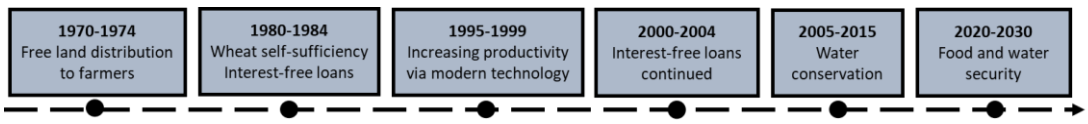

Figure 1.1 Timeline of agricultural development policies of Saudi Arabia

From 1980 to1984, wheat production self-sufficiency was a major policy for Saudi Arabia. Deployment of large-scale irrigated agricultural systems were an ongoing activity; thus, wheat production exceeded the level of self-sufficiency required for the country, resulted in a large surplus in wheat production in Saudi Arabia (Alamri and Al-Duwais 2019).

In the 1990s, the government supported the transition of large areas of desert land to agricultural land through low-cost, interest-free loans, and a policy of providing support for large irrigation projects (Alkolibi 2002). Saudi Arabia joined the ranks of the world's top wheat exporters (ranked sixth) in 1992, with total revenue of US$2.1 billion for a record 4 million tons wheat yield in 1991 (Postel 2014).

From 2000 to 2004, the policy of providing agricultural interest-free loans continued and was accessible to producers. It aimed to improve the efficiency of natural resource usage to ensure sustainable agricultural development while improving the economic performance of the agricultural sector.

The agricultural sector has made an important contribution to the Saudi Arabia gross domestic product (GDP), the contribution increased from 1.1% (1981) to 5.2% by 2001 (Al Rajhi et al. 2012). The agricultural water consumption rate is increasing by 7% annually, exceeding the rate of both the urban and industrial sectors (MEWA 2015). In reality, the focus was on growth of the sector rather than sustainability during this period.

Since 2005, groundwater resources have become scarce to meet the needs of the country’s growing population. Increasing the irrigation water for agriculture has become the only way to fulfil food demands and achieve food self-sufficiency in the country. For example, Saudi Arabia’s wheat consumption for 2016/17 was estimated to be 3.5 million metric tons, a figure similar to that of the United States (Mousa 2019). Ironically, inadequate public policies to support the agriculture sector are one of the leading causes of groundwater depletion. The reliance on aquifers as a major source of water for irrigation now accounts for more than two-thirds of total groundwater consumption (MEWA 2018).

Agricultural practices are currently facing significant challenges, particularly after the introduction of wheat into the arid cropping system. This is due to the massive water requirements for wheat production, e.g., more than 300 million m^3/year has been devoted to irrigating wheat farms since the beginning of the wheat implementation program (Elhadj 2004; Jones 2014). As a result, authorities have reversed policies supporting the production and export of wheat and have implemented new regulations aimed at restricting groundwater use.

An imbalance between environmental resilience and the demand for agricultural production is clearly seen and has forced the country to revise some of its policies relating to agricultural water use. Since the continuous extraction of groundwater in a desert climate contributes to the depletion of existing groundwater resources (Abderrahman 2003).

In 2003, the government enforced a five-year ban on the allocation of public land for farming (Cordesman 2003). Government subsidies related to wheat production were slowly phased out from 2008, and more efficient cropping systems (e.g., greenhouse-grown vegetables) were implemented. These measures were developed as part of new water management strategies. The application of the measures resulted in a 27% decrease in the area of land used for cultivation between 2007 and 2011. Significantly, the area dedicated to wheat cultivation decreased by more than 50%. Despite these policies, consistent population growth and unsustainable farming practices have increased water scarcity (Baig and Straquadine 2014). Lack of environmental awareness among investors and the absence of controls and regulations that consider environmental aspects during the implementation of development programs for wheat production, have had negative effects on land and water. Water sustainability and food security are highlighted as the top priorities for policy initiatives during the 2020-2030 period (Khan 2016). Several issues regarding agricultural expansion, however, must be tackled to achieve the necessary sustainability levels, which include measures to assess the irrigation efficiency, with a focus on providing irrigation water tailored to the actual need for each crop.

1.1.1.2 Urban policies

Rapid population growth is problematic for environmentally fragile semi-arid and arid ecosystems such as those found in Saudi Arabia (Ghanim 2019). The population growth in Saudi Arabia has been aided by revenues generated mainly from oil exports (Mubarak 2004) which have resulted in better living standards and greater employment opportunities. This has seen an increase in the urban footprint and associated demands for food production and other resources (Asif 2016; Moussa 2019).

Significant economic and social changes due to better living standards has led to higher average household sizes and increased local migration. There is a tendency for Saudi Arabia's population to move to cities because of better employment opportunities, quality education, and better services compared to rural areas (Abdulsalam et al. 2014). Often urban areas expand at the expense of agricultural land or vice versa, however, in Saudi Arabia both are expanding in the same manner.

The settlement of the Bedouin (the tribal native population of Saudi Arabia) was one of the first urbanisation projects undertaken, with migration from rural to urban areas encouraged by the government. This Saudi Arabian policy also encompassed the inclusion of Bedouin in national military service to bring the notion of 'one people' across the country. The Bedouin were given educational opportunities and encouraged to change from their previous nomadic lifestyle (Mundy and Musallam 2000; Samin 2019). Rapid urban growth has created an imbalance in the distribution of facilities and services across many regions within Saudi Arabia. Unregulated migration over the past 30 years has had many social, economic, environmental, and health impacts (Al-Khalifeh 1993). Several initiatives and comprehensive national development plans have been proposed to address the issues and regulate the development process, which includes major changes in the institutional framework for urban planning and legislation.

Despite various government strategies to ensure urban growth is sustainable, in many cases population growth has preceded the development of the strategic plans, resulting in uncontrolled developments and inadequate urban services. Unplanned urban growth, the construction of ad-hoc and unplanned housing developments, and increased waste, air, and water pollution (Deep and Saklani 2014) has led to major urban-related environmental problems such as land degradation and irreversible desertification.

In Makkah and Al-Taif, urbanisation is the main contributory factor in LULC changes (Alqurashi and Kumar 2014), likewise in Al-Kharj (Algahtani et al. 2015), Hail (Hereher et al. 2012), and Al-Khobar (Rahman 2016). From 1990 to 2017, Saudi Arabia's population density increased from 7.6 km^2 to 15.3 km^2. As a result, the increased population is now placing massive pressure on the limited natural resources, most notably on fresh water sourced from the regional, underground aquifers. Assessing LULC change and how past policies have influenced agricultural and urban expansion will assist in defining more optimal future policies on sustainable land management.

1. 2 Problem statement

Although many studies have been undertaken to map and model the impact of LULC change in Saudi Arabia, there have been few conducted in the Tabuk region. One major issue is that accurate long-term LULC maps for Tabuk are not available.

Increasing population and demand for space and food to accommodate this growth in Tabuk has put fossil groundwater at a high risk of depletion. The paucity of groundwater monitoring and comprehensive data on irrigation water use and allocation make an evaluation of impacts of LULC change on groundwater capacity difficult. Lack of an understanding of trends in LULC change, and absence of up-to-date LULC maps for Tabuk currently impedes informed water policy development for agriculture and urban planning processes.

Compounding the current situation, the Vision 2030 development projects for the Tabuk region will place additional demands on future water resources. As water use data for Tabuk city and surrounds are unavailable, alternative techniques for estimating urban and agricultural groundwater use are required based on data available.

The specific research questions covered in this thesis are:

1. What are the spatial and temporal patterns of LULC change in Tabuk?
2. What is the predicted LULC change for 2025 and 2035 in Tabuk?
3. How are changes in LULC impacting groundwater demand in Tabuk?

1. 3 Research aim

The aim of this study is to assess the impact of LULC change on groundwater resources in Tabuk city, Saudi Arabia. Specific objectives of this thesis will be achieved by:

1. Determining the pattern of LULC change over the past 30 years for Tabuk;
2. Predicting the future LULC pattern in 2025 and 2035;
3. Estimating net irrigation requirements (NIR) using the evapotranspiration (ET) model as a proxy for water consumption; and
4. Estimating urban water demand based on well abstraction data.

1. 4 Significance

Remote sensing (RS) data integrated with GIS have been used to assess and predict LULC change in arid areas globally, however, these applications rely on the availability of suitable methods and data. This research assesses the existing geospatial methods to evaluate LULC change that may be suitable for the arid environment of Tabuk. Studies that have integrated RS, GIS, hydrological and simulation modelling to evaluate the impact of LULC change on groundwater remain relatively rare for the arid environment context. It is hoped that this research will serve to inform adaptation strategies that address water availability issues due to changing in land use in arid environments.

The significance of this research can be related to several aspects of LULC change patterns and related implications, as follows:

- Groundwater is the most important natural resource in semi-arid or arid regions where surface water is severely limited (e.g., Saudi Arabia, China, and Australia). Monitoring LULC change and its impacts on groundwater could prevent and lessen excessive extraction of groundwater and permanent aquifer damage.
- The focus of this research was to assess LULC change in Tabuk, Saudi Arabia, one of the key regions targeted by Saudi Arabia's urban and agricultural development programs. When assessing the impact of LULC on limited resources in a fragile environment, detailed LULC map information is needed as a baseline tool for land managers and policymakers.
- Additional research through monitoring and predicting the impact of LULC change in arid environments is needed to protect natural resources, only then can appropriate local policies be informed. The results of such research can support a better understanding of the drivers of land change, such as governmental policies, and the corresponding impact of these policies on fragile land and groundwater resources.
- Long-term LULC change detection has not been investigated in Tabuk city and there is a distinct lack of spatial and temporal information for the region. The absence of hydrological monitoring and the lack of comprehensive data for groundwater resources is reported to be a particular issue in Tabuk.
- The impact of current well discharge practices and whether these existing practices can support the projected expansion patterns of agricultural and urban areas in 2025 and 2035 will be examined in this study.
- To date, little attention has been paid to environmental and socio-economic stability in Tabuk city. Assessing LULC change can therefore deliver essential information to aid better environmental management and planning.
- Various procedures were adopted and carried out to close knowledge gaps and proved effective in developing recommendations to lessen the impacts of LULC change in fragile environments, such as Tabuk. Consequently, this research enhances and adds new scientific information that policymakers can draw upon.

- This study is the first to address the Tabuk city's growth and impacts of agricultural and urban growth on groundwater. The study for Tabuk by Al-Harbi (2010) was from 1988 to 2008 at a small scale (i.e., 543 km^2) northwest of Tabuk city and did not include the urban development of the entire city. Detailed changes of Tabuk urban and agricultural areas on a larger scale and over a longer period are therefore essential to fill the knowledge gaps. Due to the lack of previous studies on Tabuk's agricultural area, there is a need to estimate the water demand of the agricultural area of Tabuk to ensure sound environmental and water resource management practices at the local scale. Insights related to spatial patterns in Tabuk's urban areas and the characteristics (i.e., urban growth type and patterns) form the most important findings in this research thesis.
- The research outcome could be useful for government planners and decision-makers to assess and manage agricultural and urban growth and potential adverse impact on the environment, specifically in Tabuk and other arid regions of Saudi Arabia in general. The outcomes could also be applied in other geographical locations with similar environmental features.
- This research provides past, current, and future information related to LULC in Tabuk. This temporal information can assist policymakers to develop strategies, based on rigorous scientific investigation that conserve environmental balance and ease the pressures of rapid development in the Tabuk region.
- The techniques used in this work determine the main driving force of LULC changes, which have been explored intensively and were used to predict future LULC changes. This information on LULC change is important to develop strategies for urban planning and land management.

1. 5 Scope

This thesis has drawn on limited available data and the literature surrounding land-use policies on water scarcity to assess the impacts of LULC change on fragile environment affected by unsustainable practices in Tabuk. This thesis focuses on assessing the most water sensitive anthropological activities on land (i.e., agriculture and urbanisation) as the largest consumptive uses of water in Tabuk.

Although the economic sector is also a contributor to water use in Tabuk, this sector is outside the scope of this thesis given it has less impact on water than the agricultural sector and urbanisation. Detection of LULC change, land use prediction, irrigation, and urban water requirements based on urban well discharge are used to inform this analysis.

Groundwater storage capacity depends on several components including the inflow, evaporation/evapotranspiration, water consumption and discharge. Given some of these data are difficult to find over a long period or on a large scale, this research utilizes alternative approach to understand the impact of LULC change on groundwater and understand a typical water demand in Tabuk city.

1. 6 Thesis structure

The introduction (Chapter 1) outlined the problem statement of this research followed by the research aims and objectives. Chapter 2 reviews available and current literature relating to LULC change and water use in arid environments. Chapter 3 interrogates methods and outlines the choice of techniques and technical applications associated with image analysis and data extraction used in this research to assess LULC change and groundwater usage for Tabuk.

The research results for LULC change and water use are presented in Chapter 4, which is discussed comprehensively in Chapter 5, leading to conclusions presented in Chapter 6. Baseline recommendations to lessen excessive groundwater use and possible methods to conserve groundwater resources to ensure water availability for future generations are provided in chapter 7.

1. 7 Chapter summary

Chapter 1 presented the background, problem statement, aims and objectives, and related questions that will be answered by this research thesis. The chapter also described some Saudi Arabian government policies and their impact on LULC change in Tabuk. Finally, the significance of the study, scope, and structure of the thesis were also outlined.

2 Literature review

2. 1 Land use and land cover change in arid and semi-arid areas

Land use and land cover (LULC) studies have become increasingly important in analysing and examining global environmental change (Hu et al. 2019). There has been an increasing interest in examining LULC change in arid and semi-arid regions as many developing nations work to improve conditions for their citizens by securing food sources and water resources to accommodate increasing populations. Information on LULC is vital to provide useful knowledge to inform land resource management and shape policy (Campbell and Wynne 2011). Striking a balance between the increased demand of natural resources and the actual capacity of land to support increased demands is a difficult task in arid and semi-arid areas. Many places across the world are experiencing severe stress due to the combined impacts of a growing population, the natural constraints of arid areas, and the inherent complication of a changing climate (Wang et al. 2012). Therefore, LULC change studies are used for many reasons including improving the prevailing situation, assessing land transformation processes, optimising the use of natural resources, restoration of landscapes in fragile ecosystems, modelling and predicting future trends, and implementing better environmental management strategies (Liping 2018; Wu et al. 2015).

Studying LULC change reveals several characteristics including the causes and driving forces that can be used to predict future change (Bürgi et al. 2017). The review by Lambin et al. (2011) summarised numerous cases examining changes in agricultural and urban land use. They pointed out that major underlying causes of LULC change can be categorised as natural variability, economics, demographics, governmental policies, culture, and globalisation factors.

Several studies have presented a comparative analysis of various causes of land use change (Van Vliet et al. 2016; Lin et al. 2018; Piquer-Rodríguez et al. 2018; Masini et al. 2019). As assessed by Lin et al. (2018) and Masini et al. (2019), LULC change is increasingly known to be an important driver of global environmental change.

Zewdu et al. (2016) confirmed that land use changes coupled with harsh climatic conditions are altering land cover at an alarming rate. Loures (2019), however, stated that the analysis of LULC change on where, when, and why such changes take place are at times incomplete or inaccurate thus impacting the ability to deliver sustainable outcomes.

Examples of LULC change and its implications include studies on arid and semi-arid regions of Kenya by Muriithi (2016), sustainable land use management in semi-arid regions by Rao et al. (2018), impacts of land use and climate change on water-related ecosystems by Bai et al. (2019), assessments of LULC change in semi-arid regions of India by Mondal et al. (2019), monitoring and mapping changes in land restoration in semi-arid lands by Winowiecki et al. (2018), change detection in arid and semi-arid areas of Sudan by Salih et al. (2017), and LULC change as key to understanding land degradation and related environmental impacts by Arnous et al. (2017).

Classifying LULC features has been of wide interest since the 1970s with the launch of Landsat 1 remote sensor (Anderson 1976). The computation of LULC, however, requires a powerful system besides principally remote sensing to detect the changes. From the 1980s till the mid-2000s, several technologies such as geographical information systems (GIS), spatial statistics, and global positioning systems (GPS) have been developed to generate and visualise geospatial data that provides more detailed insights on specific features in LULC (Lillesand et al. 2014). Data obtained from remote sensing can be utilised as an input into a GIS for further analysis and comparison with other data. These geospatial tools are becoming a vital component of the primary analysis and extraction of information related to urbanisation and agricultural land expansion. Accurate spatial and temporal information about LULC change of the earth's surface is very important to understand the interactions between human and natural phenomena for better land planning and management (Lu et al. 2004).

Remote sensing for LULC in arid and semi-arid areas is a non-trivial task and requires the following three issues to be tackled before providing meaningful results (Che et al. 2019; Lamqadem et al. 2019). The first issue is the accuracy of defining changes in LULC due to spectral confusion (Campbell 2002).

Detecting LULC change in arid areas can be a difficult task due to spectrally similar features (Ram and Kolarkar 1993; Thakkar et al. 2017). Processing and analysing of reflectance often produce mixed pixel (colour values) for urban and barren land, hence creating confusion between the two classes (Lu et al. 2010). Change detection of vegetation cover can also be problematic during the non-growing season (when fallow land is involved), or in the mixed woodland, grass, and bushland classes (Barati et al. 2011). To ensure that the best analytical techniques are used, different techniques need to be tested (Giri 2016). Ma et al. (2017) claimed that a specific technique applied to a specific study area may exhibit good classification accuracy but could produce inconsistent results in other study areas.

The second issue is the selection of suitable satellite imagery and applicable change detection techniques. Each satellite sensor has its limitations for scene recognition in the terms of thematic, temporal, and other interpretations (James 2002; Lu et al. 2011; Abburu and Golla 2015). For example, using traditional pixel-based classification analysis with moderate resolution remote sensing data always causes misclassification in arid urban areas due to lack of clearly defined shapes, similar textural characteristics, and mixed spectral or spatial information of urban objects.
Hence, a combination of different identification and recognition techniques are required to detect objects in remote sensing satellite images consisting of different bands and pixelated schemes (Zhang et al. 2013; Zhang et al. 2014).

The third issue, the use of remote sensing requires additional inputs from various ancillary heterogeneous information sources. Sources may include the digital elevation model (DEM), climate data, digital land use, land cover maps, field data, topography, and spatial models (Franklin and Wulder 2002). Myburgh and Van Niekerk (2013) stated that textual information, contextual information, and ancillary data may also impact considerably on feature extraction and the accuracy of classification. In many developing countries, however, there is usually a lack of existing digital data in a form that can be automatically utilised (Banskota et al. 2014).

2.1.1 Remote sensing of LULC change

To assess and monitor LULC change, remote sensing data set combined with ancillary information in a GIS, have been used as a valuable source of data (Lillesand et al. 2014). Various applications for remote sensing include detection of urbanisation, quantification of vegetation cover and agricultural land, and detection of landscape change (Zhao et al. 2013; Galletti et al. 2014) which utilise multi-temporal data (Coppin et al. 2004; Allam et al. 2019). The level of information derived from remote sensing images is dependent upon the resolution of the multi sensors utilised (Hansen and Loveland 2012). Coarse resolution sensors only provide basic LULC information; medium resolution sensors can provide more advanced information on LULC enabling assessment of changes at a regional scale, and high-resolution sensors enable researchers to map and analyse temporal changes of LULC in greater detail to aid in planning and management.

Detailed spatial and temporal information together with advanced remote sensing and GIS modelling has provided a great opportunity to understand the LULC process and supports better management of land, and effective mitigation of land degradation at global and regional levels (Thenkabail et al. 2018; Borrelli et al. 2017, Eerens et al. 2014). The spatio-temporal analysis of cropland mapping in semi-arid areas of the Nile in Egypt (1984–2015) provides an example of the effectiveness of such analysis to identify cropland trends and LULC dynamics (Xu et al. 2017).

Change detection is the process of identifying differences in the state of an object by observing it several times (Singh 1989). Detecting the changes that have occurred by identifying the nature of change, measuring the area extent of change, and assessing the spatial pattern of change are important aspects of land use dynamics, which can support effective management of natural resources (Macleod and Congalton 1998).

There are several change detection methods within remote sensing applications pertaining to LULC such as image rationing, image differencing, change vector analysis, image regression, and post-classification comparisons. The selection of a suitable change detection technique is very important and is determined by the

complexity of the study area and its particular characteristics including the availability and quality of data, and the amount of spatial information desired. There is not a single technique that fits all LULC change detection scenarios (Bhagat 2012). However, detailed reviews on change detection techniques suggest that the most widely used digital LULC change detection method is the post-classification comparison technique (Coppin et al. 2004; Lu et al. 2004; Singh 1989).

The post-classification comparison technique detects the nature of the LULC change by determining the 'from-to' change. It accomplishes this by comparing classified images individually across different dates (Jensen 2004). Data from these different dates are separately classified and then individually compared to detect any changes (Singh 1989). The technique relies on appropriate pre-processing of the imagery for successful post-classification analysis, namely, image registration, atmospheric correction, and image enhancement (Campbell 2002; Canty 2014).

The accuracy of post-classification comparison change detection appears to be superior to that of other methods such as image differencing, image rationing, and principal component analysis. In research conducted in semi-arid regions of Egypt, the post-classification technique recorded an accuracy of 67% for the classified change image, whereas image differencing, image rationing, and principal component analysis yielded accuracies of 53%, 57%, and 48%, respectively (Afify 2011). Similar results were obtained by Rozenstein and Karnieli (2011), who suggested that the post-classification technique should use ancillary data to improve accuracy. The results showed an improvement in accuracy by up to 10% (giving an overall accuracy of 81%). Post-classification comparison changes detection technique applied to coastal zones of Egypt yielded a classification accuracy of 96%-98% (El-Hattab 2016).

The technique has also been found to provide accurate results when applied to land surface imagery recorded from a large variety of climatic zones, including the Mediterranean, tropical, arid, and semi-arid regions (Mas 1999; Yin et al. 2011). Post-classification techniques, therefore, have become essential tools for detecting LULC change to develop policies and strategies for better LULC management (Peiman 2011).

Additionally, the post-classification technique minimises the effect of atmospheric and sensor differences since the data from two dates are separately classified. Therefore, individual image classification accuracy plays a key role in the accuracy level of post-classification technique (Coppin et al. 2004).

Classification is a statistical tool for extracting information from satellite imagery to derive the spatial patterns of LULC change. The selection of an appropriate classification method is essential for extracting reliable information from satellite data. The general approach of image classification has historically been pixel-based and can be divided into two main categories: 1) unsupervised, and 2) supervised classification (Campbell and Wynne 2011). Numerous techniques in the supervised classification process have been developed to assess variation in LULC such as maximum likelihood classification (MLC) as parametric classifiers, and minimum distance classification (MDC) and newly developed support vector machine (SVM) as a non-parametric classifier, and artificial neural network (ANN) (Vapnik 1999). The hybrid classification approach combines characteristics of both supervised and unsupervised classifications (Lillesand et al. 2014). The object-based image analysis classification by Walter (2004) has gained popularity in more recent times.

Several attempts have been made to detect LULC change using the pixel-based classification technique (Al-Ahmadi and Hames 2009; Soffianian et al. 2010; Yin et al. 2011; Ghaffar 2015; Mohammady et al. 2015). They reported that the pixel-based technique was valuable for assessing LULC change in arid and semi-arid areas. However, pixel-based classification requires additional steps to improve accuracy and visual interpretation in most cases. Several issues in using pixel-based classification has been highlighted by Goodin et al. (2015). Such problems can be encountered due to similar reflectance of different objects producing similar spectral responses of different surface features (from both urban and barren land). This was experienced in a study conducted in Chile by Rojas et al. (2013), requiring additional photointerpretation and fieldwork to overcome mixed classification between bare soil and built-up areas.

Similarly, manual masking may be necessary to reduce misclassification of complex terrains such as valleys with shadows that can produce similar spectral characteristics to urbanised areas, as experienced in a study in Cairo, Egypt, by Mohammady et al. (2015).

In addition, pixel-based classification can be inadequate for assessing agricultural land in arid and semi-arid areas. Fallow farmland can appear like urban areas since both exhibit high reflectance at visible infrared wavelengths. Lamqadem et al. (2019) suggested that issues of mixed pixels when extracting data about agricultural lands using spectral mixture analysis yielded high accuracies in arid Morocco. Allam et al. (2019) applied MLC and normalised difference vegetation index (NDVI) over an arid region of Egypt to produce accurate agricultural classified maps. Chen et al. (2019) found that object-based image analysis (OBIA) can significantly reduce the salt-and-pepper effect that generally exhibits when using pixel-based approaches for complicated agricultural land compared to object-based classifications. Several other studies suggested that using the OBIA technique can accurately define a spatially complex agricultural landscape (Kramm et al. 2017; Lebourgeois et al. 2017; Ma et al. 2017; Naboureh et al. 2017; Aslami and Ghorbani 2018; González et al. 2019; Silver et al. 2019).

Many researchers, including Myint et al. (2011), Kux and Souza (2012), and Ye et al. (2018), have investigated the utility and effectiveness of object-based image segmentation in detecting change in urban and agricultural areas within arid and semi-arid settings. For example, the urban class of OBIA provided higher accuracy compared to a pixel-based MLC classification in a study by Myint et al. (2011).

Similarly, when Zhang et al. (2019) compared the results of pixel-based classification with OBIA classification they found that the OBIA technique significantly improved the extraction and accuracy when analysing urban areas.
In semi-arid Argentina, a 2019 study by González et al. tested five pixel-based classifications, including MLC and SVM algorithms, with OBIA. The results indicated that OBIA increased accuracy by up to 35% more than pixel-based classifications.

The key to OBIA is that it picks up on textural, spectral, and spatial features so that an accurate analysis can be delivered (Lang 2008; Chen et al. 2018), which differs to the pixel-based approach that analyses the spectral properties of each pixel (Bhaskaran et al. 2010).

Various researchers have performed comparisons on object-based and pixel-based image classification approaches to detect LULC change in arid and semi-arid areas including studies in Jordan (specifically the Dead Sea) by Al-Bilbisi and Makhamreh (2010), semi-arid regions of Saskatchewan by Duro et al. (2012), Saudi Arabia by Alqurashi and Kumar (2014), Mexico by Gutiérrez et al. (2012), and China by Zhang and Jia (2014). The outcomes of these studies concluded that OBIA shows more accurate change detection than those achieved by pixel-based classification algorithms.

Table 2.1 summarises previous studies of LULC change detection in arid and semi-arid areas and suggests that the three most commonly used methods are: a) spectral indices (making use of two satellite imagery bands), b) supervised classification (MLC), and c) object-based image analysis (OBIA).

Table 2.1 Summary of arid and semi-arid regions LULC studies

LULC change detection technique	Approach	Country	Satellite data	Reference
Post-classification comparison	PCA, Tasseled cap transformation (TCT)	Saudi Arabia	Landsat	Madugundu et al. 2014
Post-classification modifications	OBIA	Arizona	ASTER	Galletti & Myint 2014
Post-classification comparison	OBIA, pixel-based of RF	Uzbekistan	SPOT	Conrad et al. 2015
Post-classification comparison	OBIA, MLC image classification	Arizona	QuickBird	Myint et al. 2011
	OBIA, NDVI	Brazil	WorldView	Kux & Souza 2012
Post-classification comparison	ISODATA & MLC	Egypt	Landsat	El-Hattab, 2016
	SVM, NDVI	Arizona	Landsat	
Post-classification comparison & binary change maps	SVM	Nigeria	Landsat	Mahmoud et al. 2016
Land use trajectories analysis	OBIA, SVM & RF	Kazakhstan	Landsat, RapidEye	Löw et al. 2015
	NDVI	Niger	Landsat	Nutini et al. 2013
Cluster analysis	Near spectral mixture analysis (NSMA), decision tree (DT) classifier, cluster analysis	China, USA	Landsat	Zhang et al. 2015
Post-classification comparison	MLC	Egypt	Landsat	El-Kawy et al. 2011
Post-classification comparison	MLC	Pakistan	Landsat	Hassan et al. 2016
Post-classification comparison	MLC, DT, ISODATA, SVM	India	Landsat	Kantakumar & Neelamsetti 2015
Post-classification comparison and binary maps	NDVI	Egypt	Landsat	Megahed et al. 2015

Several methods are available to evaluate the accuracy of image classification techniques, with the mostly used error matrix (EM). An EM represents the individual accuracies of each LULC class, and the commission and omission errors (misclassifications) that have occurred (Campbell 2002; Congalton 1991).

The technique includes calculations of user accuracy, procedural accuracy, overall accuracy, and kappa coefficient. Lu and Weng (2007) suggested a combination of high-resolution imagery and ancillary data can improve the classification results.

The ability to obtain accurate geospatial information is crucial when using satellite image spectral data for land management, as this information is essential in understanding the interaction between human activities and consequent LULC change. Different techniques have been used in research conducted previously in arid areas of the world, and the selection of an appropriate classification method is regarded as crucial in extracting reliable information from any satellite data available. An accurate definition of past and current LULC change can be used to simulate future change and provide potentially sustainable development opportunities (Alexakis et al. 2014). Accurate prediction of future changes can also protect existing natural resources from irreversible damage, as well as enabling planners to predict and plan for future urban growth.

Various modelling techniques are used to predict LULC change that can highlight potential impacts on natural resources based on current land use practices. Predicting land use change on fragile landscapes can be used to conserve and protect areas from irreversible damage through informed planning and management. Land use models can be used as decision support tools for urban planning to further inform decision makers and urban planners (Kazak 2018). Great efforts have been made to develop models that can simulate and explore land use change at different scales (Corner et al. 2014; Chen et al. 2016; Lyu et al. 2018).

Substantial progress in spatial modelling of land use change has been made when special datasets have become available from remote sensing. Data from remote sensing imagery and GIS can be used to simulate future LULC change by mapping spatial distribution options that may assist in a sustainable development (Alexakis et al. 2014). Mapping the trend of future changes in LULC has been the main objective of many remote sensing studies around the world (Vaz et al. 2015; Su et al. 2011; Guan et al. 2011; Al-Sharif and Pradhan 2014; Corner et al. 2014; Halmy et al. 2015).

Several models with differing levels of complexity can be used to predict future land use change (Table 2.2). These land use models can be used as a predictive model (e.g., Markov chain); or an explorative model (e.g. agent-based) (Verburg et al. 2004; Mallampalli et al. 2016). Verhagen (2012) states that predictive models can simulate future landscapes under various scenarios. Conversely, Fudge et al. (2013) describes that explorative models explain the interaction between landscape patterns and the driving forces of change. Land use modelling approaches have been reviewed extensively over decades by Batty (2008, 2012, 2017). A thorough review of the most utilised modelling approaches can also be found in Briassoulis (2000) and Dang and Kawasaki (2016).

Table 2.2 Land use model characteristics

Model	Remark	Data dependency	References
Markov chains	• Statistical analysis • Probability of one state change to another based on historical land use development • No spatial dimension • Simulate changes between two or more land use types • Does not consider the factors of land use change	Low	**India** (Mishra et al. 2016; Das & Sarkar 2019)
Cellular automata	• Change is based on neighbourhood cell • Flexible and applicable • Simplicity • Spatially explicit modelling • Allocate a cell to one land use class • Modelling a complex dynamic system	Low	**Hongkong SAR, China** (Chen et al. 2016), **China** (Zhang et al. 2011)
CLUE-S	• Statistical and empirical models • Spatially explicit	Medium	**India** (Maria et al. 2016), **China** (Yi et al. 2012)
ANN	• Suitability maps • Transition rules calculated via the neural network • Predict complex patterns of LULC • Allocate a cell to one land use class	Low	**Iran** (Ansari & Golabi 2019)
LR	• Statistical binary model • Based on driving variables	Medium	**Mongolia** (Tsutsumida et al. 2015), **Mumbai** (Shafizadeh & Helbich 2015)
SLEUTH	• Based on cellular automata • Need for historical maps	Medium	**China** (Lyu et al. 2018)
Agent-based	• Incorporate the effect of human decision making on land use • Often not spatially explicit • No need for historical maps • Does not consider the neighbourhood interaction • Bound on the behaviour of individuals/group agent	High	**China** (He, Li et al. 2017)
Integrated models	• Integration of multiple modelling approaches e.g., integrating MCCA • Benefits from both models	Medium to high	**Libya** (Al-sharif and Pradhan 2014), **Egypt** (Halmy et al. 2015), **Mexico** (Berlanga-Robles and Ruiz-Luna 2011), **Nigeria** (Mahmoud et al. 2016)

Among the aforementioned land use models, integrated model of Markov chain and cellular automata (MCCA) is commonly used for urban growth modelling and land use change prediction (Singh et al. 2015; Zhang et al. 2011). Cellular automata (CA) is a mathematical technique in which the behaviour of the system is produced by a set of probabilistic rules based on the state and neighbourhood of the cells. Whereas Markov chain (MC) models are stochastic models that provide a transition probability matrix for each pixel from the past and current state to the next state (Petit et al. 2001). The MC model, however, is more practical for describing and quantifying land use change but does not consider spatial characteristics or the patterns of land use for predicting the future (Muller and Middleton 1994; Sang et al. 2011).

Sang et al. (2011) noted that both models MC and CA can predict land use change independently, but when combined the MCCA model provides a more accurate prediction of land use change, as it allows for prediction of land use change on a spatial basis based on transition probability and contiguous neighbourhood cells. The MCCA is a preferred predictive model within the geospatial field due to its effectiveness for simulating urban growth and analysing LULC dynamic scenarios (Al-Sharif et al. 2014; Ghosh et al. 2017; Gidey et al. 2017). As Santé et al. (2010) and White and Engelen (2000) stated, the MCCA model has become a powerful tool in spatio-temporal dynamic modelling due to its simplicity, fixability, ability to model complex dynamic systems, and compatibility with most spatial datasets incorporated with GIS (Abdullahi and Pradhan 2018).

Over the last two decades, the MCCA model has provided land use predictions with realistic and satisfactory results across the world including Egypt (Halmy et al. 2015), USA (Puertas et al. 2014), China (Sang et al. 2011; Zhang et al. 2011; Yang et al. 2014; Feng et al. 2018; Lu et al. 2019), Japan (Guan et al. 2011), India (Kumar et al. 2014; Munshi et al. 2014), Libya (Al-Sharif and Pradhan, 2014), Turkey (Akın et al. 2015; Bozkaya et al. 2015), United Arab Emirates (Yagoub and Al Bizreh 2014), Ecuador (Barona and Mena 2014), Mozambique (Henriques and Tenedório 2009), Bangladesh (Ahmed and Ahmed 2012; Corner et al. 2014), Nepal (Rimal et al. 2017), Cyprus (Louca et al. 2015), and Portugal (Araya and Cabral 2010).

The reliability of LULC models depends on the driving forces used for LULC change prediction and modelling (Wang et al. 2012; Celio et al. 2014; Chen et al. 2016). Biophysical and socioeconomic factors are the main factors considered when modelling and predicting future LULC (Lambin et al. 2001). Proximate causes and neighbourhood variables are also important when modelling LULC change. The factors selected are dependent on data availability and the objectives of the study. In developing countries, however, consistency and quality of available data are the main challenges. Eastman and Toledano (2018) stated that integration models (e.g., MCCA) works well when limited historical data is available. Eastman (2009) reported that MCCA models are also ideal for modelling land use in areas where data is unavailable. Use of the MCCA model is also beneficial in settings where LULC change occurred at a fast rate (Singh et al. 2015).

2. 2 Impact of LULC changes on groundwater

Over two billion people depend on groundwater as their main water source globally (Famiglietti 2014). Understanding the impacts of LULC change on groundwater is essential for optimal management of natural resources. Groundwater is extracted at an alarming rate and groundwater levels have significantly declined in many areas. This has been observed in Vietnam (Minderhoud et al. 2017), central Punjab of India (Kaur and Vatta 2015), India (Fishman et al. 2011), and Pakistan (Steenbergen et al. 2015). These studies identified groundwater depletion as a major concern resulting from land use change.

Groundwater is the most important natural resource in arid and semi-arid regions where surface water is severely limited. Effective water management is critically significant for these countries due to the scarcity of water, for example, Saudi Arabia with virtually no available surface water resources. Most of the country - apart from areas in the south - are affected by low and irregular precipitation.

Groundwater extraction and seawater desalination are currently the primary sources of water in Saudi Arabia. With no surface water available, agricultural expansion is dependent on groundwater from both shallow and deep aquifers that underlie many parts of the country (Al-Ibrahim 1991; Al-Ahmadi 2009; Madani et al. 2019).

These aquifers supply the major share of irrigation water for agricultural production which now account for more than two-thirds of total groundwater consumption, making the groundwater resources become crucial in meeting the fundamental requirements of Saudi Arabia's increasing population. There is no recharge available for the deep aquifers, shallow aquifers recharged only after heavy rainfall (Al-Ibrahim 1991). According to the World Bank, water scarcity has the potential to cause extreme societal stress in the Middle East. The economic impact of water scarcity could put the country at risk 6% decrease of GDP by 2050 due to water-related losses in agriculture, climate change, health, income, and prosperity (World Bank 2018).

Al-Salamah et al. (2011) modelled the groundwater of Saq Aquifer in Buraydah Al Qassim in Saudi Arabia over the period 2008 to 2035. Their modelling indicated that, at current pumping rates, a drawdown of the water table by up to 28m could be expected by 2035. A recent government report confirmed that some regions in Saudi Arabia could expect a depletion in the water reserve for the next 12 years (MEWA 2018). Al-Naeem (2014) also investigated the effect on groundwater levels and salinity due to excessive pumping of the groundwater from Saq Aquifer in the Hail region and indicated that the water table had decreased by 25m over the studied period 2002 to 2013. The excessive drawdown in the aquifer also led to a deterioration in water quality in terms of increased levels of salinity.

The desert climate and unsustainable human activity are depleting water resources and contributing heavily to stress on groundwater sources in Saudi Arabia (Gassert et al. 2013; Vincent 2008). More than 80% of the water use for agriculture, industry and daily consumption is withdrawn annually in Saudi Arabia (Gassert et al. 2013).

Substantial climatic fluctuations in recent decades have already caused a decline in rainfall and groundwater recharge (Almazroui et al. 2012; Tarawneh and Chowdhury 2018). Future use of groundwater in Saudi Arabia is projected to increase massively, due to climate change (rise in temperature) and recurrent droughts. Saudi Arabia is ranked 9th out of the 33 countries worldwide that are expected to face a major water crisis by 2040 (Maddocks et al. 2015) (Figure 2.1).

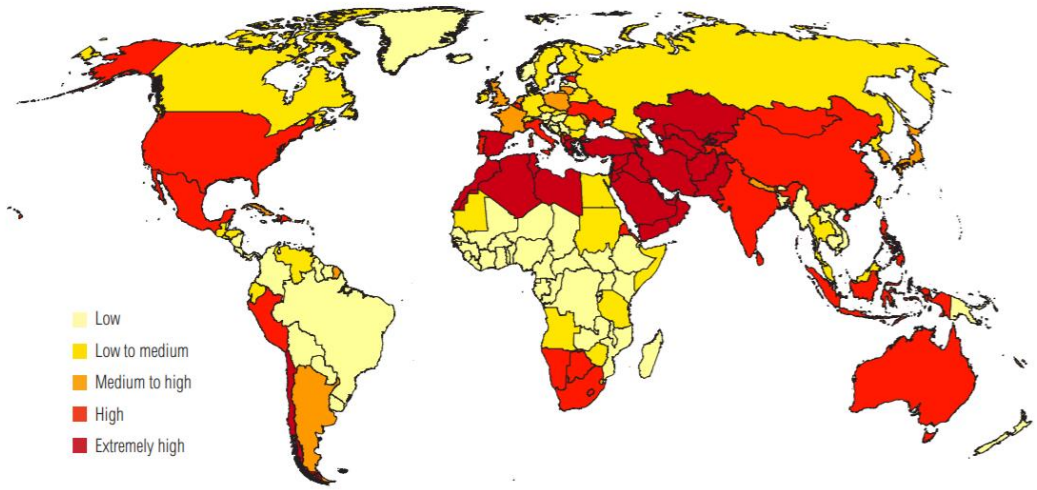

Figure 2.1 Distribution of water stress across the world, showing Saudi Arabia marked as extremely high (Source: Luo et al. 2015)

Saudi Arabia has a very fragile desert environment, therefore, assessing the impact of LULC change on groundwater to optimise water management strategies is of great importance (Sowers et al. 2011; Luo et al. 2015). Groundwater management, however, requires insight on groundwater usage, demand, and discharge. When national data is lacking or unreliable, it may be necessary to obtain estimates from models and satellite imagery. While modelled data may be useful, it cannot replace real measurements taken onsite. Even more so in developing countries, such data is not always available because it is not regularly monitored or is not monitored at all. Thus, data can be extrapolated using alternative tools and models based on available limited data to solve issues related to gaps in data. Several approaches can be used to assess the impact of LULC change on groundwater. The most direct approach is relating LULC changes to water table fluctuations. The following section explains some of the common evapotranspiration (ET) models as enabler to estimate crop water requirements used in recent research.

2.2.1 Evapotranspiration (ET) models

Evapotranspiration plays a key role in irrigation water management at local, regional, and global scales. ET has been considered one of the most promising approaches to estimate agricultural water requirements in a given area. Crop water requirements (CWR) can be defined as the amount of water required to compensate for the water loss through evapotranspiration of a crop (ET_C) (Savva and Frenken 2002). The Food and Agriculture Organization (FAO) has provided several models and equations for ET values to allow accurate CWR estimation, since direct measurements of ET are too expensive and time-consuming to conduct.

Several models exist for calculating ET based on available meteorological data which is a key variable in the models (Allen et al. 1998). These models can be classified into three groups: solar radiation-based, temperature-based, mass-based, or a combination thereof, to estimate ET values as shown in Table 2.3.

Table 2.3 Evapotranspiration models

Model	Parameter	References
Penman-Monteith	$Tmean, Rs, RH, u, es$	Allen 1998
Ivanov	$Tmean, RH$	Romanenko 1961
Kharrufa	$Tmean,$	Kharrufa 1985
Thornthwaite	$Tmean, \varphi$	Thornthwaite 1948
Schendel	$Tmean, RH$	Schendel 1967
Hargreaves-Samani	$T, u, Tmin, Tmax, RH, n,$	Hargreaves et al. 1985
Blaney-Criddle	$T, n, RHmin, \varphi, u$	Allen and Pruitt 1986
FAO Blaney Criddle	$T, n, RHmin, \varphi, u, H$	Doorenbos and Pruitt 1977
Hamon	$Tmean$	Hamon 1963
Baier-Robertson	$Tmin, Tmax, \varphi$	Baier & Robertson 1965
Ravazzani	$Tmean, Tmin, Tmax, Ra$	Ravazzani et al. 2012
Linacre	$Tmean$	Linacre 1977

es is the saturation vapour pressure, T is the average daily air temperature, u is the mean daily wind speed at 2m, H is the elevation, φ is the latitude, Tmin is the minimum air temperature, Tmax is the maximum air temperature, Tmean is the mean air temperature, RH is the average relative humidity, n is the actual duration of sunshine, RHmin is the minimum relative humidity, Rs is the solar radiation

The Penman-Monteith equation (Cai et al. 2007) is a well-recognised ET model and widely used by researchers as being the most accurate model for estimating ET (Azhar and Perera 2011; Muhammad et al. 2019). The model requires several climatic parameters and solar radiation values to compute ET values of the agricultural area.

In most developing regions, real-time solar radiation data is not always available, and can be inconsistent, which limits the use of the Penman-Monteith model. Rezaei et al. (2016) suggested that empirical temperature data can be used to calculate ET values when data is not available. Comprehensive studies that focused on the comparison of ET estimation models under different climatic conditions have been done in Mexico (Quej et al. 2019), China (Feng et al. 2017), Senegal (Djaman et al. 2015), and Spain (Senatore et al. 2020). These studies concluded that the temperature-based model could estimate ET values satisfactorily when using limited data, as well as under a variety of weather conditions. Djaman et al. (2015) showed that two best temperature-based equation models, as compared to the Penman-Monteith equation model, were the Romanenko (Ivanov) and Schendel models. Similarly, Poyen et al. (2016) noted that the Ivanov equation fits best if data on air temperature and relative humidity for the location under inspection are available. Therefore, the temperature-based model was selected to be used in this research.

Previous studies have suggested that the selection of ET models that suit a specific climate zone is crucial since ET estimation depends on the climatic region and the availability of climatic inputs (Djaman et al. 2015; Poyen et al. 2016; Muhammad et al. 2019). Evaluating the performance of selected ET models is, therefore, necessary to ensure that the most accurate results possible are used to inform management of agricultural practices in arid and semi-arid areas.

2.2.2 Saudi Arabian (regional-based) ET model

Historical government-supported agricultural expansion has led to massive land use change. Saudi Arabia has now embarked on programs and plans to strike a balance between development and preserving groundwater resources. To achieve this requires access to accurate data regarding actual agricultural water use. One of the main approaches put forward to determine agricultural water use is through evapotranspiration estimation.

Estimating ET is crucial in a country such as Saudi Arabia where agricultural irrigation is the primary consumer of water (>85%) and uses a resource which is likely to be significantly impacted by climate change. The sprinkler irrigation system used to irrigate large agriculture areas (specifically wheat and clover cultivation) is still in use in most agricultural regions. This process is highly prone to evapotranspiration loss, especially when operating in conditions of elevated temperature. These systems operate in an environment which lacks rigorous irrigation policies and laws, and where irrigation occurs without any consideration of the quantity of water used.

Often meteorological data including solar radiation data, is not available especially in developing countries such as Saudi Arabia. Therefore, simple temperature models are widely used and preferred. Early examples of research into ET estimation includes that by Al-Taher et al. (1992) in Al-Hassa Oasis, Saudi Arabia, which compared three models (Blaney-Criddle, Pan Evaporation, and Jensen-Hais), and developed a model that was specific for the case study area. The results indicated that more climatological parameters were required to provide a more accurate estimation. When Al-Ghobari (2000) evaluated five ET estimation models (FAO-Penman, Jensen-Haise, Blaney & Criddle, Pan Evaporation, and calibrated FAO-Penman), results indicated that the calibrated FAO-Penman model provided the best ET estimation. It was noted, however, that not all methods could be transferred between different climatic regions or could provide the best outcomes under all weather conditions.

Khan et al. (2016) computed potential evapotranspiration (PET) within a variety of climatic conditions in Saudi Arabia, specifically, an arid climate (Riyadh), humid climate (Jeddah), and moderate climate (Abha) using the temperature-based empirical equation of Thornthwaite. This study found PET varied depending on the climatic conditions. The humid climate had the highest PET values followed by the arid climate. Previous studies have concluded that the climate data available on a specific climate zone determines the most suitable model for ET estimation. For sustainable agricultural practice and efficient use of water, accurate ET and CWR estimations are important to be ascertained.

2. 3 Chapter summary

Much has been written on the topic of land use and land cover in arid and semi-arid areas. The key areas examined in this literature review were:

1. Land use and land cover (LULC) change in arid and semi-arid areas with an in depth look at the use and challenges of remote sensing to assess and monitor LULC change;
2. The relationship between LULC change and groundwater, highlighting the role of appropriate environmental management strategies to conserve limited water resources;
3. The need for insights on groundwater usage, demand, and discharge for good groundwater management and land use planning;
4. The value of land use modelling to protect natural resources from irreversible damage, and support policymakers in their efforts to conserve the environment;
5. Predicting the future through the use of land use models and discussing optimal models (i.e., MCCA) that are relevant to the Tabuk city examined in this research work;
6. The use of evapotranspiration models (i.e., ET temperature-based model) to estimate crop water requirements (CWR) in agricultural areas and thus support irrigation water management.

Although several studies have assessed LULC change and model their potential future in arid areas, spatiotemporal analysis and modelling in arid Saudi Arabia have received little attention. Therefore, the appropriate and the most useful techniques found in the literature can be utilised in the study area to achieve the aim of this research. This research will apply models to specifically examine the situation of LULC change in the Tabuk city of north-western Saudi Arabia which comes with its own unique set of factors that are currently impacting the sustainability of natural resources, in particular groundwater.

3 Materials and methods

This chapter is divided into two main sections, starting with a description of the study area Tabuk city, followed by the analysis section presenting data utilized and detailed analysis. The data include primary and secondary data from remote sensing imagery, meteorological records, crop planting and harvesting data, and well abstraction data to estimate water demand.

All of the tools and analyses used to evaluate changes in agricultural and urban land use areas with a focus on groundwater demand for Tabuk are presented in the analysis section of the chapter.

3. 1 Description of Study area and data

3.1.1 Study area

This study is focused on Tabuk city within the north-western Tabuk region of Saudi Arabia which is located between 28˚23 to 28˚39 N and 36˚35 to 36˚57 E, covering an approximately 4,212km^2 area (Figure 3.1).

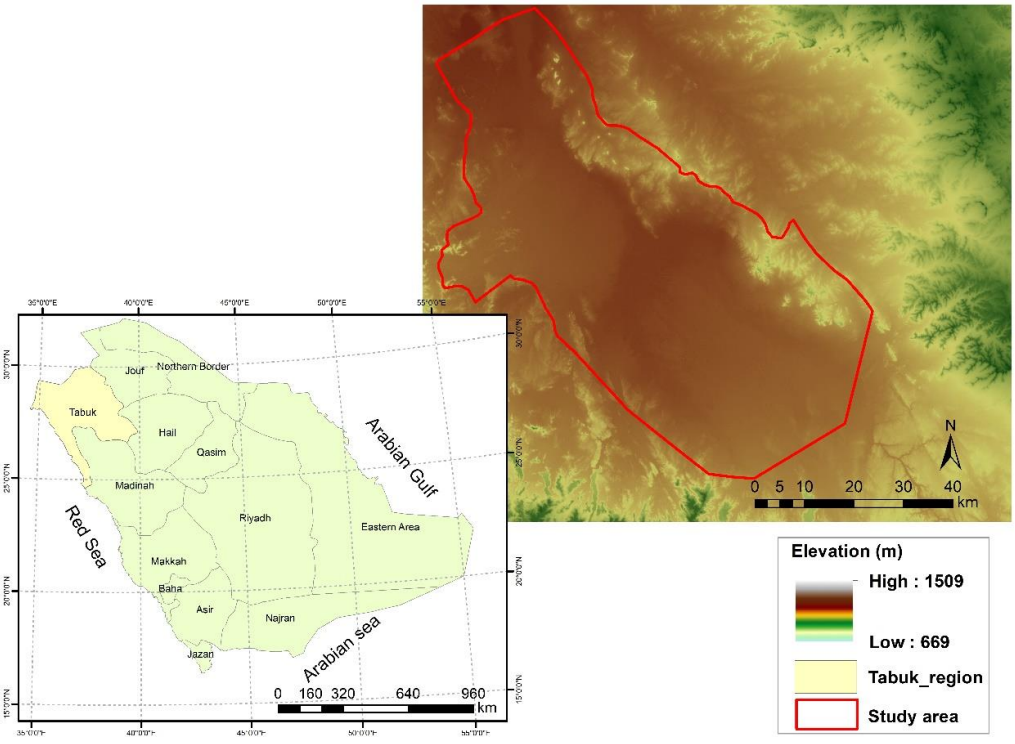

Figure 3.1 Study Area (Tabuk) Locality

Tabuk is situated in the Arabian Shield area and consists predominantly of sedimentary lithological units, as typified by the rocks of the Hijaz Mountains and the Arabian rocky plateau. The soil type of Tabuk is sandy loam which is generally suitable for irrigated agriculture in the northwest and southeast of the city (Al Harbi 2010).

The topography of the city of Tabuk is relatively flat between two mountain ranges (>1500 m above sea level), namely, Mount Sharora and Mount Guanem in the eastern part of the province, and Hijaz and Midian mountain ranges in the west. Tabuk is located on three valleys, Al-Akhdar valley runs to the west, and Abu-Nashefa and Dhaban valleys run to the east and northeast, respectively. The centre and northern areas of Tabuk consist mainly of desert and valleys with an altitude varying from 600 to 800m above sea level (ASL).

Tabuk has a desert climate type of arid-desert-hot or "BWh" according to Koppen's classification scheme (Table 3.1).

Table 3.1 Koppen climate classification scheme

Symbol	Climate	description
B W h	Arid Desert Hot	Dry desert, mean temperature > 18°C, evaporation higher than precipitations (no more than 200 mm annually).

The daily-average temperature in Tabuk ranges from 15°C to 30°C and rarely experiences below 1°C or above 42°C. The warmest months are June to September (summer) with an average maximum temperature of 34°C. December to February (winter) are the coldest months with an average minimum temperature of 4°C.

The average yearly precipitation for Tabuk between 1985 and 2015 was 32 mm, ranging from 1 mm to 92 mm per year (Table 3.2) which is the lowest amount of rainfall in Saudi Arabia (Hasanean and Almazroui 2015). June to September receive insignificant precipitation (0-3 mm) with irregular rain fall between January to December (0-92 mm), with snowfalls experienced every two to three years. The low rainfall leads to recurrent arid conditions in Tabuk.

Table 3.2 Monthly precipitation in Tabuk, 1985-2015

	Precipitation (mm) by month												
Year	Jan	Feb	Mar	Apr	May	Jun	Jul	Aug	Sep	Oct	Nov	Dec	**Total**
1985	0	2	4	4	0	0	0	0	0	0	10	59	**79**
1986	1	0	18	12	0	0	0	0	0	1	17	0	**49**
1987	0	1	0	0	0	0	0	0	0	26	0	14	**41**
1988	9	0	1	12	2	0	0	0	0	53	0	2	**79**
1989	0	0	6	2	1	0	0	0	0	0	20	18	**47**
1990	1	0	0	0	0	0	0	0	0	1	0	2	**4**
1991	36	0	25	0	0	0	0	0	0	6	0	1	**68**
1992	2	1	0	0	0	0	0	0	0	0	3	1	**27**
1993	1	1	0	5	0	0	0	0	0	10	0	18	**35**
1994	5	1	0	0	1	0	0	0	2	24	13	0	**46**
1995	0	0	11	0	1	0	0	0	0	0	0	0	**12**
1996	0	0	1	0	0	0	1	0	0	0	11	4	**17**
1997	21	0	2	0	3	0	0	0	0	7	0	0	**33**
1998	3	2	3	0	2	0	0	0	0	0	0	0	**10**
1999	2	14	11	0	0	0	0	0	0	0	0	0	**27**
2000	7	2	0	0	0	0	0	0	0	1	8	4	**22**
2001	2	0	2	12	2	0	0	0	0	0	0	0	**18**
2002	2	0	0	0	0	0	0	0	0	1	3	0	**6**
2003	0	0	0	0	0	0	0	0	0	0	0	1	**1**
2004	5	1	0	0	0	0	0	0	0	0	0	0	**6**
2005	8	0	0	1	0	0	0	0	0	0	0	0	**9**
2006	0	6	8	0	6	0	0	0	0	0	0	0	**20**
2007	8	2	1	1	2	0	0	0	0	1	0	0	**15**
2008	8	1	0	0	0	0	0	0	0	0	2	1	**12**
2009	0	1	0	0	23	0	0	0	0	1	4	0	**29**
2010	39	0	1	0	5	0	0	0	0	0	0	4	**49**
2011	4	3	0	5	0	0	0	0	0	0	0	0	**12**
2012	0	5	0	9	0	0	0	0	0	17	1	0	**32**
2013	76	6	0	0	1	0	0	0	0	0	0	9	**92**
2014	1	2	24	0	5	0	0	0	0	3	0	10	**45**
2015	0	2	0	0	0	0	0	3	0	10	42	0	**57**
Average	**8**	**2**	**4**	**2**	**2**	**0**	**0**	**1**	**0**	**5**	**4**	**5**	**32**

Source: GAMEP, 2015

3.1.2 Data acquisition and analysis

To assess the changes in urban and agricultural land use and corresponding impact on groundwater, primary and secondary data sources were required. Primary data were obtained from the analysis of satellite images, while secondary data were captured through climate data, field observations, a survey using GPS, personal communications, and water and agricultural experts from government ministries.

More details about these datasets and preparation are provided in the following sections.

3.1.2.1 Satellite data acquisition and preparation

Multi-date Landsat Thematic Mapper (TM), Enhanced Thematic Mapper Plus (ETM+), and Operational Land Imager (OLI) for 1985, 1990, 1995, 2000, 2005, 2009 and 2015 to assess land use and land cover in Tabuk were acquired for this study from Earth Explorer (USGS Earth Explorer (https://earthexplorer.usgs.gov/)) (Table 3.3). As satellite data for the year 2010 was not available, 2009 data was used instead. Images with minimal cloud cover (<10) were selected for March or April of each year assessed. These months equate to the spring season with high vegetation growth and provided optimum contrast between LULC classes. The images were selected to minimise the impacts of any seasonal variation. The specific time interval selected allows an examination of LULC changes over five distinct periods to evaluate urban and agricultural expansion in Tabuk.

Table 3.3 Satellite data used to assess land use/land cover land in Tabuk city

Data type	**Date of acquisition /time-period**	**Path/row**	**Source**	**Description**
Landsat 5	26-03-1985	173/40	USGS	TM
Landsat 4	08-03-1990	173/40	USGS	TM
Landsat 5	22-03-1995	173/40	USGS	TM
Landsat 7	27-03-2000	173/40	USGS	ETM
Landsat 7	10-04-2005	173/40	USGS	ETM+
Landsat 7	20-03-2009	173/40	USGS	ETM+
Landsat 8	14-04-2015	173/40	USGS	OLI
DEM	2011	173/40	ASF	12.5m

Ancilliary SPOT S5 data (at 2.5m resolution) for 2005, 2008, 2010, and 2014, sourced from King Abdulaziz City for Science and Technology (KACST), were used to support LULC classification. Topographic maps were used for geometrical rectification of Landsat data, and to assist in image classification, LULC classification, and validation (Table 3.4). Two topographic maps at the scale of 1:100,000 and 1:500,000 were obtained from the Ministry of Petroleum and Mineral Resources (MPMR) of Saudi Arabia. The 1:500,000 scale map was updated using aerial photography from 1983.

The Saudi Arabia General Commission for Survey (GCS) provided access to a combined dataset including road networks, agricltural well locations, and topographic line map (TLM) at the scale of 1:50,000 and joint operations graphic (JOG) at the scale of 1:250,000. These maps were based on aerial photographs taken in 1981 and updated in 2009 through ground truthing from various Saudi ministries. Because multi-date Landsat data were used in this work, a number of topographic maps of various years were also sourced to support LULC classification and validation.

Table 3.4 Topographic map details used to ground truthing of remotely sensed data

Scale	ID	Year	Source
1:50 000	4624-11	1994	GCS
1:100 000	1	1991	MPMR
1:250 000	NH 37-13	1988-1991	GCS
1:500 000	NH37-SW	1980-81	MPMR

In addition to using topographic maps, a field survey was carried out as part of this study from December 2015 to February 2016 to obtain ground truthing data that supported land use classification of the study area. A handheld Garmin global positioning system (GPS) with an accuracy of ±5m was used to collecting information related to LULC. A total of 488 locations (random sample points for different LULC) were recorded and subsequently converted to a shapefile in GIS (Figure 3.2).

3.1.2.1.1 Classification scheme

Selecting the LULC classification scheme is an essential step since it affects the interpretation of remote sensing data. The classification scheme developed by Anderson (1976) offers four levels of increasing detail from level I to level IV (Giri 2016). Andersons's classification system is flexible and adaptable to meet user demands which can be general LULC classification at large scales (i.e., first and second level) or detailed LULC classification at smaller scales (i.e., third or fourth level). Anderson (1976) stated that the type and amount of LULC information acquired from different sensors rely on the resolution of each sensor. For example, level I LULC information can be compiled effectively using Landsat satellite images.

This work utilises Landsat data, therefore, Anderson scheme level I with main LULC classes would be considered for Tabuk city (Table 3.5). The existing LULC classification system of Tabuk city outlined by Al-Harbi (2010) was also adapted to assess LULC changes in the study area. There are four primary classes which typically present the arid environment, that were identified and designated in this study (Table 3.5 and Figure 3.2). These nominally were barren land, urban area, agricultural land, and water classes. During the LULC classification determination process, high-resolution SPOT images and field data were utilised.

Table 3.5 LULC classification scheme

Code	Class	Description
1	Barren land	Desert sand, mountain, bare exposed rock, mixed bare land, and dry salt flats
2	Urban area	Residential, commercial, and industrial areas; settlements; and transportation infrastructure
3	Agricultural land	Cropland and pasture fields, greenhouses, harvested and fallow lands
4	Water	Ponds or small lake

Adapted from Anderson 1976; Al-Harbi 2010.

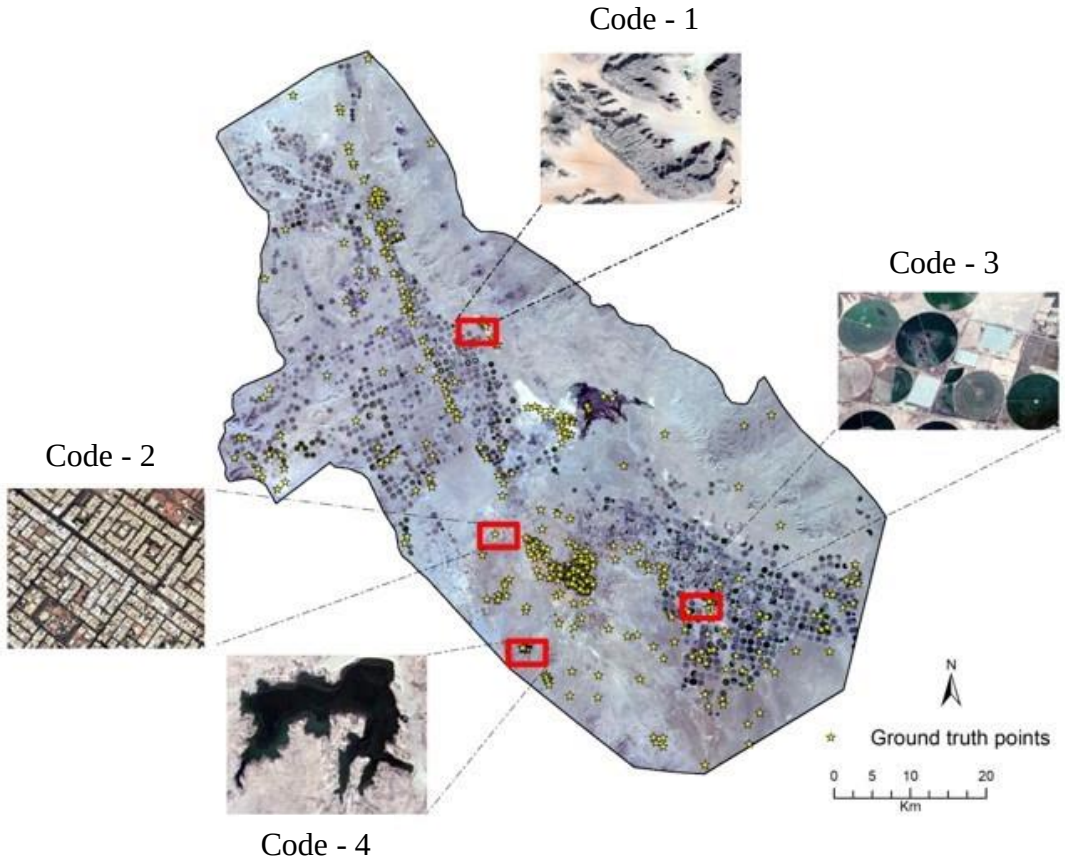

Figure 3.2 Ground truthing points from fieldwork in 2015 and LULC classification codes

3.1.2.1.2 Image pre-processing

Before any change detection procedures can be used, geometric and atmospheric corrections must be carried out for images acquired during different periods impacted by haze and dust present in the atmosphere during satellite overpass (Chavez 1996). Multi-date Landsat images (L1 product) were geometrically corrected and rectified to the Universal Transverse Mercator (UTM) system (zone N37). Atmospheric correction, including radiometric calibration, was applied to minimise any atmospheric effects and the digital numbers (DN) converted to top-of-atmosphere (TOA) reflectance (Chavez 1996). The dark object subtraction (DOS) method was used to correct for atmospheric scattering. Base and warp pre-processing image-to-image registration technique were also used (Jin 2018).

This technique aligned the images and generated automatic tie points between the base image (Landsat ETM+ of 2000) and the warped image (Landsat TM of 1985). A total of 50 ground control points (GCPs) were generated and distributed across all images. The nearest neighbourhood re-sampling method was used to align multi-year images, which resulted in an overall root mean square error (RMSE) of 0.46 pixels. The geometrically and radiometrically corrected images were then clipped to the study area boundary.

3.1.2.2 Climate and crop data

Climatic data from the General Authority for Meteorology and Environmental Protection (GAMEP) was obtained from their Tabuk meteorological station (ID 40375), located at 28° 36’ N, 36° 56’E. Daily climate data were sourced from 1985 to 2015 to align with the Landsat data being analysed. Climate data included daily maximum, minimum and mean, temperature (Tmax, Tmin, Tmean), rainfall (RF), and relative humidity (RH). Climate analysis focused on measured meteorological data available during the growing seasons. These variables have a direct and indirect impact on the evapotranspiration process (Table 3.6). Evapotranspiration (ET) is based on the Ivanov model (1961), a description of the model is presented in section 3.2.3 of this thesis.

Table 3.6 provides a summary of the variables and parameters used to determine past water demands for irrigated agriculture in the study area. Crop data (e.g., crop name, planting, and harvesting dates) were sourced from the Saudi Statistical Yearbook (SSYB 2015), Agricultural Tabuk Region Calendar and the Agriculture Census (Table 3.6).

Standard crop coefficient values were obtained from the Food and Agriculture Organization (FAO) database for each crop of interest i.e., wheat, clover, potato, and maize. The corresponding irrigated areas were ascertained from remotely sensed data used in the study. Daily climate data were divided into four main growing seasons for each crop. Season I wheat is grown during November to February, season II clover (berseem) during March and April, season III potato during September and October, and season IV maize from May to August (Figure 3.3). Each crop field is irrigated with a centre-pivot sprinkler system (Figure 3.4), which allows crop farming throughout the year.

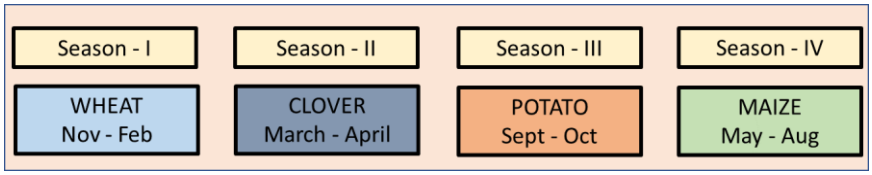

Figure 3.3 Crop calendar of Tabuk

Figure 3.4 Typical irrigation system in Tabuk (images from fieldwork in 2015)

Climatic conditions were analysed for the study period using data from monthly air temperature, relative humidity, rainfall, and wind speed for Tabuk to assess variation. The analysis showed that the climate was relatively stable, and the data are presented in appendix A.

Table 3.6 Definition of key crop water requirement parameters and variables

Symbol	Description	Units	Source
	Climate variables		
$Tmax$	Maximum Air Temperature	°C	GAMEP, FAO & Ivanov model
$Tmin$	Minimum Air Temperature		
$Tmean$	Mean Air Temperature		
P	Precipitation	mm	
ET_o	Evapotranspiration	mm	
$Eff\ rain$	Effective Rainfall	mm	
RH	Relative Humidity	%	
	Crop parameters		
_	Crop planting date	_	SSYB & Tabuk Agriculture Calendar
Kc	Crop Coefficient	_	FAO
ETo	Reference Evapotranspiration	mm/day	Ivanov model
ETc	Evapotranspiration water requirement	mm/day	Ivanov model & FAO
_	Crop field size	km^2	Remotely sensed data

3.1.2.3 Water abstraction data

Groundwater is the main source of water for Tabuk and is used for different purposes. The study area of Tabuk overlies the Saq Aquifer which is the major contributor of fossil groundwater in the area. Saq Aquifer is unconfined in the southeastern part of the study area while it is confined in the northeastern part. It is characterised by an average transmissivity of 1,572 m^2/day which indicates high potentiality while the average storativity is $2.86x10^4$ m^3 indicating confined conditions. Due to extreme hot weather conditions, there is very limited local recharge in the unconfined part of the Saq Aquifer.

The Saudi Arabian Ministry of Environment, Water and Agriculture (MEWA), formerly referred to as the Ministry of Agriculture and Water (MAW), were the main source of groundwater data used to generate the initial dataset of water abstraction in Tabuk. Limited data were available for agricultural and urban water use in Tabuk.

Data record with respect to water supply for urban areas was very limited and available only in archived hard copy tabular form, which were mostly inconsistent and/or incomplete. Completed dataset was available for urban areas covering well abstraction (discharge), well pumping run time, and well installation year between 1995 and 2015 (Table 3.7).

The geographical location of the urban tube wells was captured during a field inspection in 2015 using a GPS. A total of 28 flowing artesian wells were currently in use for domestic purposes in Tabuk city – some wells were opened recently (2018) and around three closed from 2010 to 2015 (MEWA 2015). This study considered the working wells (28) during the period of study. Urban wells were drilled to depths of 500m to 825m. Water production from wells were generally constant throughout the year (MEWA 2015). The number of wells utilized in this research is summarized in (Table 3.8).

Table 3.7 Urban well information

Well ID	Suburb	Coordinates		Installation year	Flowrate (m^3/hours)	Pumping run time hours/day
		Latitude	Longitude			
1	Alazizeah	261400	3142428	1995	136	22
2	Alkhaldieah	261003	3141181	1995	108	19
3	Alfaysliyah-1	262675	3142603	1995	144	22
4	Alfaysliyah-2	262781	3142584	2005	272	22
5	Alrabwah	264087	3142856	2007	216	21
6	Aljumrak	260055	3144277	2004	408	22
7	Alsanabel	258596	3143262	2006	360	18
8	Alsaadah	262673	3132576	2003	340	21
9	Alsalihiyah	260412	3142092	1999	272	22
10	Almanchiha	261903	3141792	1995	408	21
11	Sultana-1	262611	3143674	1999	528	22
12	Sultana-2	263523	3144079	2003	340	22
13	Alsuleimaneh	260860	3145479	2002	288	18
14	Demage	257034	3144891	2006	160	20
15	Almuruj-1	264242	3145236	2001	336	21
16	Almuruj-2	262815	3146915	2006	272	18
17	Almuruj-3	260994	3148080	2014	312	20
18	Alrayan	260499	3150737	2014	288	7
19	Alhmraa	261773	3139646	2010	272	10
20	Almassif	260419	3148746	2007	340	14
21	Alwurud	263894	3144662	2001	272	22
22	Alsheikh	260560	3140928	2008	264	19
23	Alrowdah-1	257034	3144891	2004	264	21
24	Alrowdah-2	257122	3144917	2014	340	23
25	Algadesiah-1	257040	3146763	2007	216	18
26	Algadesiah-2	257033	3147518	2011	264	14
27	Algadesiah-3	255801	3148751	2014	360	10
28	Alnahdah	258596	3143262	2001	340	23

Source: MEWA, 2015

Table 3.8 Well category by sector

Category	Number	Data source
Agricultural (irrigation) wells	466	GCS (2009-2014)
Urban (domestic) wells	28	Field data (2015)

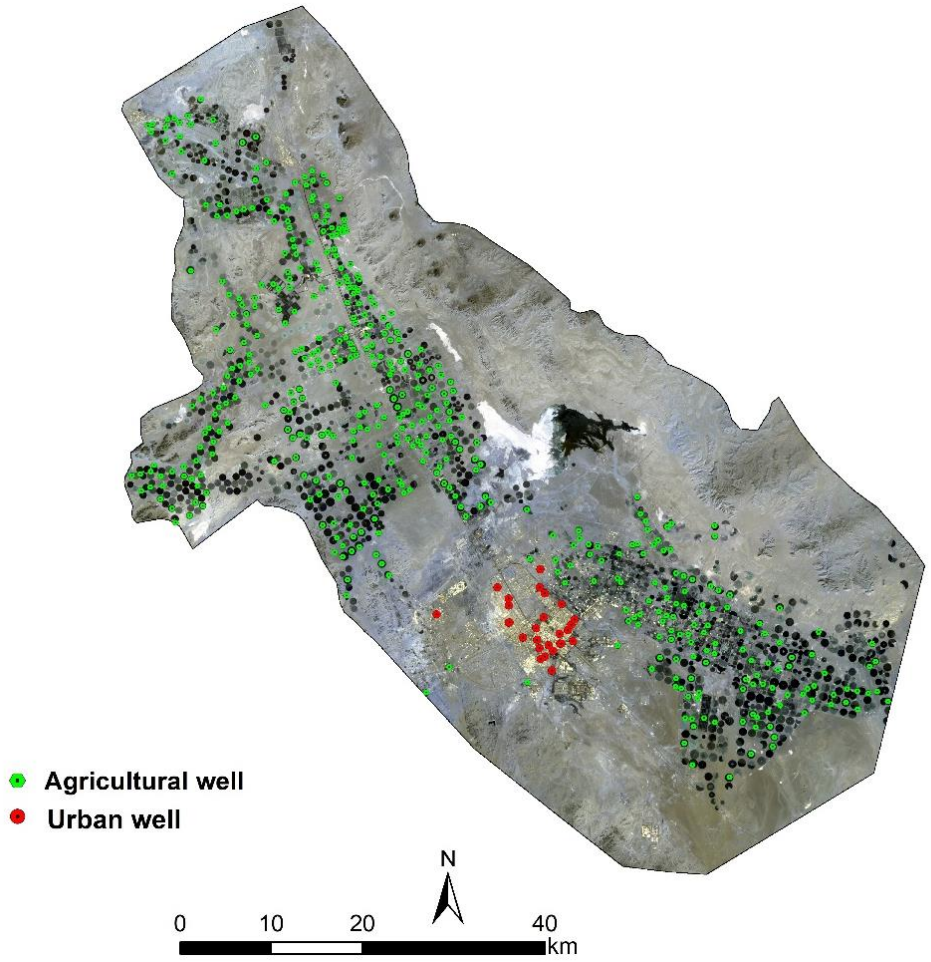

Figure 3.5 Spatial distribution of drilled wells in Tabuk (draped over Landsat 8 imagery 2015), black circles represent agricultural crops

Advanced technologies for extracting urban water are distributed in each suburb of Tabuk city (Figures 3.5 and 3.6) which may account for the increasing pressure on groundwater due to heavier pumping capacity.

Figure 3.6 Examples of urban wells in Tabuk city showing the technology used (Source: 2015 fieldwork)

Statistical and census data issued by the Central Department of Statistics and Information (CDSI) of Saudi Arabia were utilised to describe Tabuk's demographic characteristics.

Tabuk has been selected for this study as it is a good example of an area which has undergone significant LULC change since the 1980s. Currently, the area is also at greater risk of deterioration due to population pressures, intensive agricultural activities, and changing climatic conditions.

3. 2 Analytical techniques

3.2.1 Analysis of LULC change in Tabuk between 1985 and 2015

3.2.1.1 Image classification technique

The selection of a ‘best’ LULC image classification technique is subjective and depends solely on the study purpose (Kantakumar and Neelamsetti 2015). Any selected method must, however, be informative and able to distinguish effectively between classes, such as those representing arid, agricultural, and urban areas. Several classification approaches have been developed to extract land cover information and changes from remotely sensed imagery (as discussed in chapter 2). None of the methods is expected to be 100% accurate in all situations, however, the research literature has identified three classification techniques that have been widely used in arid and semi-arid area studies, namely, maximum likelihood classification (MLC) and support vector machine (SVM) which are both supervised classification techniques, and object-based image analysis (OBIA). These image classification techniques were considered for the study area with several factors considered to select the most suitable classification method for this study. The factors include classifier accuracy, convenience, and effective separation between the LULC classes, classifier applicability, and computing time.

Object-based image analysis (OBIA) was selected as the best option to classify each Landsat image to four main LULC categories in Tabuk (Table 3.5). The main advantage of the OBIA technique was that it groups the image pixels into objects based on similar spectral, spatial, colour, and textural features (Costa et al. 2017) rather than using individual pixels to classify satellite data such as MLC (Chen et al. 2019).

The technique of OBIA has been shown to perform better in areas of complex spectral characteristics such as Tabuk, where urban areas readily mix with barren and inactive agricultural land. Using a pixel-based classification in such instances can lead to misclassification (see appendix B).

To determine the pattern of LULC change over 30 years (1985-2015) for Tabuk, remote sensing image classification, accuracy assessment, and change detection were used. A workflow showing stages in LULC classification through to change detection is shown in Figure 3.7.

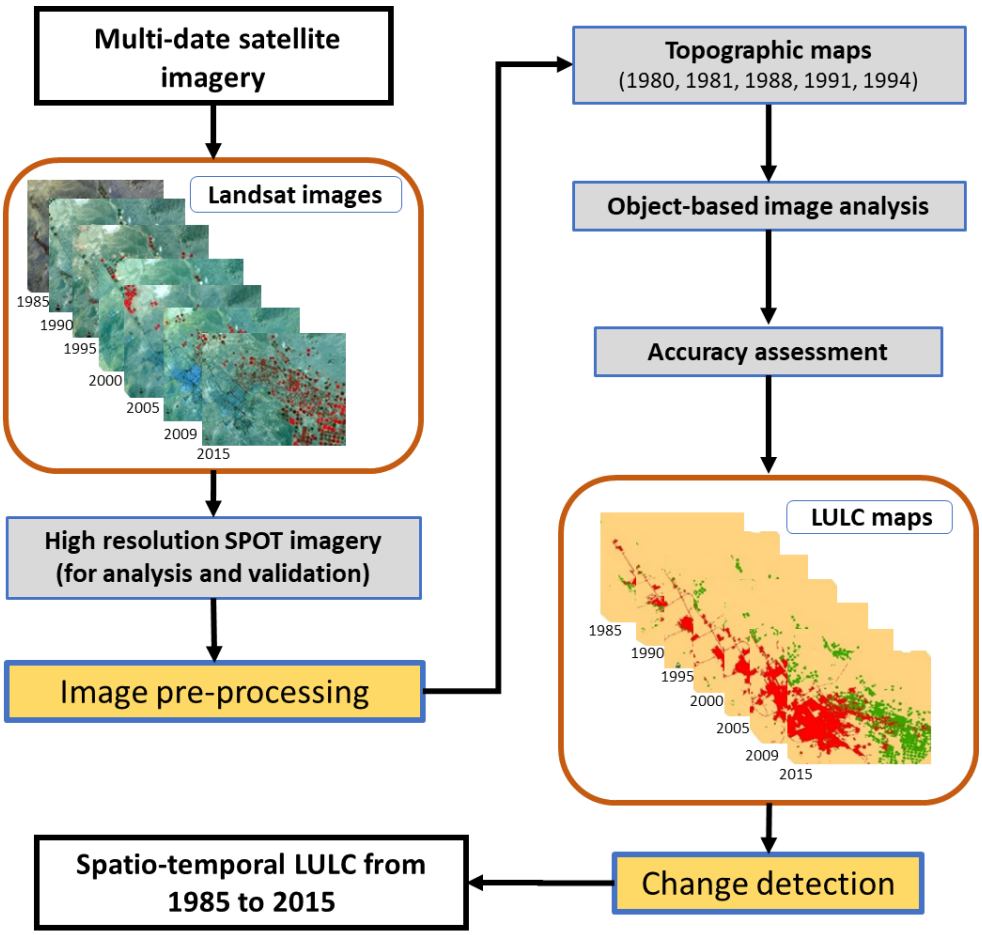

Figure 3.7 Workflow of stages for image classification to LULC change detection in for Tabuk, 1985-2015

3.2.1.2 Object-based image analysis (OBIA)

Object-based image analysis in this study uses a segmentation process to establish LULC classes in the study area within the ENVI 5.1 software application. The segmentation process is a crucial step in OBIA because it determines the interpretation of the image data into LULC type based on different spatial and spectral characteristics. Various scale levels were tested during a preliminary analysis (trial and error) to set the scale level that suited the spectral and spatial LULC characteristics for Tabuk and to produce the best outcome.

In the feature extraction tool, an edge-based segmentation algorithm was used to create LULC classes. The OBIA algorithm created lines along the strongest intensity gradients making it an effective edge detector. In the segmentation process, the determination of the scale level (SL) defines the size of an object in an image. Various SL (e.g., 10 to 70) were tested to find the appropriate scale for the study area. The most appropriate scale for the study area was selected based on the smallest feature. The SL for the edge segment algorithm was adjusted to 10 (on a scale from 0 to 100) as the lower the SL the more effective the spectral information and vice versa. In this case, a value of 10 worked well to separate two features, giving the strongest intensity gradients along lines. The next step was the use of a merging method which aggregated small segments into larger areas as the merging value increased based on homogeneity (using a scale from 0 to 100). The full lambda schedule merging method was applied and adjusting the merge level (ML) to 97 delineated LULC class boundaries. A default value of 3 was used for the texture kernel size and was set prior to the settings for segmentation merging. Examples show an initial segmentation process to accurately classify agricultural land and urban areas using satellite data from 2015 (Figure 3.8).

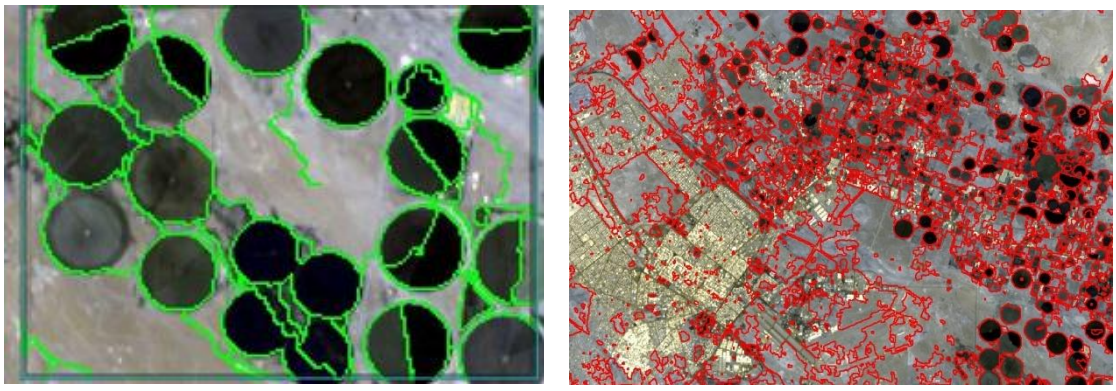

(a) (b)

Figure 3.8 Example of segmentation process using satellite imagery from 2015: (a) initial segmentation step preview; (b) segmentation after selection of parameters

3.2.1.2.1 Training sample

Training samples were interactively selected and then assigned segments to each LULC class using reference data. The training samples for each image were defined and labelled manually. A representative sample of 100 features were evenly distributed over the entire image and assigned different LULC classes. Varied object sizes, shapes, colours, and intensities were considered when selecting the training samples (Figure 3.9) to obtain optimal classification results.

Figure 3.9 Selecting training samples for identifying LULC classes, example from 2015 satellite imagery

K nearest neighbour (KNN), principal components analysis (PCA), and support vector machine (SVM) are the three classification methods available within the feature extraction tool. For this study, KNN was applied to assign each object in the image with an appropriate LULC class. The KNN technique has the ability to classify each object based on its proximity to neighbouring training regions by computing the Euclidean distance between them. The KNN method is less sensitive to noise in the training dataset and is stricter than the other mentioned methods.

The KNN method also differentiates between similar classes effectively, therefore, it produces a more accurate classification result (Tsai et al. 2011; Pragunanti et al. 2020). These are the main advantages of utilising the KNN method in this study. All the Landsat datasets underwent the same segmentation process, the same setup of scale and merge level, and the same classification method and parameters. Finally, the LULC classified objects were exported as thematic vector layers.

3.2.1.3 Accuracy assessment

An error matrix was utilised to measure the degree of closeness of the outputs (thematic map) to the true values, including overall accuracy, producer's accuracy, user's accuracy, and kappa coefficient (Cohen 1960; Congalton and Green 1999; Foody 2002; Lu and Weng 2007).

The error matrix represents not only individual accuracies of each LULC class, but also any misclassifications made through commission and omission errors (Campbell 2002; Congalton 1991). Reference datasets (from high-resolution images), ancillary data, field visits and associated field knowledge were all used to improve the classification and final accuracy assessment results as recommended by Lu and Weng (2007). A total of 500 points were randomly generated using stratified random sampling for each LULC map in this study. Field data were used as reference data for the 2015 imagery. For other images, reference data were gathered from high-resolution images and near synchronous topographic maps. Appendix C contains the EM tables of LULC reference data for 1985, 1990, 1995, 2000, 2005, 2009, and 2015.

The degree of agreement between the classified results and the reference data were calculated using the Kappa coefficient (Cohen 1960; Congalton 1991):

$$Kappa = \frac{N\sum_{i=1}^{k} x_{ii} - \sum_{i=1}^{k}(x_{i+} \times x_{+i})}{N^2 - \sum_{i=1}^{k}(x_{i+} \times x_{+i})} \quad \text{(eq. 1)}$$

where,

k is the number of rows in the error matrix

x_{ii} is the number of observations in row *i* and column *i*

x_{i+} and x_{+i} are the marginal totals of row *k* and column *i*

N is the number of observations in the matrix.

3.2.1.4 Change detection (post-classification techniques)

The most widely used change detection technique, i.e., pixel-by-pixel post-classification comparison method (Raja et al. 2012), was applied to quantify the changes in LULC between years.

A post-classification comparison was conducted using classified remote sensing images across different periods to determine 'from–to' change in LULC categories and provide information on the rate and direction of LULC change.

3.2.1.5 Urban growth analysis

Several landscape matrices have been developed and widely used for assessing the spatial-temporal pattern of urban growth and consequent land use change. Landscape metrics including spatial metrics aimed at identifying different stages of urbanisation such as shape, size, pattern, and land-use structure over time. Urban spatial growth and type for this study were measured using the urban growth analysis tool (UGAT) developed by Angel et al. (2007). Extension, infill, and leapfrog are the main growth types. The term extension development is used where new developments extend into the outer regions relative to existing urbanised areas (Angel et al. 2012).

Infill development refers to new development occurring within existing urbanised areas, while leapfrog development occurs in areas distant from existing urbanised pixels. A detailed description of the tool can be found in Angel et al. (2007).

The direction and buffer zone of urban growth from the Tabuk city centre between 1985 and 2015 was quantified using a bearing distance tool in GIS. Lines extending from the city centre were drawn with equal intervals of 45° from the north in a clockwise direction, resulting in a total of eight directions i.e., N, NE, E, SE, S, SW, W, NW (Zhang et al. 2016). The buffer zones were created and overlaid with urban growth at regular intervals of 5km^2 from the city centre. The Tabuk administrative centre was used as the city centre, obtained from Google Earth.

3.2.1.6 Population growth

To analyse the relationship between population and urban expansion, population data were sourced from the Central Department of Statistics and Information (CDSI) census data and the United Nations (UN) statistical data.

Population rate growth was calculated for each period as follows:

$$Population\ change = \frac{(pop_{Present} - pop_{Past})}{pop_{Past}} \times 100 \qquad \text{(eq. 2)}$$

$$Population\ growth\ rate = \frac{Population\ change}{N} \qquad \text{(eq. 3)}$$

where, *N* is the number of years (5 years).

The data on population numbers did not include the large numbers of visitors that visit the area on religious pilgrimage. In 2018, a total of 185,388 people came through Halat Ammar port (which links Saudi Arabia with Jordan, Lebanon, Turkey, and Europe) to perform the Hajj pilgrimage (CDSI 2018) placing additional pressure on Tabuk's resources. Further visitors arrive from Duba port (which is a commercial port connecting Tabuk with Egypt).

3.2.2 Predicting LULC change for 2025 and 2035

To gain a comprehensive understanding of the land use change in Tabuk city, a simulation model was adapted. The model was based on the Markov chain and cellular automata (MCCA) integration model. Data acquired from remote sensing imagery for historical LULC data (1985-2015) and biophysical factors (elevation and slope) and proximity (distance from wells, distance from roads, and distance from existing agricultural land and urban areas) were used as input data for the model (Figure 3.10).

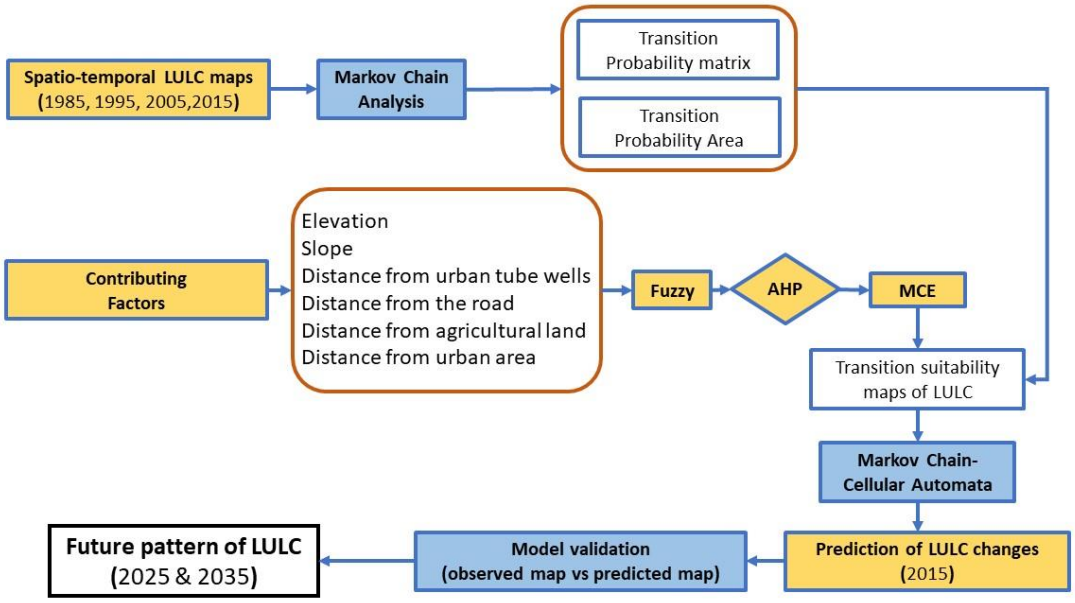

Figure 3.10 Workflow showing steps for predicting LULC change patterns in Tabuk

The following section briefly explains the integrated Markov chain (MC) and cellular automata (CA) model used in this work.

3.2.2.1 Land use modelling

The integration model of MC and CA was used to simulate land use change from 2015 to 2025 and 2035 covering a period of 20 years using TerrSet modelling software. The MC is an empirical/statistical stochastic model to estimate LULC change probability of occurrence from one state to another between time *t1* and *t2*

using transition matrices (Eastman 2009). According to Tang et al. (2007), the simple matrix in eq. 4 can calculate the entire landscape spatial transition model as:

$$N_{t+1} = N_t \times P_{ij} \quad \text{(eq. 4)}$$

where N_{t+1} represents the state of the land-use at times $t + 1$ and time t, respectively. P_{ij} is a square matrix, which cell P_{ij} is the transition probability in a state from landscape i to j during times t and $t+1$.

Transition probability is calculated as follows:

$$P = (P_{ij}) = \begin{vmatrix} P_{11} & P_{12} & \cdots P_{1n} \\ P_{21} & P_{22} & \cdots P_{2n} \\ \cdots & \cdots & \cdots \\ P_{1n} & P_{2n} & \cdots P_{nn} \end{vmatrix} \quad \text{(eq. 5)}$$

where, P is the transition probability, P_n is the state probability of any time, Pij is the probability of change from current state (i) to another state (j) in next time t (Guan et al. 2008) which has to meet the following condition:

$$0 \leq P_{ij} \leq 1 \mid (i, j = 1, 2, 3, \ldots, n) \quad \text{(eq. 6)}$$

where a probability near '0' represents low transition and a probability near '1' represents a high transition.

The MC model generates transition probabilities, transition area matrices, and a set of conditional probability images (Eastman 2016). The transition probabilities determine the probability of each land cover class being converted into another class, while transition area matrices represent the number of pixels that are likely to change from one class to another class. Conditional probability images report the probability that each land cover type would be converted at each pixel after the specified number of time units (Eastman 2016). In this research, the MC model was used to compute two transition matrices from LULC maps of 1985, 1995, 2005, and 2015.

Datasets were selected at 10-year intervals. During the calibration phase, the 1985 LULC data was used to initialise the model. A background area was assigned a value of 0.0, and the proportional error was defined as 0.6 based on the OBIA overall accuracy of LULC classified maps. The MC model is ideal for describing and quantifying land use change and does not consider the spatial characteristics of the patterns of land use when predicting future change (Muller and Middleton 1994; Sang et al. 2011). Spatial characteristics were added to land use modelling using CA (Eastman 2016). There are four elements within the CA model: cell space, cell states, transition rules, and time steps (White and Engelen 2000). This helps integrate the MCCA model to incorporate neighbourhood effects into future predictions.

The MCCA model includes information on how LULC change has occurred, or would occur, and where the change has taken place spatially. The MCCA consists of four elements: 1) multi-temporal maps, essentially a land cover image; 2) a transition function, which refers to Markov transition area; 3) transition suitability maps; and 4) simulated future land use change maps (White and Engelen 2000). Prior to the use of the MCCA model, transition suitability maps were generated for each LULC type

3.2.2.2 Suitability criteria

Information on land-use change is required to provide an understanding of the interaction between environmental systems, and biophysical and geophysical factors that drive growth. Determining driving factors used in the prediction of agriculture and urban expansion is, therefore, an essential step in developing the MCCA model (Clarke et al. 1996). In this study, suitability maps were created using specific factors that are affecting and driving urban and agriculture growth based on data availability. Available data on the factors chosen for analysis were collected and processed to generate the transition suitability maps of urban and agriculture classes individually according to experts' knowledge (personal communications with the Ministries of Agriculture and Water in Tabuk city).

These factors are generally continuous in nature (e.g., slope), which indicate relative suitability of certain areas (Eastman 2016).

Five factors consisting of two biophysical elements (elevation and slope) and three proximity elements (distance from tube wells, distance from roads, and distance from existing agriculture and urban areas) were considered in this study (Figure 3.11). The following five factors were considered as follows for urban growth in Tabuk:

1. Distance from agricultural and urban tube wells: location of urban and agricultural tube wells for 1995, 2005 and 2015 were converted into a shape file;
2. Distance from roads: road data for 1995 and 2005 were digitised in GIS. Topographic maps and high-resolution images were also used for validation at this stage;
3. Distance from agricultural land and urban areas: agricultural land and urban areas were extracted from classified LULC maps; and
4. Elevation and slope: elevation was calculated using a 15m digital elevation model (DEM), and the slope of the study area was calculated (as a percentage) from DEM data.

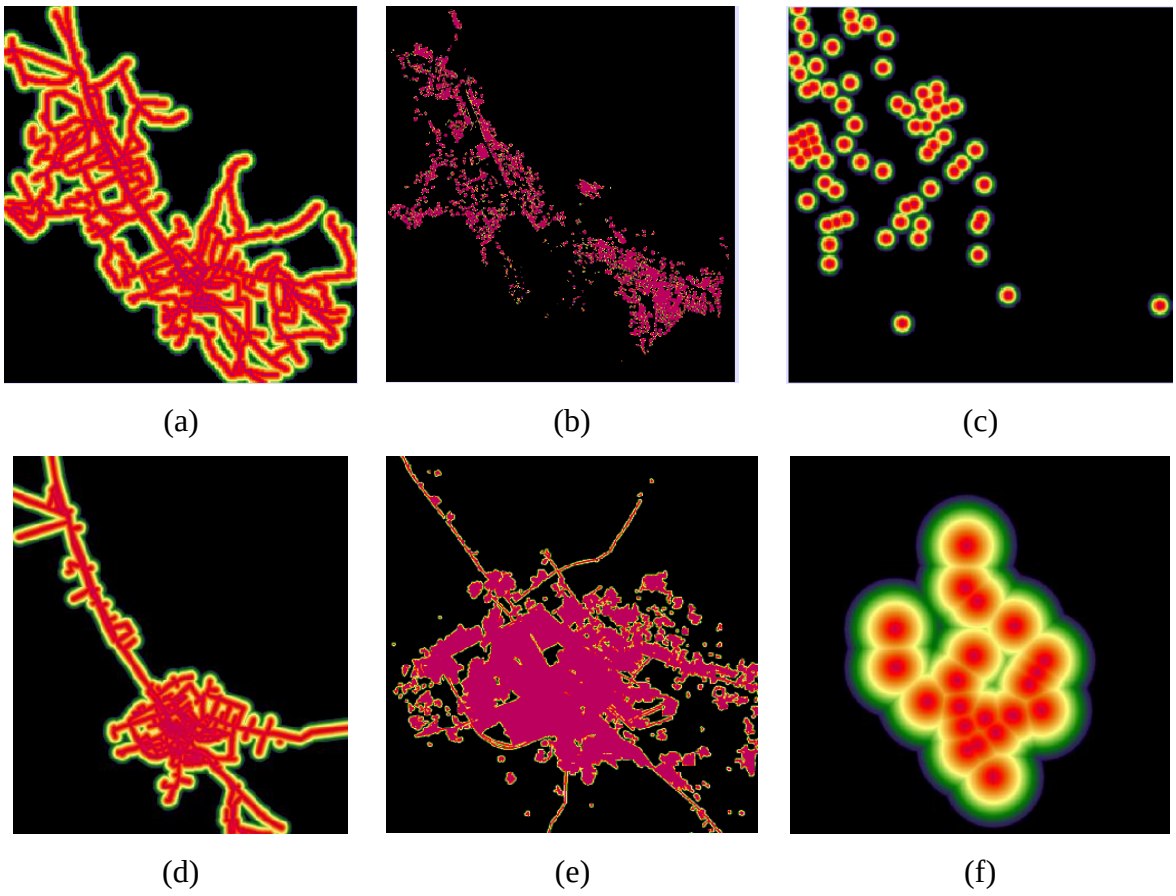

Figure 3.11 Proximity factors considered in this study: (a) distance from road to agricultural area; (b) distance from existing agricultural area; (c) distance from agricultural well; (d) distance from road to urban area; (e) distance from existing urban area; and (f) distance from urban well

A fuzzy membership function (FMF) was applied to assess the possibility of the suitable locations of biophysical and proximity factors considered. The FMF evaluated the possibility of each pixel changing from one class in the past to a new class in the future. FMF is characterised by a fuzzy membership grade that ranges from 0.0 (non-membership) to 1.0 (complete membership) (Eastman 2016). In this study, several FMF function types were used to investigate the effect of each factor including sigmoidal, J-shaped, and linear (Table 3.9).

The selection of the fuzzy function was based on a visual analysis considering the current state of agricultural and urban growth. For example, as shown in Table 3.8, the values ascribed to slope were set between ‘0’ and ‘40’. Flat areas attract more agricultural and urban growth while areas with high slope experience minimal or no growth. A higher value in slope and elevation would indicate decreasing suitability (Murayama 2012).

A similar assumption was applied to distance from roads, distance from existing urban, and distance from an urban tube well (Table 3.9).

Table 3.9 Fuzzy parameters for factors driving urban and agricultural growth

Factors	**Function shape**	**Function type**	**Control points**
Distance from urban well	Monotonically decreasing	J-shaped	0-250
Distance from road	Monotonically decreasing	J-shaped	0-50
Distance from existing urban area	Monotonically decreasing	Linear	0-100
Elevation	Monotonically decreasing	Sigmoidal	0-800
Slope	Monotonically decreasing	Sigmoidal	0-40
Distance from agricultural well	Monotonically decreasing	J-shaped	0-250
Distance from existing agricultural land	Monotonically decreasing	Linear	0-400

The FMF also standardised the values by re-scaling driver maps into the range from 0 to 255, where '0' indicated least suitability, and '255' indicated higher suitability. These factors were then weighted using the analytical hierarchy process (AHP) based on their relative importance for urban and agricultural growth (Satay 1980; Eastman 2016). The weight of each factor was developed from a series of pairwise comparisons. A pairwise comparison is a rating of the relative importance of two factors related to the suitability for agriculture and urbanisation (Murayama 2012). The factors weight is calculated from the pairwise comparison. The consistency ratio (CR) of the matrix were derived as shown in Table 3.9. The CR of the overall weighting factor for each period in this study was within a satisfactory level (Eastman 2016) (Tables 3.10 and 3.11). A detailed description of the pairwise comparison method can be found in (Satay 1980).

Table 3.10 Relative weights for each factor of urban growth

	Relative weight – urban growth		
Factors	**1995**	**2005**	**2015**
Distance from well	0.1941	0.1267	0.1522
Distance from road	0.1941	0.1573	0.1965
Distance from area	0.1609	0.1922	0.1672
DEM	0.2566	0.2468	0.2624
SLOPE	0.1941	0.2770	0.2217
Total	1	1	1
Consistency ratio	0.03	0.05	0.04

Table 3.11 Relative weights for each factor of agricultural growth

	Relative weight – agricultural growth		
Factors	**1995**	**2005**	**2015**
Distance from well	0.1463	0.1962	0.1492
Distance from road	0.2251	0.1487	0.2230
Distance from area	0.2347	0.2254	0.1452
DEM	01463	0.1708	0.2623
SLOPE	0.2476	0.2589	0.2203
Total	1	1	1
Consistency ratio	0.05	0.02	0.05

Multi-criteria evaluation (MCE) is a decision support tool that enables suitable locations for urban and agriculture growth to be determined based on several criteria (Eastman 2016). MCE requires two inputs: 1) extracted weight factors, and 2) constraint maps. Using a boolean intersection method (BIM), constraint maps were generated for 1995, 2005 and 2015 (Figure 3.12). The maps record a value of ‘0’ for areas where development was excluded, and ‘1’ for areas where development was permitted.

1995 **2005** **2015**

(a)

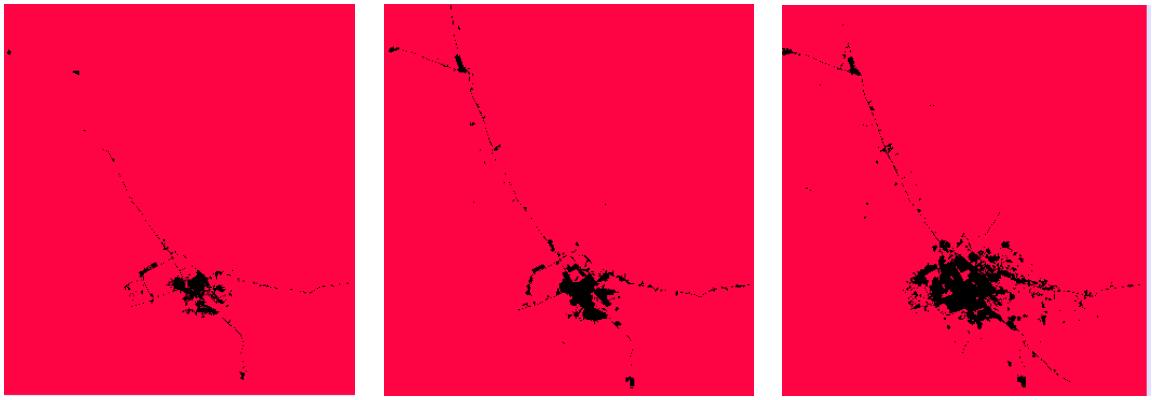

1995 **2005** **2015**

(b)

Figure 3.12 Constraint maps for 1995, 2005, and 2015 for (a) agricultural growth (in black); and (b) for urban growth (in black)

MCE was then employed by using the weighted linear combination (WLC) technique. Suitability maps for agricultural and urban classes using the five criteria were generated individually. The MCE method was utilised for agricultural and urban land uses. The suitability maps for other land cover types (i.e., barren land and water) were based on the spatial distribution of each land cover type. Each type was assigned a weight (‘1’ for suitable sites, and ‘0’ for non-suitable sites) to obtain a final suitability map for each land cover type.

Spatial characteristics were added to the urban land use modelling using CA (Eastman 2016). As mentioned earlier, there are four elements within the CA model: cell space, cell states, transition rules, and time steps (White and Engelen 2000). The use of this type of modelling added a spatial dimension to the final product and provided information on the likely distribution of transitions to the Markov chain analysis. Observed urban and agricultural growth between 2005 and 2015 was used to test the model. The maps developed from the modelling were compared with observed 2005 and 2015 land use maps.

Three major steps were followed in the modelling process. The first step was to determine the probability matrices and transition rules between the two-past dates 1985 and 1995 and use MC to predict the probabilities of change for the next date 2005. The second step combined the MC and CA models to determine the spatial pattern of land use change at the next date (2005) based on the CA contiguity filter. The filter allowed land use cells to grow out to contiguous suitable areas based on neighbour cells and its proximity to existing areas with the use of suitability maps. Finally, the results were compared with the actual maps for the year 2005. The LULC area of 1995 was used as the basis to predict LULC changes for the year 2005. Markov transition areas that were created from the Markov chain modelling of 1985 and 1995 were used in association with transition suitability data for 1995. The predicted land use maps were then integrated using a multi-objective land allocation (MOLA) procedure. This procedure worked by dividing the transition areas with the number of iterations. The MOLA procedure helped to resolve the land allocation conflict within each time step. The MOLA procedure determines a compromise solution based on the information from a set of suitability maps, one for each objective (Eastman 2016).

The outputs of each MOLA procedure were overlaid to produce the prediction for the new LULC maps at the end of each iteration. Using the CA contiguity filter the suitability of each pixel for the LULC classes was weighted. In this research, a 5×5 contiguity filter was chosen for the CA model to define the neighbourhood rules as shown in eq. 7. This ensures that changes are not random (Eastman 2003).

Previous works indicated that the use of a 5×5 contiguity filter results in a more accurate prediction (Araya and Cabral 2010, Sang et al. 2011, Mondal et al. 2012, Halmy et al. 2015). The higher the number of pixels in a class of land cover in the neighbourhood, the greater the value of suitability for this land cover.

$$Window\ size = \begin{bmatrix} 0 & 0 & 1 & 0 & 0 \\ 0 & 1 & 1 & 1 & 0 \\ 1 & 1 & 1 & 1 & 1 \\ 0 & 1 & 1 & 1 & 0 \\ 0 & 0 & 1 & 0 & 0 \end{bmatrix} \quad \text{(eq. 7)}$$

A similar process was applied to predict urban growth in 2015.

3.2.2.3 Model validation

Actual and predicted LULC maps for 2015 were compared statistically using the quantity and allocation disagreement method (Pontius 2002), which measures the agreement between prediction and actual maps. Seven agreement and disagreement components used in the method are agreement due to chance, agreement due to quantity, agreement due to location at the stratified level, agreement due to location at the grid cell level, disagreement due to location at the grid cell level, disagreement due to location at the stratified level, and disagreement due to quantity (Eastman 2016). The model also calculates Kappa index of agreement (KIA) and three more useful variants of the KIA, such as Kappa for no information (Kno), Kappa for grid-cell level location (KLocation), and Kappa for stratum-level location (KLocationStrata). A detailed description of each expression is provided by Pontius and Suedmeyer (2004).

Based on a successful validation with high agreement, the MCCA model was judged suitable for modelling agricultural and urban growth in 2025 and 2035. The 2015 observed map was used as a base map. The transition probability matrix for 2005-2015, and the associated suitability maps, were used to predict agricultural and urban growth in 2025. The same process was applied to predict agricultural and urban growth in 2035 using the 2025 as a base year and the transition probability matrix for 2005-2015.

3.2.3 Estimating Tabuk water requirements

Estimating water demand in agricultural land (for crops) and for urban use was calculated for years 1995, 2005 and 2015 to provide an overall indication of non-renewable fossil groundwater consumption for Tabuk. The analysis relied on estimates of agricultural water use from ET modelling and urban water use from urban well and discharge to estimate Tabuk's water use demand.

3.2.3.1 Net irrigation requirements (NIR)

Knowledge of crop irrigation requirements for most crops grown in Tabuk is limited. To quantify net irrigation requirements, evapotranspiration, crop evapotranspiration (crop water requirement), effective rainfall, irrigated land area and irrigation efficiency were estimated. This study assumed that irrigation water was available throughout the growing season. NIR is calculated by the following equation:

$$NIR = ET_c \times Crop\ area - Eff_{rain} \quad \text{(eq. 8)}$$

where,

NIR is net irrigation requirement (m^3/area/period)

ET_c is crop reference evapotranspiration (mm/period)

Crop area is irrigated land in (km^2)

Eff_{rain} is effective rainfall (mm/period)

To estimate the net irrigation requirements for all crops in Tabuk, reference crop evapotranspiration, crop evapotranspiration, and effective rainfall were calculated as follow.

3.2.3.1.1 Calculating evapotranspiration (ET)

Evapotranspiration (ET) has been considered one of the most promising approaches for estimating agricultural water requirements in a given area (Mattar et al. 2016).

With several methods that exist to measure ET value for a given climate data (as discussed in Chapter 2), Penman-Monteith (Allen et al. 1998) is the most commonly used, under various climatic conditions. The model, however, requires several climate parameters such as solar radiation and soil information. For many developing countries like Saudi Arabia, weather data needed to compute Penman-Monteith in most Saudi's regions, are often incomplete, inconsistent, and/or not available. This considers as limitation of using Penman-Monteith to compute the ET in this study.

Based on available climate data and a reasonable ET value obtained in preliminary analyses, the empirical Ivanov model developed by Romanenko (1961), was adopted over Kharrufa (1985), Schendel (1967), and Hargreaves and Samani's (1985) models. The empirical Ivanov model has proved to be robust and straightforward and has been widely used in various climate settings (Tabari et al. 2013; Djaman et al. 2015; Djaman et al. 2017; Muhammad et al. 2019). The Ivanov model requires simple calculations using the most readily available climate data, daily mean temperature (°C) and relative humidity (%) and were used to estimate evapotranspiration rates for the 30-year period.

Ivanov ET model is expressed as:

$$ET = 0.00006\,(25 + T_{mean})^2\,(100 - RH) \quad \text{(eq. 9)}$$

a. Estimating crop evapotranspiration ET_c

Estimation of crop evapotranspiration (ET_c) is a product of crop coefficient (K_c) and Evapotranspiration as follows:

$$ET_c = K_c \times ET \quad \text{(eq. 10)}$$

where,

ET_c is evapotranspiration water requirement (mm/day)

K_c is crop coefficient which varies by crop development stage, and growing season

ET is reference crop evapotranspiration (mm/day)

The calculation procedure for K_c consists of three steps: 1) identifying crop growth stages (initial, mid, and late development); 2) determining the length of growth stages; and 3) defining corresponding K_c coefficients for each crop growth stage.

Three distinct growth phases related to the three different crop coefficients (K_c), and the normalised ET value over the full growth phase of the crop can be equated as follows:

$$ET_c = \frac{(K_{c1} \times ET + K_{c2} \times ET + K_{c3} \times ET)}{3} \quad \text{(eq. 11)}$$

Crop evapotranspiration assumed that the crops were free from disease, and well-fertilised in a large field under non-stressed or restricted soil and water conditions (Allen et al. 1998). The daily ETc values were first calculated for each crop, and then aggregated to annual and monthly values.

3.2.3.1.2 Effective rainfall analysis for Tabuk

Effective rainfall analysis for Tabuk was estimated based on a probability analysis using and equation from Smith (1992). The monthly and annual estimated probability of the dependable level of rainfall exceedance for Tabuk corresponded to wet (20%), average (50%), and dry (80%) using following steps.

The total rainfall amounts of Tabuk was tabulated. Total rainfall data were arranged in descending order, then the plotting position was tabulated as:

$$F_a = \frac{M}{1+N} \times 100 \quad \text{(eq. 12)}$$

where,

F_a is plotting position (%)

M is rank number

N is number of records.

The dry value of 80% was used as articulated by Smith (1992) for arid areas where most rainfall values were below 100 mm/month. Given a sprinkler irrigation system is used in Tabuk, the irrigation efficiency was adjusted to 70% following guidance from Doorenbos and Pruitt (1977). Accumulated K_c was used to estimate the total irrigation water requirements, and it was assumed that the proportion of the irrigated area was the same for each crop.

3.2.3.2 Groundwater modelling and drawdown effect

The drawdown effect of groundwater in Tabuk city is calculated based on Theis groundwater model (Theis 1935). The model assumes a fully penetrating well in an unconfined homogeneous isotropic aquifer. The flow of water from the well is considered as unsteady and follows radial principle of a cylindrical equation. A well is assumed to be located at the centre of the aquifer, having a constant discharge rate (Q). The static water level (h_0) is considered as an initial condition towards the solution of Theis formulation, which remains uniform over the aquifer domain. The hydraulic head is considered to be undisturbed and is equivalent to the initial static level h_0 as a boundary condition. According to Theis' assumptions, the spatial coordinates are defined such that the head lies in the spatial xy-plane, whereas the vertical axis z specifies the height of the head which dropped with respect to the ideal horizontal flow conditions (Wang et al. 2015).

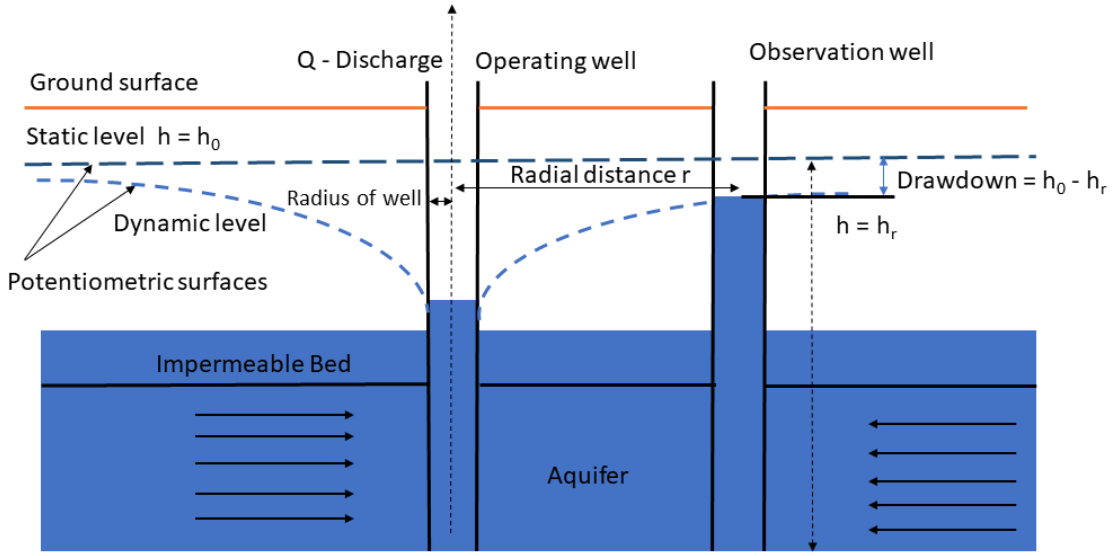

Figure 3.13 A single pumping fully penetrated well and an observation well in an ideal setting of aquifer as described by Theis (Source: Wang et al. 2015)

Figure 3.13 shows the features setting by Theis (1935), of an ideal aquifer, with a fully penetrating pumping well. The position of the potentiometric surfaces i.e., initial and during pumping are represented by dashed lines. The drawdown effect of the aquifer is a function of radial and saturated flow (Wang et al. 2015) as shown and formulated in the equation (eq. 13). The reduction in the piezometric surface with respect to its initial state is represented by aquifer drawdown (S) and is given by a generalised equation as follows:

$$S = h_0 - h_r(x, y, t) \quad \text{(eq. 13)}$$

where,

S is the aquifer drawdown rate

h_0 is the static water level

h_r is the dynamic water level

The Theis (1935) solution (eq. 14) can be extended to dealing with conditions where the constant pumping rate and the operating well assumptions are considered, as follows:

$$S(x, y, t) = \sum_{i=1}^{n} \frac{Q}{4\pi T} W \frac{St\, r^2}{4T\, t} \quad \text{(eq. 14)}$$

where,

Q is the well discharge rate

T is transmitivity constant

St is storativity of aquifer

r is the distance between wells

W is the well function

Groundwater drawdown in the aquifer occur as a response to spatially distributed functioning wells. In the two dimensional (x,y) extent of the aquifer, the drawdown at any observation point (x,y) and time (t) due to a well field with a number (n) of operating wells, each one with a discharge rate (Q), and an operating starting time (t_i) can be calculated as:

$$S(x,y,t) = \sum_{i=1}^{n} \frac{Q}{4\pi T} W \frac{St\, r_i^2}{4T\, t-t_i} \quad \text{(eq. 15)}$$

where,

i is the well number

r_i is the distance of the observation point (x,y) from well i

x_i, y_i is the well coordinates

$$r_i = \sqrt{(x-x_i)^2 + (y-y_i)^2} \quad \text{(eq. 16)}$$

3.2.4 Urban water use

To quantify the water consumption of urban areas a preliminary assessment was conducted based on all data found from 1995 to 2015. By calculating hourly and daily water abstraction (discharge) for Tabuk, the urban water quantity use was estimated. This process allows for a rough analysis of past and current water demands for the urban areas of Tabuk. Assessment of water use and demand to provide a rough indication was critical given groundwater is the main water source for the city's urban requirements.

3. 3 Chapter summary

This chapter started by providing a general overview of Tabuk covering its geographical location, topography, and climate. Fundamental information on the datasets used in this research, including primary remote sensing data and secondary data including climate, crop, and water data were also described.

In the second part of the chapter, the analytical techniques used for each of the research components were explained in three subsections. The methodology used to determine Tabuk city's spatio-temporal pattern was discussed in the first subsection. More specifically the steps described covered: image classification of Landsat images using OBIA, accuracy assessment using the error matrix method, and LULC change detection technique 'from-to' during the period 1985-2015. To define growth types of urban areas in Tabuk city, UGAT was utilised and the direction of urban expansion was identified.

Methods used to predict LULC for 2025 and 2035 were discussed in the second subsection of this chapter. The Markov chain (MC) method was used on LULC maps for the period 1985-2015 to establish transition probability matrices between LULC categories. Cellular automata (CA) modelling was used to add spatial characteristics and model neighbourhood interactions. The integration model of MCCA was used to predict LULC in 2025 and 2035, respectively.

The third subsection outlined the methodology used to historically estimate water demand for agricultural land and urban areas of Tabuk city. Agricultural irrigation requirements were estimated using evapotranspiration values based on climate data, and for urban demand the estimation was based on urban well production. Several steps were applied including estimation of evapotranspiration, crop evapotranspiration, the crop coefficient of each crop, crop water requirements, and net irrigation requirements over agricultural land changes between 1985-2015. The dataset of urban wells including groundwater pumping, well working hours, and the year wells were opened was utilised to roughly estimate water use in the urban area of Tabuk city.

4 Results

The significant change in LULC seen in Tabuk city due to the expansion of agricultural and urban land areas over a 30-year period (1985-2015), has increased the demand for non-renewable groundwater in the city. This chapter presents the results, analysis, and findings on LULC change and water demands modelled on available historical data and predictions of future expansion of agricultural and urban lands. Model based calculations were performed to estimate the net irrigations water requirements for agricultural lands using climate data from weather station. Groundwater levels, drawdown effect, and net flow are calculated for existing urban areas (using the well dataset) and are predicted for future land use.

4. 1 Spatio-temporal LULC changes between 1985 and 2015

4.1.1 Object-based image analysis

LULC maps generated show a significant increase in the pattern of LULC change of Tabuk over a 30-year period from 1985 to 2015 (Figure 4.1). Over the 30 years, a total of 731 km^2 (17.30% of the study area) of barren land was converted to agricultural and urban areas (Table 4.1). The comparison maps of LULC change detection to understand the spatial and temporal pattern of change can be seen in Figure 4.1.

Based on the OBIA classification (Table 4.1), the main land cover class for the classified 1985 map was a barren land with areas of 4051 km^2 (96% of the total study area). The other LULC categories of agricultural land and urban area covered areas of 112 km^2 (3%) and 48 km^2 (1.14%), respectively. By 2015, Tabuk experienced a dramatic increase in agricultural land by 414%, adding 464 km^2, to become 576 km^2 (14% of the study area). Urban areas increased by 556% over the same period, adding 267 km^2, to become 315 km^2 (7.48% of the study area). Bare land remains the dominant LULC category with 3320 km^2 (78%) in 2015 (Table 4.1).

Gain and loss of barren land, agricultural land, and urban area land-use types, as well as their contribution to net change, were quantified for each epoch (Table 4.2).
The most notable change detected for agricultural land expansion from 358 km^2 to 528 km^2 was during the 2000-2005 (Table 4.2), a total of 170.5 km^2 (60%) (Table 4.1). The rate of growth of agricultural land was also high between 1995-2000, a total of 131 km^2 (58%) (Table 4.2 and Table 4.3).

Until the period 2005-2009, agricultural land expansion was seen to increase at a greater rate than urban land (Table 4.2). While urban land growth was increasing over the 30-year period, the peak in the rate of growth of urban areas was observed in the period 2009-2015 (Table 4.2). The most significant increase of urban area, from 204 km^2 to 315 km^2 (111 km^2), was observed between 2009-2015, which is a 25% increase in area (Tables 4.2 and 4.3). The generated LULC maps of Tabuk (Figure 4.1) show that urban areas encroached into agricultural land during this period.

Table 4.1 Area statistics of LULC change (km^2) and class percentages (%), 1985-2015

Year	Land cover/ use Categories					
	Barren land		Agricultural land		Urban area	
	Area (km^2)	%	Area (km^2)	%	Area (km^2)	%
1985	4051	96	112.5	2.67	48.3	1.14
1990	3995	94	152.3	3.61	64.4	1.52
1995	3897	92	226.7	5.38	88.1	2.09
2000	3732	88	357.8	8.49	122.1	2.89
2005	3539	84	528.3	12.5	145.0	3.44
2009	3484	82	524.4	12.4	203.6	4.83
2015	3320	78	576.6	13.6	315.1	7.48

Table 4.2 Area gain/loss of LULC classes (km^2) across six time periods in Tabuk

LULC classes	Year						Total
	1985-1990	1990-1995	1995-2000	2000-2005	2005-2009	2009-2015	
Barren land	-55.87	-98.22	-164.96	-193.43	-54.84	-163.61	-730.92
Agriculture	39.78	74.43	131.03	170.50	-3.85	52.23	464.12
Urban area	16.08	23.78	33.94	22.93	58.63	111.44	266.79

Table 4.3 Total of change/unchanged (%) for each LULC classes in Tabuk

	LULC class	Year (From To)						
		1985-1990	1990-1995	1995-2000	2000-2005	2005-2009	2009-2015	1985-2015
No change	Barren land	98	97	94	90	87	85.2	97
	Agriculture	1	2	4	7	10	10.3	1.35
	Urban area	1	1	2	3	3	4.4	1
	Total	100	100	100	100	100	100	100
Change	To barren land	45	37	32	31	47	37	11
	To Agriculture	44	52	58	60	35	38	61
	To urban area	11	11	11	10	18	25	28
	Total	100	100	100	100	100	100	100

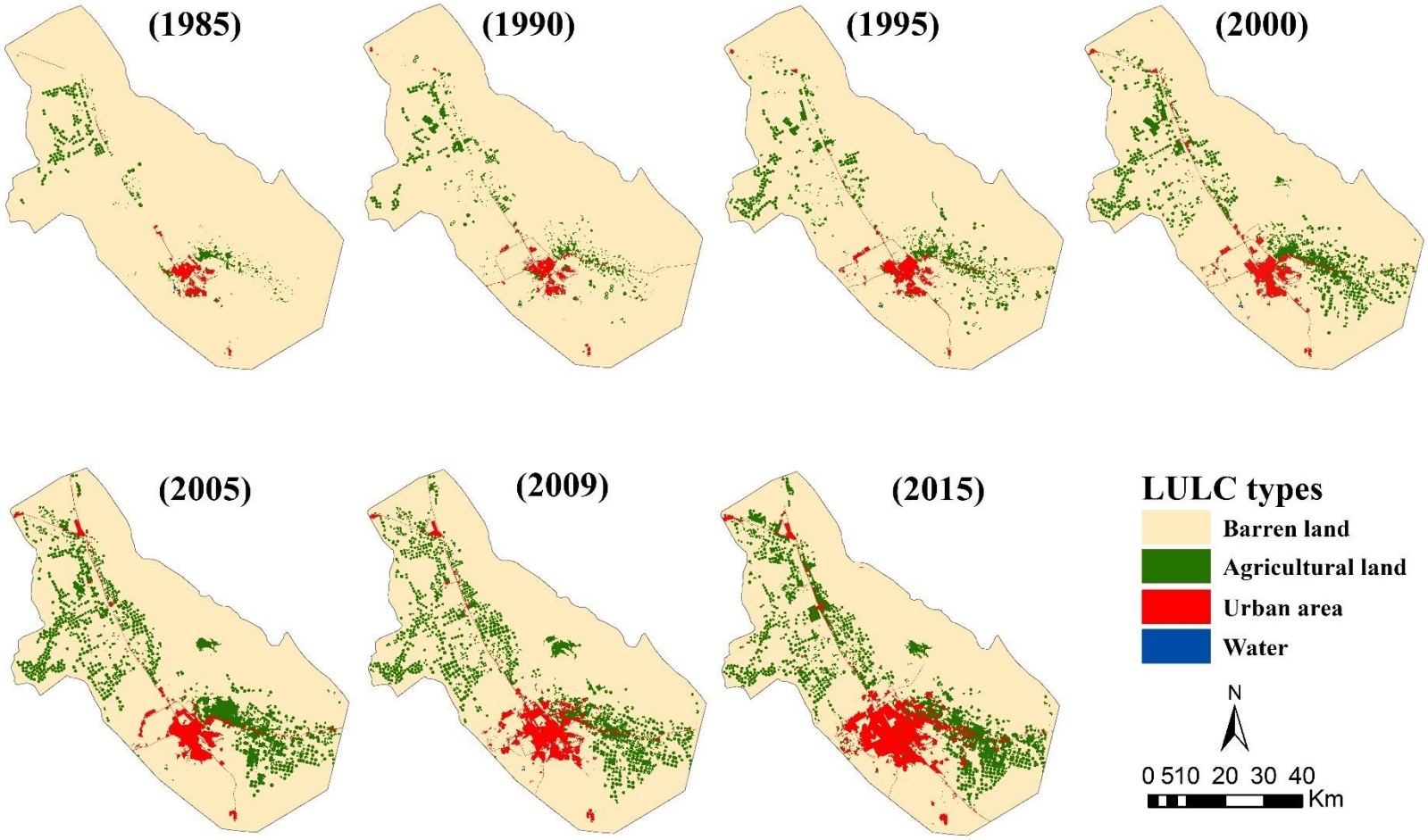

Figure 4.1 LULC maps of Tabuk between 1985 and 2015

4.1.2 Accuracy assessment

The accuracy of the classification results supports the effectiveness of using OBIA to generate land cover maps in the arid environment of Tabuk. Water accounted for less than 1% of the study area and was difficult to classify due to the medium resolution of Landsat imagery (i.e., 30 m resolution).

The overall accuracy for all years (1985-2015) was very high, ranging from 93% to 97% and a Kappa coefficient from 0.90 to 0.96 (Table 4.4), showing the strength of using the OBIA method for land use classification in an arid landscape. The precision of defined classes indicated by producers' and user's accuracy was above 81% for barren area, agricultural land, and urban area classes for each year (Appendix C).

Table 4.4 Classification accuracy and Kappa coefficients

Year	**Overall accuracy** (%)	**Kappa coefficient**
1985	94	0.91
1990	97	0.96
1995	94	0.91
2000	95	0.93
2005	96	0.94
2009	97	0.95
2015	93	0.90

The OBIA approach used in this study produced smooth classification results without the issue of mixed pixels. However, the accuracy of the results and visual interpretation showed the limitation of using OBIA in Landsat images when assessing the water class within the study area. Due to spatial resolution (30m) and the size of the object, misclassification occurred in the barren class even though this class had distinct spectral differences with water. Using a cost-effective medium resolution imagery still provided satisfactory OBIA classifications to answer the questions on LULC for accurate identification of agricultural and urban classes, without requiring additional expert analysis and computational time. The results provide detailed information on LULC changes that were previously unavailable for Tabuk city.

4.1.3 Spatial agricultural growth and direction between 1985 and 2015

Generally, the directional trends for agricultural growth between 1985 and 2015 were mainly toward the northwest and southeast of the study area (Figure 4.2) which was the north and southeast of Tabuk city central area. The existing city limits were to the south and south-west portions of Tabuk. Agricultural crops in the study area are predominantly cultivated under centre pivot irrigation systems. In 1985, intensive crop irrigation (represented as crop circles) was limited, with many small agricultural holdings evident, centred north of the city and in the outer north-western areas. By 2015, the smallholdings were intermingled with many large, intensively irrigated areas with the expansion mainly occurring northwest and southeast of Tabuk city. There was a marked increase in agricultural expansion for the periods 1985-1990 (44%), 1990-1995 (52%), 1995-2000 (58%), and 2000-2005 (60%) (Table 4.3). There was a slight reduction in agricultural land area between 2005-2009 (-1%), however, agricultural land expansion picked up again in 2009-2015 (38%) although the growth was slower than the previous periods 1985 to 2005 (Figure 4.2).

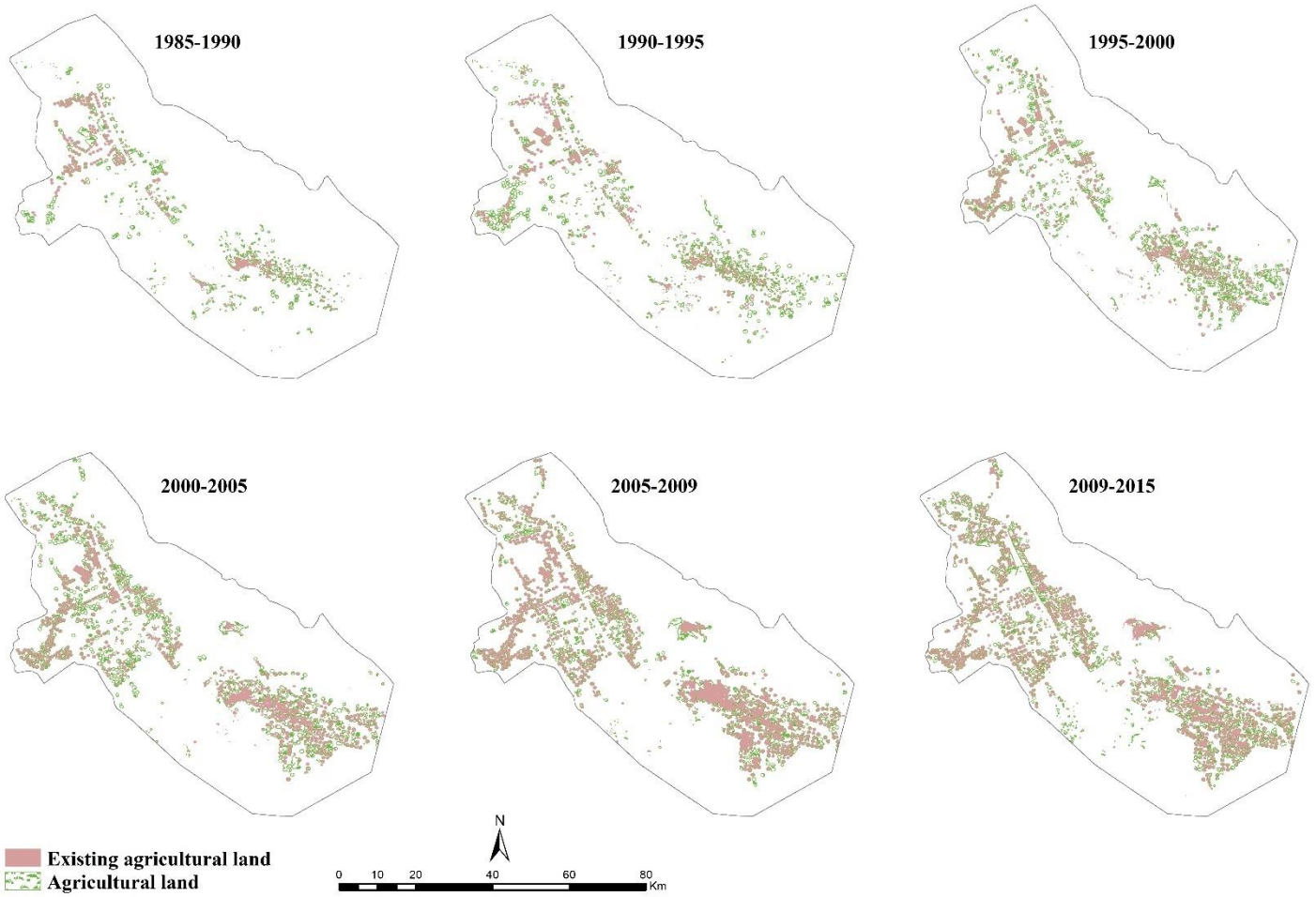

Figure 4.2 Increase in agricultural land in Tabuk between 1985-2015

4.1.4 Urban growth type and direction between 1985 and 2015

Three different growth types of Tabuk's urban expansion were identified, namely extension, infill, and leapfrog (Figure 4.3). The results indicate that the dominant type of urban growth for the period 1985-2015 was the extension type (Figure 4.3 and Table 4.5). For example, the contribution of the extension type accounted for 72% (389 km^2) growth of the total urban area between 1985 and 2015. Leapfrog growth type accounted for 17% (91 km^2) of Tabuk's urban development, and infill growth type accounted for only 11% (58 km^2) (Table 4.5). The extension growth type in Tabuk occurred primarily on the outer edges of the existing urban boundary, while the infill growth type occurred within the gaps surrounding the existing urban areas within the city centre (Figure 4.3). Leapfrog type growth happened on the outside of the urban boundary area (Figure 4.3). Most of the urban expansion in Tabuk between 1985 and 2015 was within buffer distances of 5-15km^2 from Tabuk city central. For each period, the extension urban growth type was consistently dominant (63-79%). Infill growth type peaked between 1990-1995 at 20% and only at 3% between 2005-2009. Leapfrog urban growth type was at maximum growth between 1995-2000 (25%) (Table 4.5).

The general direction of urban growth in Tabuk was towards the south, northwest and west between 1985 and 2015. The expansion was directed to the southeast and south of Tabuk central, with some new developments extended towards the west and northwest between 1985-1990 and 1990-1995 (Figure 4.3). During the period of greatest urban growth between 2009 and 2015, expansion was occurring in all directions with some emphasis on the northwest and western directions noticeable from 2005-2009.

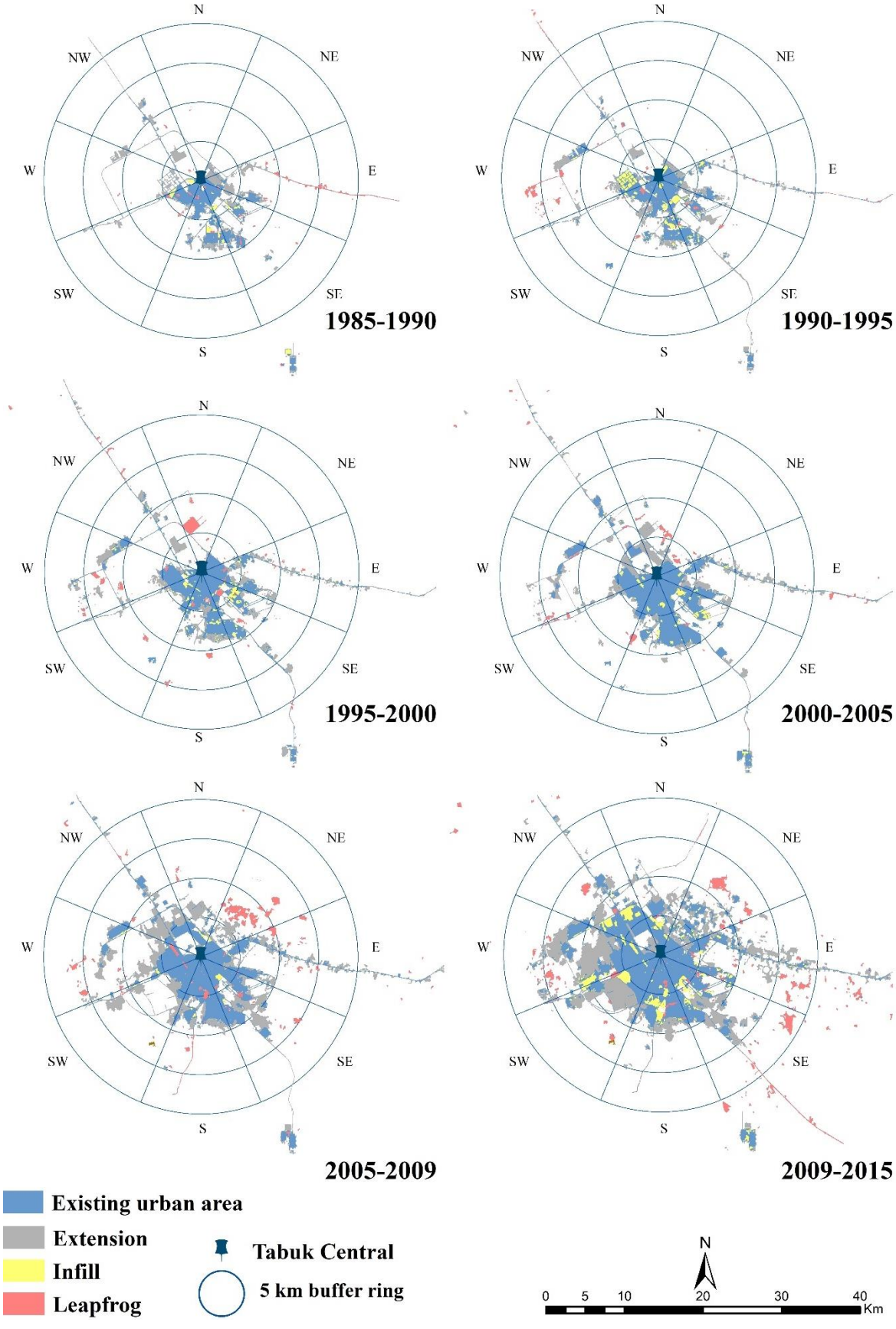

Figure 4.3 Urban growth types and direction, 1985–2015

Table 4.5 Urban growth types, 1985-2015

Period	Urban growth type (area in km^2)			Urban growth type (area in %)		
	Extension	Infill	Leapfrog	Extension	Infill	Leapfrog
1985-1990	31.64	4.22	7.33	73	10	17
1990-1995	31.28	9.73	8.73	63	20	18
1995-2000	41.99	6.98	16.09	65	11	25
2000-2005	58.96	7.49	8.82	78	10	12
2005-2009	91.97	3.96	19.97	79	3	17
2009-2015	133.19	25.68	30.47	70	14	16
Total	**389.04**	**58.07**	**91.41**	**72**	**11**	**17**

4.1.4.1 Population growth

Urban area expanded in line with population growth in the period 1985-2015 (Figure 4.4). Urban area expansion positively correlated with the increase in population size (r^2 = 0.94) (Figure 4.5), demonstrating a strong relationship between urban area expansion and population growth. The population of the study area increased 288% over the 30-year period, from 165,000 in 1985 to 657,000 people in 2015. Population growth rate was greatest during the period 1985-1990 (10%), 1990-1995 (6%) and 2009-2015 (6.2%). All other periods showed population growth rates between 2-3 %. Between 2000-2005 a drop in the relationship between urban area and population was observed (Figures 4.4 and 4.5). In this period the population was observed to have increased by 31% which was greater than the other periods studied.

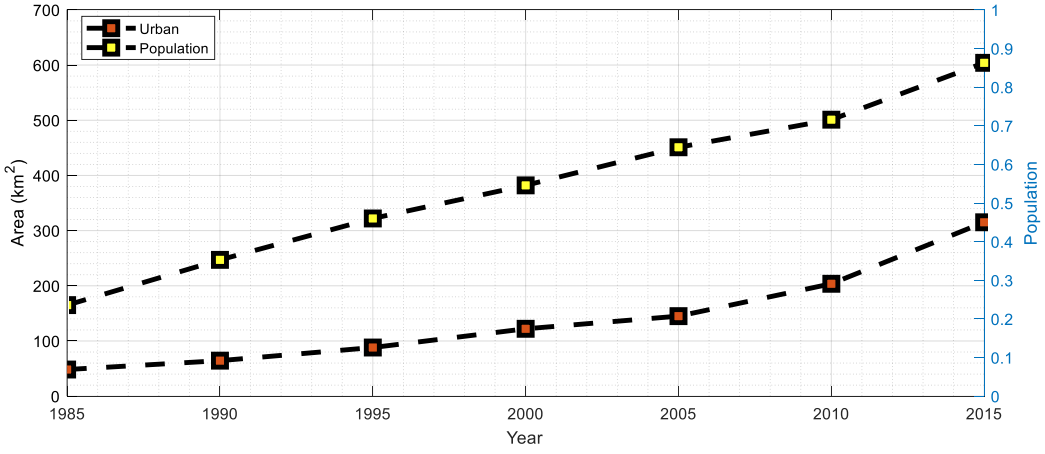

Figure 4.4 Urban area and population growth in Tabuk, 1985-2015

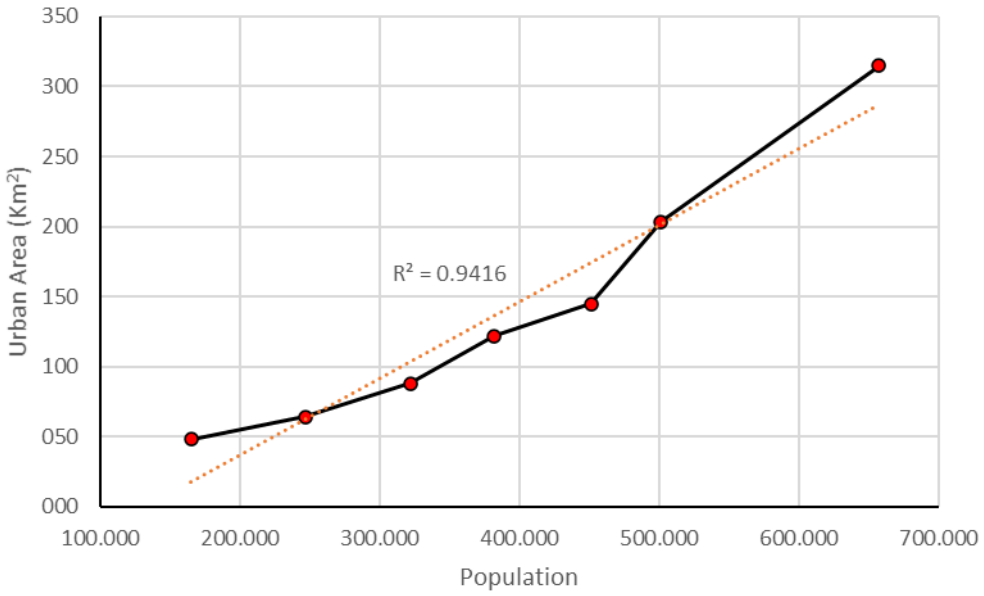

Figure 4.5 Relationship between urban area and total population

4. 2 Prediction of LULC

This section presents the results of the future land use prediction pattern change for both agricultural land and urban areas in Tabuk in 2025 and 2035, respectively.

4.2.1 Transition matrices

Transition probabilities of LULC based on Markov chain (MC) analysis for 1985-1995, 1995-2005, 2005-2015 and 2015-2025 (Table 4.6) consistently showed agricultural class changing to urban class as 4%, 6%, 6%, and 10% respectively. The probability of barren class transitioning to agricultural land class was 4%, 10%, 6%, and 10%, and barren to urban class was 1%, 2%, 5%, and 8%. In contrast, agricultural land class transitioning to barren land class probabilities were the highest at 54%, 27%, 27%, and 42% respectively. The water class was the smallest of the classes and predictably had the biggest impact for transition probability to change either to the barren land class (81%, 15%, 15%, and 26%), agricultural land class (20%, 5%, 18%, and 21%), or urban class (14%, 0%, 28%, and 36%).

Table 4.6 LULC transition probability matrices, 1985-2025

Year			**1995**		
	Class	Barren land	Urban area	Agricultural land	Water
1985	Barren land	0.9450	0.0111	0.0438	0.0001
	Urban area	0.1618	0.7856	0.0527	0.0000
	Agricultural land	0.5390	0.0447	0.4163	0.0000
	Water	0.8091	0.1380	0.0529	0.0000
			2005		
	Class	Barren land	Urban area	Agricultural land	Water
1995	Barren land	0.8888	0.0150	0.0963	0.0000
	Urban area	0.1504	0.8370	0.0126	0.0000
	Agricultural land	0.2730	0.0572	0.6695	0.0003
	Water	0.1509	0.0000	0.2000	0.6491
			2015		
	Class	Barren land	Urban area	Agricultural land	Water
2005	Barren land	0.8946	0.0455	0.0599	0.0000
	Urban area	0.0998	0.8436	0.0566	0.0000
	Agricultural land	0.2658	0.0595	0.6748	0.0000
	Water	0.1477	0.2795	0.1795	0.3932
			2025		
	Class	Barren land	Urban area	Agricultural land	Water
2015	Barren land	0.8207	0.0827	0.0965	0.0000
	Urban area	0.1885	0.7196	0.0919	0.0000
	Agricultural land	0.4230	0.1024	0.4746	0.0000
	Water	0.2658	0.3631	0.2164	0.1546

4.2.2 Model validation

The performance of the MCCA model was validated when comparing the simulated map against the actual map for 2015 (Figure 4.6), with the KIA, Kno, Klocation, KlocationStrata being 87%, 91%, 89% and 89%, respectively.

There was little difference between the actual and simulated maps of the study area as seen for agricultural land area (actual was 577 km^2 and simulated was 570 km^2) and urban area (actual was 315 km^2 and simulated was 313 km^2) (Figure 4.7), reinforcing a high degree of confidence in the simulation model used. Results from the MCCA model used to predicted land areas in 2015 indicate that the model can be used to simulate agriculture and urban growth for 2025 to 2035 with reasonable confidence.

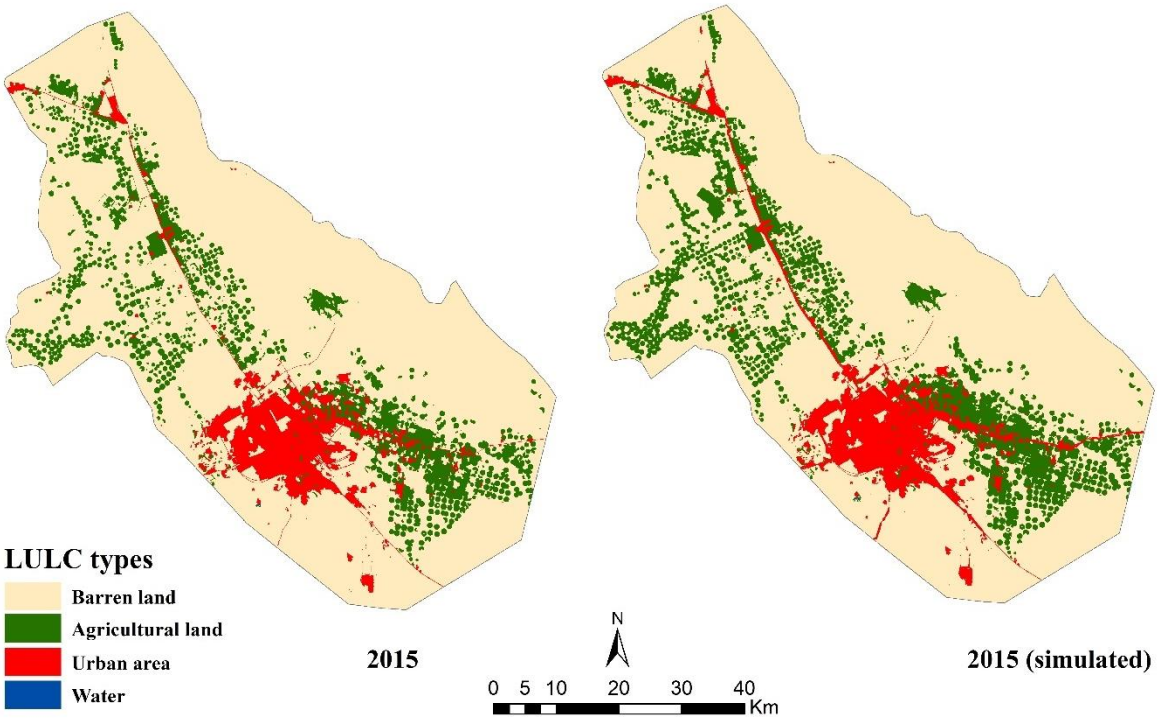

Figure 4.6 Comparison of the actual versus simulated LULC map, 2015

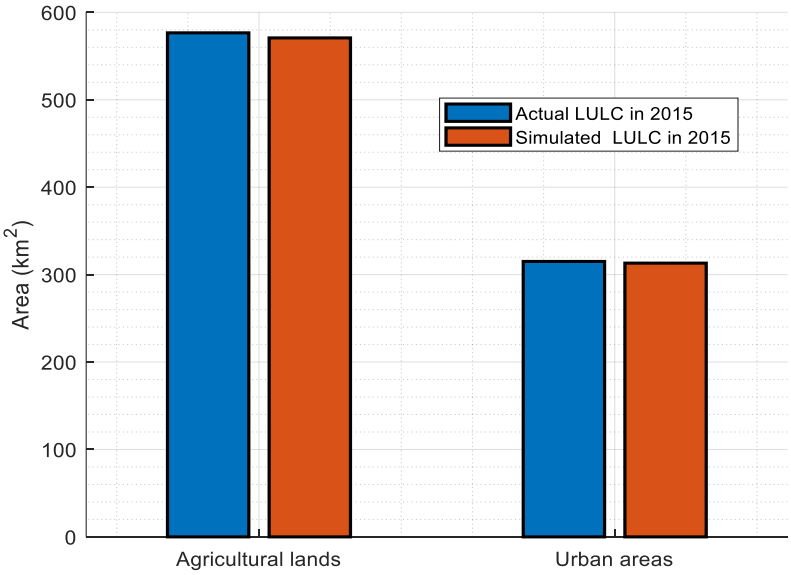

Figure 4.7 Area of actual versus simulated LULC (agricultural and urban), 2015

4.2.3 Tabuk future LULC pattern

Based on a study area of 4212 km^2, the MCCA model predicted an increase in agricultural land from 577 km^2 (14% of the study area) in 2015, to 606 km^2 (15% of the study area) in 2025, and 701 km^2 (17% of the study area) in 2035 (Table 4.7). Urban areas were predicted to increase from 315 km^2 (8% of the study area) in 2015, to 362 km^2 (9% of the study area) in 2025, and 453 km^2 (11% of the study area) in 2035 (Figure 4.8). Encroachment between agricultural land and urban area in Tabuk was evident when both land classes were in close proximity (Figure 4.8). Predicted increases in agricultural land and urban areas was at the expense of fragile barren land with a decrease in barren lands of approximately 76 km^2 and 187 km^2 in 2025 and 2035, respectively (Figure 4.8).

Table 4.7 Future agricultural and urban land area change in the study area up to 2035 simulated using MCCA model

Year			**Area change as gain (km^2 / %)**	
	2025	**2035**	**2015-2025**	**2015-2035**
Agricultural land **(km^2)**	606	701	30	125
Agricultural land **(%)**	15	17	5	22
Urban areas **(km^2)**	362	453	47	138
Urban areas **(%)**	9	11	15	44

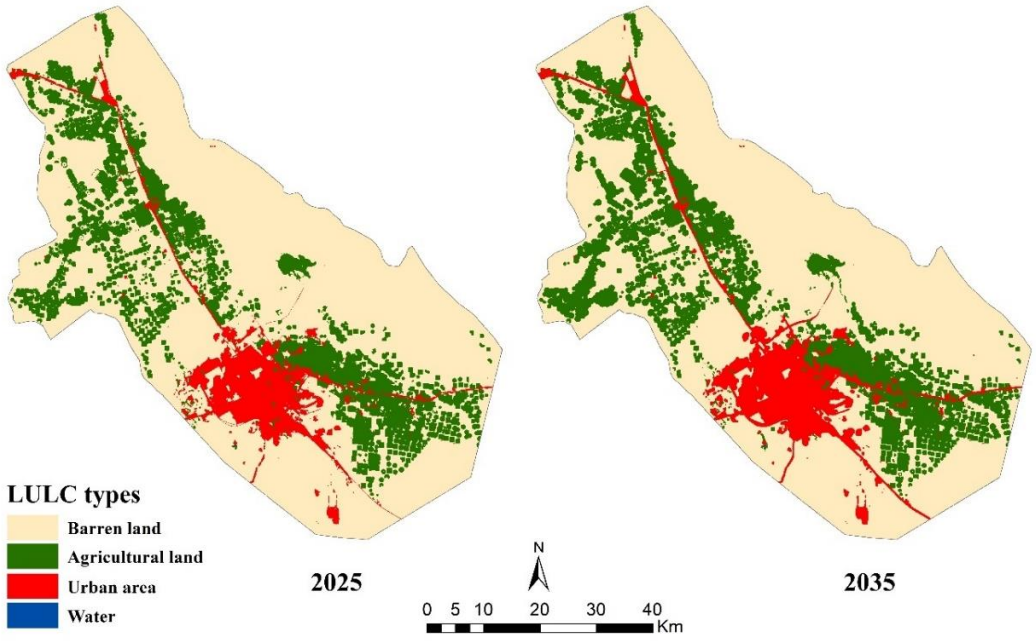

Figure 4.8 Simulated LULC of Tabuk, 2025 and 2035

4. 3 Agricultural and urban water demand

The combined total estimated water consumption for agricultural water (for crops) *and* urban water for 1995, 2005 and 2015 was $1.38x10^{10}$ m^3, $3.26x10^{10}$ m^3 and $4.36x10^{10}m^3$, respectively (Table 4.8). Due to the continuing increase in population, total annual urban water consumption in the study area rapidly increased from $0.57x10^7$ m^3 in 1995 to $3.24x10^7$ m^3 in 2005, and $4.93x10^7$ m^3 in 2015. The proportion of agricultural water consumption was largest during the period 1995-2015 (Table 4.8). Although urban water use was increasing rapidly, its proportion in the overall total water consumption of Tabuk was very small.

Estimated urban water consumption accounted for only a maximum of 0.13%, while agricultural demand exceeded 99% of all water use estimated for each of the three years (Table 4.8). All irrigation and urban water use were met by pumping groundwater from the Saq Aquifer.

The approach used to estimate the agricultural water consumption in this study provided critical insights on water consumption in Tabuk. The approach also helped to estimate historical CWR and NIR values and identify crops that consume more water than others.

Table 4.8 Overall agricultural and urban water consumption in Tabuk

Year	Estimated water use (m^3)			Percentage water use	
	Agricultural (x 10^{10})	**Urban (x 10^7)**	**Total (x 10^{10})**	**Agricultural**	**Urban**
1995	1.38	0.57	**1.38**	99.96	0.04
2005	3.26	3.24	**3.26**	99.89	0.11
2015	4.36	4.93	**4.36**	99.87	0.13

The results for each analytical component used for estimating agricultural crop water demand and urban water requirements are presented in the sections that follow.

4.3.1 Net irrigation requirements (NIR)

The total estimated yearly water demand for irrigated agricultural areas has increased significantly since 1985 ($0.14x10^{10}$ m^3) to 2015 ($4.36x10^{10}$ m^3) (Figure 4.9 and Table 4.9).

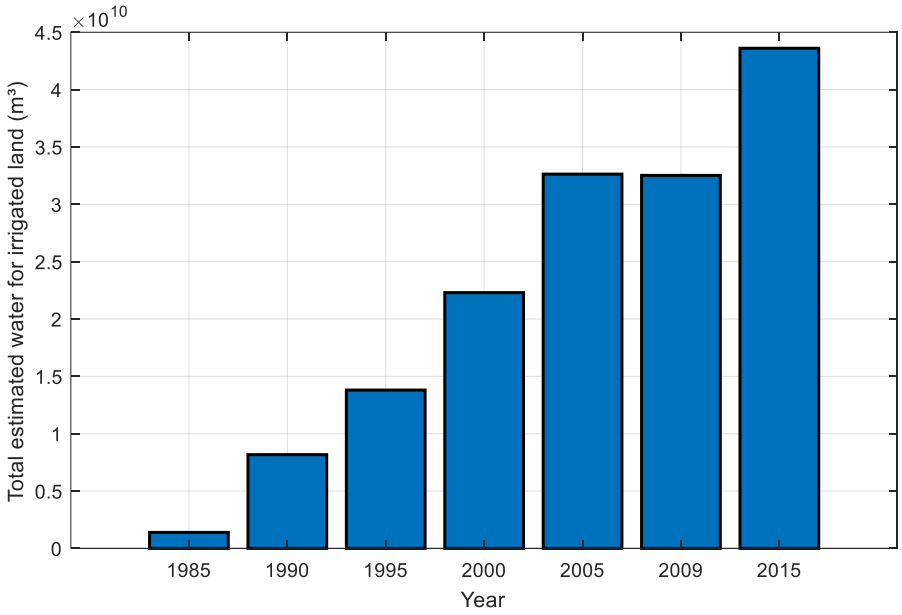

Figure 4.9 Total estimated water use by irrigated land, 1985-2015

Estimated water demand for agriculture peaked during 1985-1990, increasing significantly by 486% from 1985 to 1990 (Figure 4.9 and Table 4.9). There was a steady increase in water demand at around 60-70% from 1990 to 2000. In the 2005-2009 period, estimated water use remained stable as indicated by the small difference in water use and zero gain or loss (Table 4.9).

Table 4.9 Difference and percentage gain/loss of estimated water demand for irrigation of all crops for six periods in Tabuk

Period	Difference (m^3)	% Gain/loss
1985-1990	6.78 $x10^{10}$	486
1990-1995	5.63 $x10^{10}$	68
1995-2000	8.85 $x10^{10}$	62
2000-2005	10.33 $x10^{10}$	46
2005-2009	-0.01 $x10^{10}$	0
2009-2015	1.11 $x10^{10}$	34

To estimate NIR, data from evapotranspiration (ET), crop water requirements (CWR) and effective rainfall as inputs (NIR = ET_c × Crop area – Eff rain). Net irrigation requirement results for crops (wheat, clover, potato, and maize) during 1985-2015 are presented in detail at the end of the irrigated agriculture assessment.

4.3.1.1 Evapotranspiration

Daily evapotranspiration (ET) showed an increasing trend between 1985 and 2015 based on fitting slope (y=0.0001+6.4767), with average daily ET for Tabuk ranging from 5.8 to 9.13 mm/day (Figure 4.10).

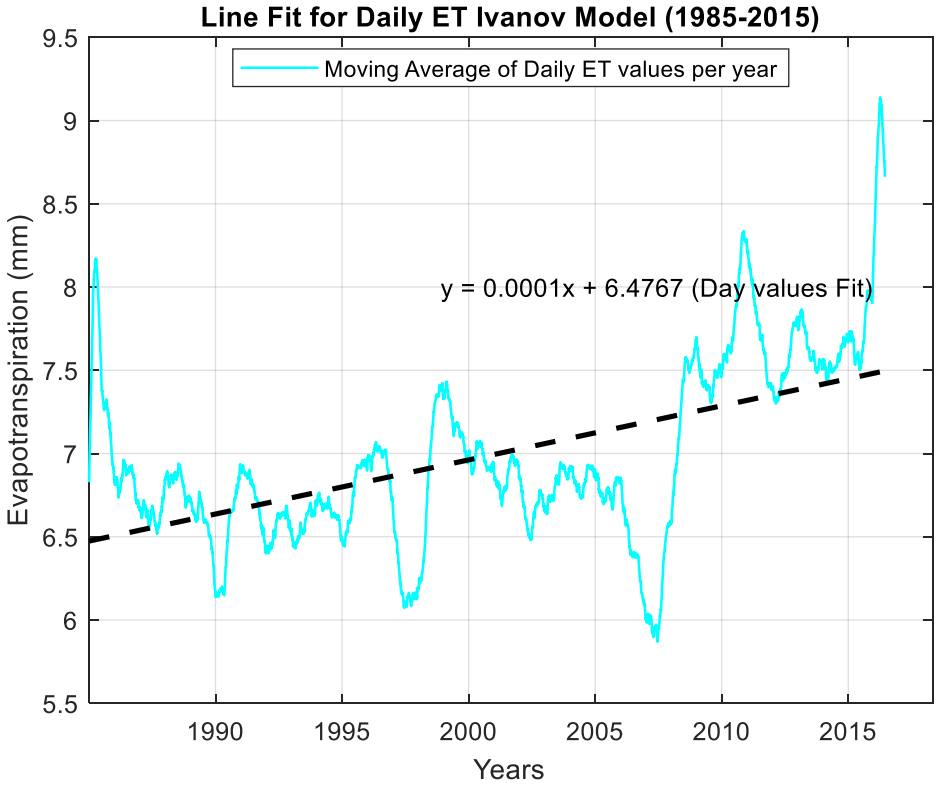

Figure 4.10 Evapotranspiration (ET) in Tabuk

Evapotranspiration estimated across the seasons during 1985-2015 was fairly stable with slight variations. Spring ranged from 12.40 to 22.64 mm/month, summer ranged from 11.71 to 23.32 mm/month, autumn ranged from 9.62 to 20.41 mm/month, and winter ranged from 7.01 to 18.65 mm/month (Figure 4.11). Cooler weather produces lower ET values.

(a)

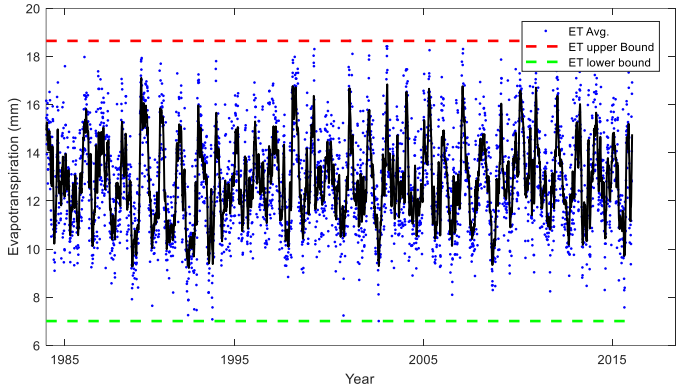

(b)

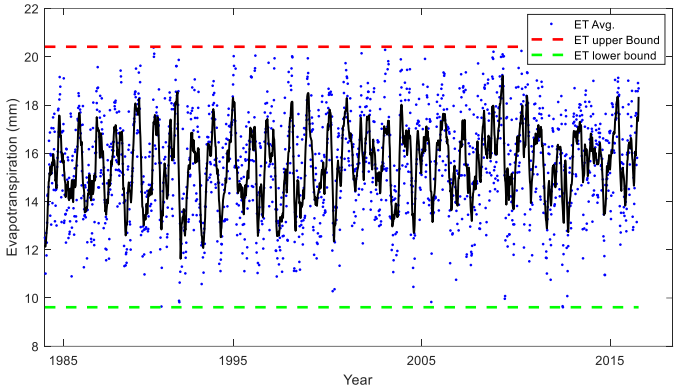

(c)

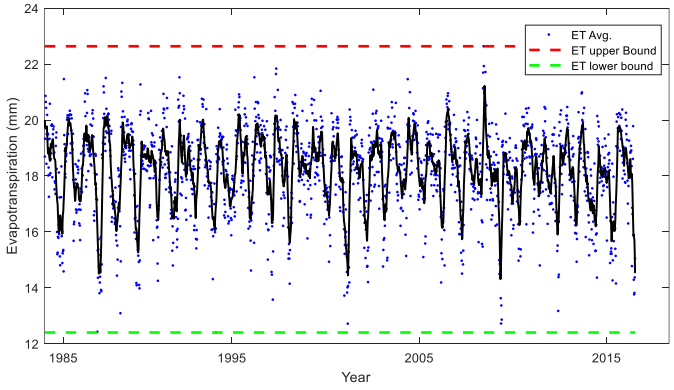

(d)

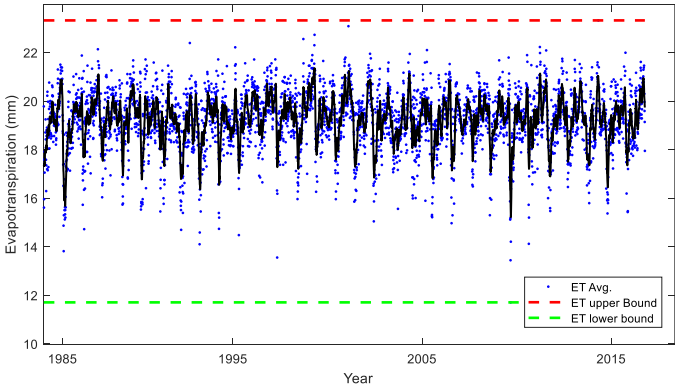

Figure 4.11 Monthly variation of reference evapotranspiration (mm), 1985-2015: (a) winter; (b) spring; (c) autumn; and (d) summer (10 day moving average in black)

4.3.1.2 Crop water requirements (CWR)

Growing stages and crop coefficient values (K_c) were obtained and tabulated for wheat, clover, potato, and maize to estimate crop water requirements (Table 4.10). The parameter K_c varies based on the type of crop and the stage of crop development during seasonal growth (e.g., initial stage, mid-season, and late season).

Table 4.10 Growing stages and K_c for each crop

Crop	**Growing stages (days)**				Total days	Planting-harvesting date	**Crop (Kc)**		**Coefficient**
	Initial	Crop Development	Mid-season	Late			Initial	Mid	Late
Wheat	20	30	50	30	120	Nov-Feb	0.7	1.15	0.40
Clover	10	20	20	10	60	Mar-Apr	0.4	0.90	0.85
Potato	25	30	30	30	60	Sept-Oct	0.5	1.15	0.75
Maize	20	35	40	30	120	May-Aug	0.3	1.2	0.35

Source: FAO and SSYB, 2015

Total CWR between 1985 to 2015 was highest for maize (1.35640×10^5mm) and then wheat (1.07260×10^5 mm), potato (0.82612×10^5 mm), and clover (0.63144×10^5 mm). Maize was grown for a longer period over the summer season from May to August when there were high temperatures, zero precipitation, and crop water requirements measuring from 21.66 to 43.15 mm/month. Annual CWR was highest for potatoes (ranging from 29.76 to 54.33 mm/month) which was generally grown for two months from September to October each year during the study period. Wheat, grown during November to February, was had the lowest water demand (ranging from 15.77 to 41.96 mm/month). Water demand for clover, grown from March to April (spring), ranged from 20.67 to 43.89 mm/month (Figure 4.12).

(a) Wheat

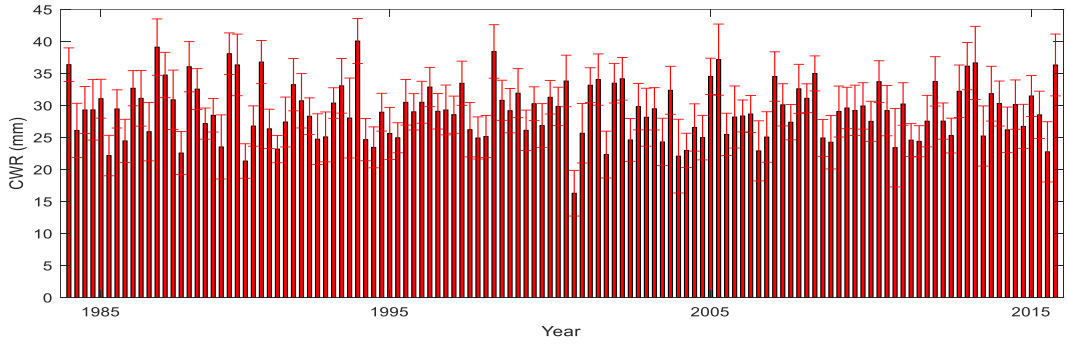

(b) Clover

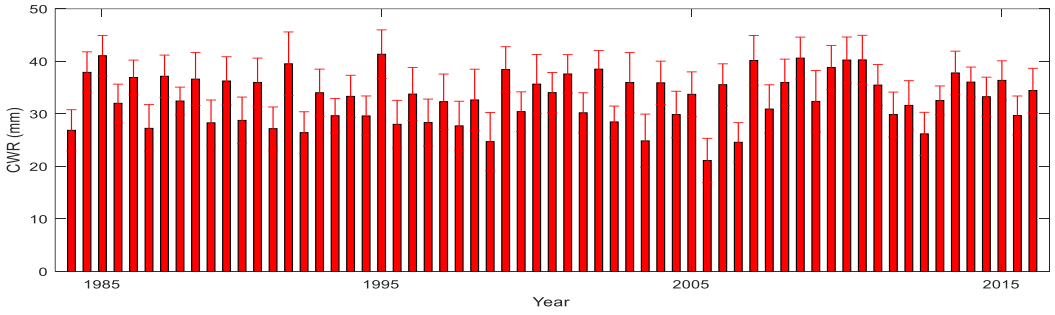

(c) Potato

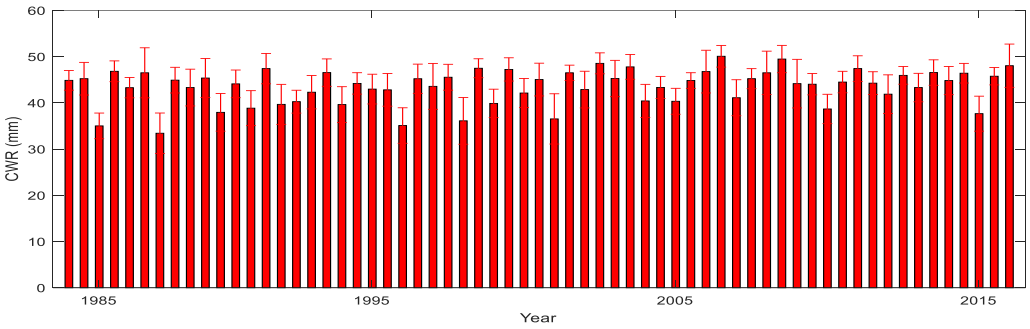

(d) maize

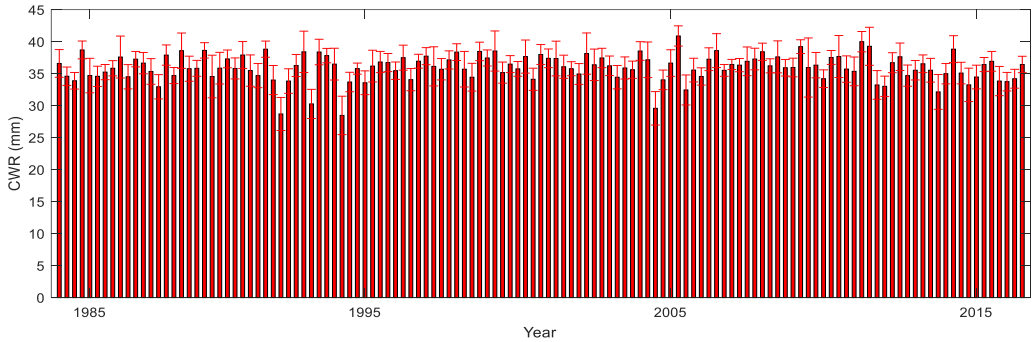

Figure 4.12 Crop water requirement in Tabuk, 1985-2015: (a) winter (wheat); (b) spring (clover); (c) autumn (potato); and (d) summer (maize)

4.3.1.3 Effective rainfall analysis

Effective rainfall in Tabuk was calculated to use in the net irrigation formula. There was no significant variation in rainfall for the 30-year period classified overall as 'dry' according to thresholds set by Smith (1992) (Table 4.11). The rainfall was 12mm/month in January, and close to zero from June to September. From February to May effective rainfall was estimated between 3 and 6mm/month (Table 4.11). Tabuk's dependable level of rainfall probability of exceedance measured P_{80}=11.98mm=P_{dry}, P_{20}=50.75mm=P_{wet}, and P_{50}=25.13mm=$P_{average}$ for the study period.

Table 4.11 Monthly effective rainfall (mm) in Tabuk using Smith (1992) classification of wet (20%), average (50%), and dry (80%), 1985-2015

Month	**JAN**	**FEB**	**MAR**	**APR**	**MAY**	**JUN**	**JUL**	**AUG**	**SEP**	**OCT**	**NOV**	**DEC**
Dry	3	1	1	1	1	0	0	0	0	2	2	2
Average	8	2	4	2	2	0	0	1	0	5	4	5
Wet	12	3	6	3	3	0	0	1	0	8	7	7

Note: raw precipitation data are in Table 3.2

4.3.1.4 Irrigation demand by crops

The net irrigation requirement for each crop increased constantly over the study period (1985-2015) (Figure 4.13) due to an increase in the planting of irrigated crops. The total NIR between 1985 to 2015 was highest in maize 38% (total of $5.47x10^{10}$ m^3), followed by wheat 28% (total of $4.30x10^{10}$ m^3), and potato at 19% (total of $3.21x10^{10}$ m^3). Clover showed the lowest crop irrigation demand at 15% ($2.46x10^{10}m^3$).

(a) Wheat

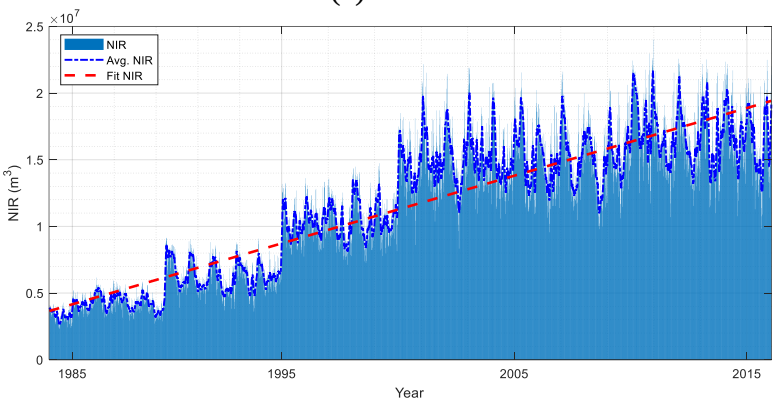

(b) Clover

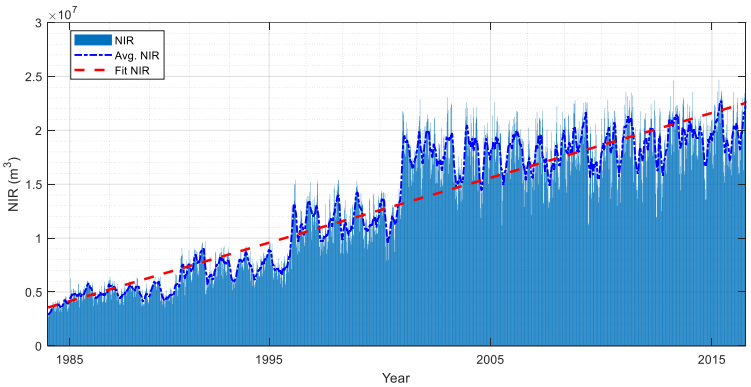

(c) Potato

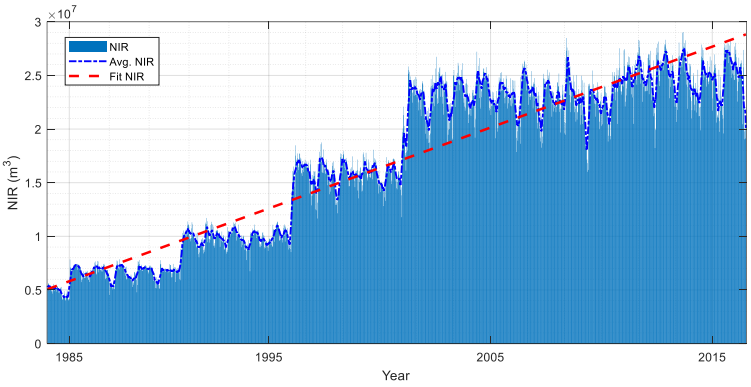

(d) Maize

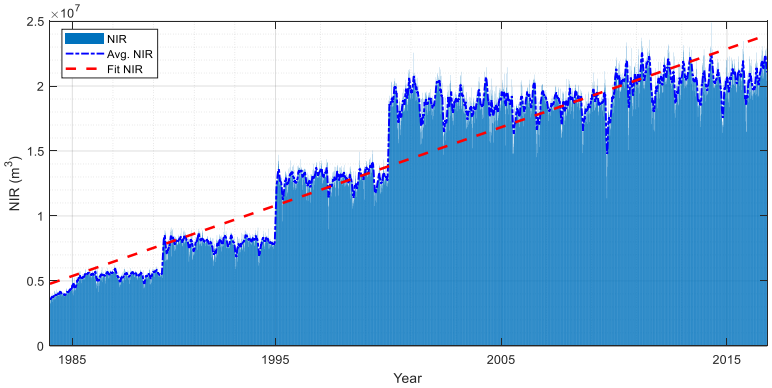

Figure 4.13 Net irrigation requirement in Tabuk, 1985-2015: (a) wheat; (b) clover; (c) potato; and (d) maize

4.3.2 Fossil groundwater discharge and levels

Groundwater levels and drawdown effects of urban areas shown in Figures 4.15 and 4.16 were calculated (see eq. 13, eq. 14 and eq. 15 in chapter 3). Figures 4.14 and 4.15 show the contour line plot of the drawdown distribution, obtained at time t=7300days (20 years), in an aquifer with the hydrogeological parameters given in Table 4.13. The well static water level (h_0) before pump, transmitivity (T), and storativity (St) of Saq Aquifer is listed in Table 4.12.

Table 4.12 Saq Aquifer hydrogeological parameters

h_0 (m)	**T (m^2/day) = K x h_0**	**Storativity (unit)**
90	1,572	2.86×10^{-4}

The plots in Figures 4.14 and 4.15 were plotted in MATLAB based on eq. 10 described in chapter 3. The drawdown rate was calculated based on the Theis equation (Theis 1935) with time-varying operation rates of wells situated in different (x,y) map locations. A constant pumping rate is considered in the calculations, followed by the principle of superposition to deal with scenarios where the constant pumping condition was not met. The well operation rate was considered a time dependent function and the drawdown values were computed by first using convolution and then integrated to obtain the final solution.

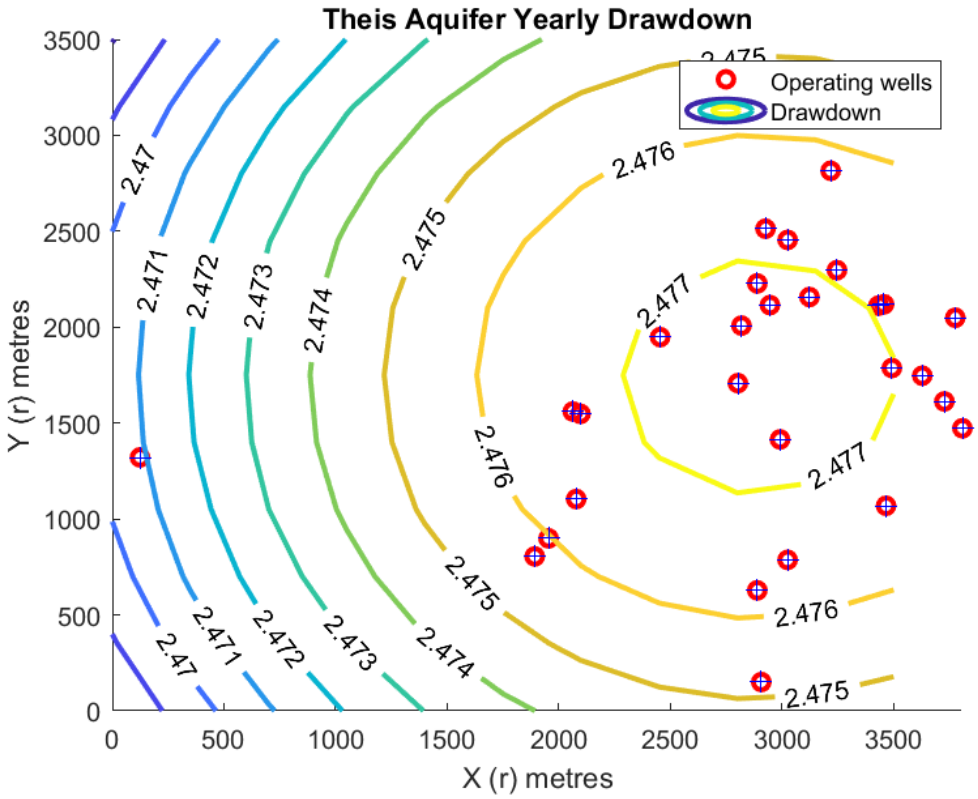

Figure 4.14 Groundwater drawdown contour map in 2015 plotted using Theis equation

The contour plot values for annual drawdown effect of the operational urban wells were quantified (Figure 4.14). To calculate the effect of pumping on the groundwater levels in Tabuk city, a grid of observation well data (Figures 4.14 and 4.15) was used to monitor groundwater levels over 20 years from 1995 to 2015. The yearly drawdown was varied based on well location and pumping rate, ranging between 2.470 to 2,477 of groundwater levels in the study area over the 20-year period (Figures 4.14). The well data including the well coordinates were obtained from the map of Tabuk's urban area and the simulated drawdown effect contour map was overlaid to show the groundwater drawdown levels in the area (Figure 4.15).

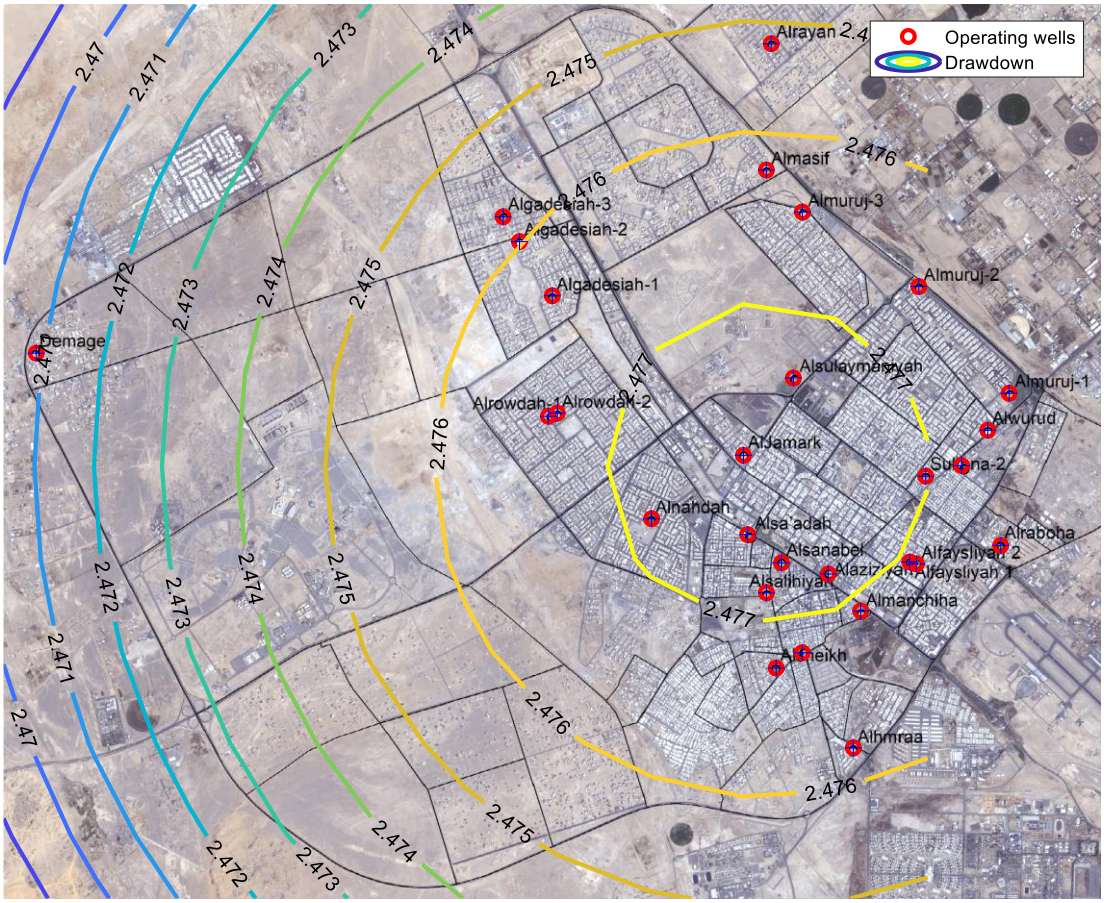

Figure 4.15 Groundwater drawdown contours in 2015 using Theis equation plotted over Tabuk city map

The total estimated groundwater discharge flow for all urban wells increased exponentially by 820% (Figure 4.16) from 1995 to 2015. For example, the total discharge (production) in 2015 from all urban wells was estimated to be $2.15 \times 10^7 m^3$/day. The water level dropped substantially because of heavy well pumping to cater for the increased water demand stemming from expanding urban and agriculture lands (well data was not available at the time of writing this thesis). It was also noticed that the depth-to-groundwater increases with time, which implied a continuing water level drop in the area with an average drop rate of 10-15 m/year. The recharge of the Saq Aquifer was low compared to operational well discharge which was made apparent by the water levels of the observation wells where the depth-to-groundwater increased from 75 m to 110 m. The groundwater level drop was attributed to extensive pumping of groundwater to meet urban and agricultural needs, especially irrigation.

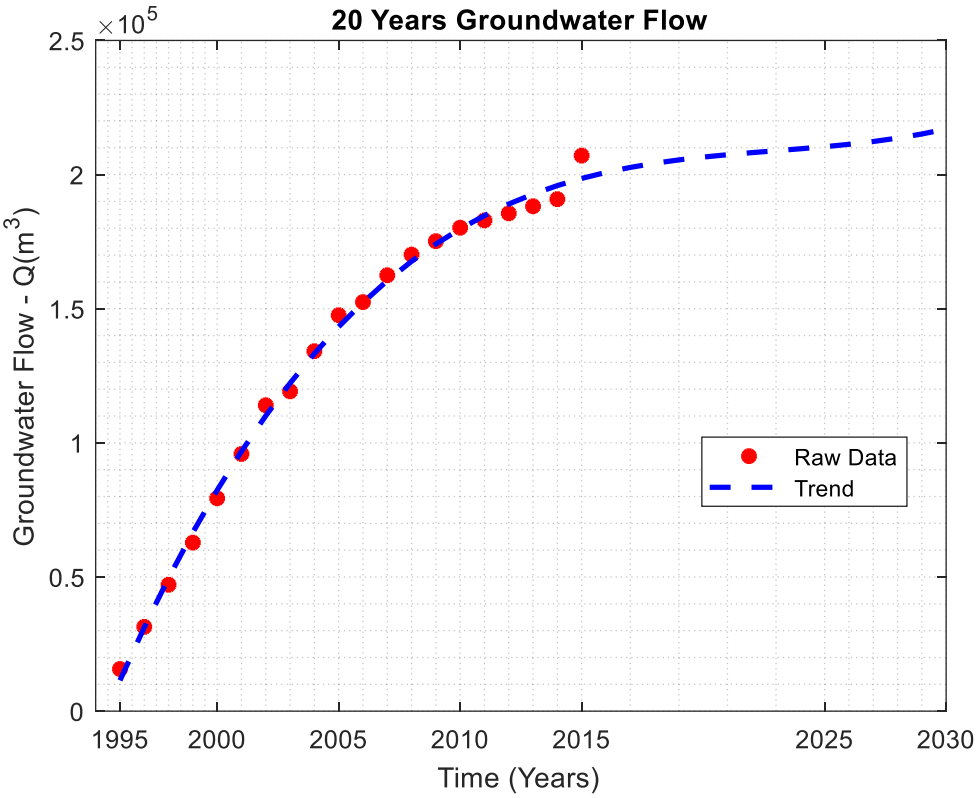

Figure 4.16 Groundwater flow data for years 1995-2015

In Figure 4.16 an asymptotic trend can be observed, showing that groundwater flow will remain uniform or slightly increased for the next 20-year period, 2015-2035.

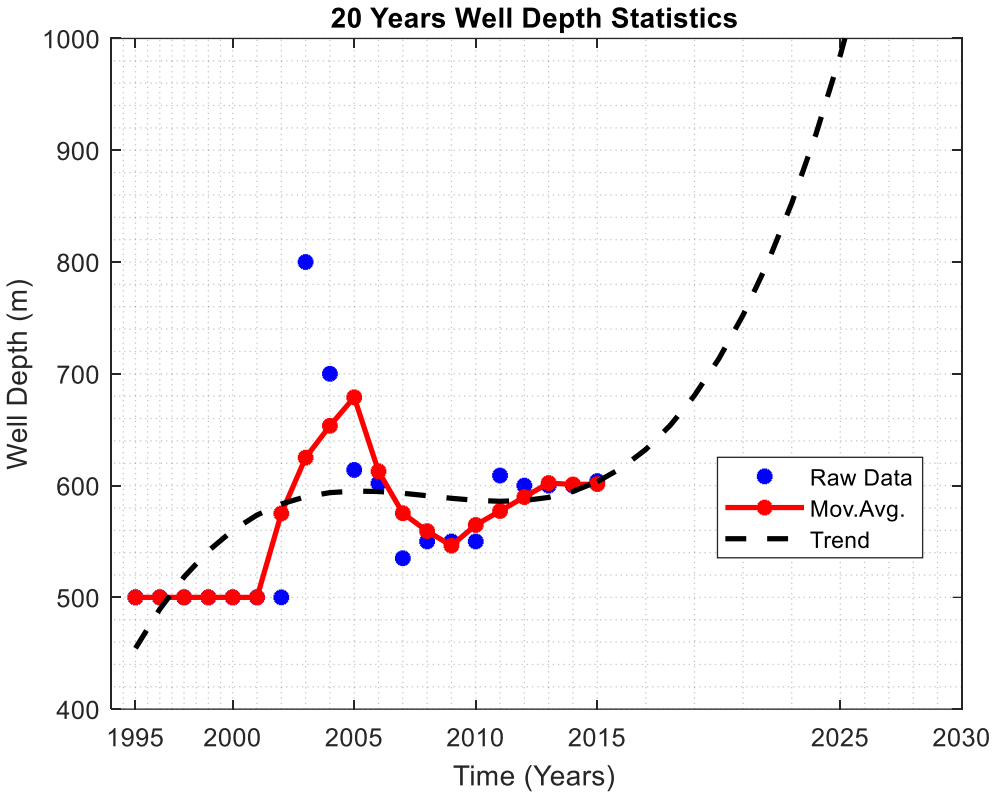

Figure 4.17 Well depth data for years 1995-2015

In Figure 4.17 a sharp increase in the well depth data trend was observed showing an increase in the well depth requirement for the next 20-year period (2015-2035). This indicates that better water resource management in Tabuk is required as a priority as the trending line is unsustainable meaning well depths cannot increase ad infinitum.

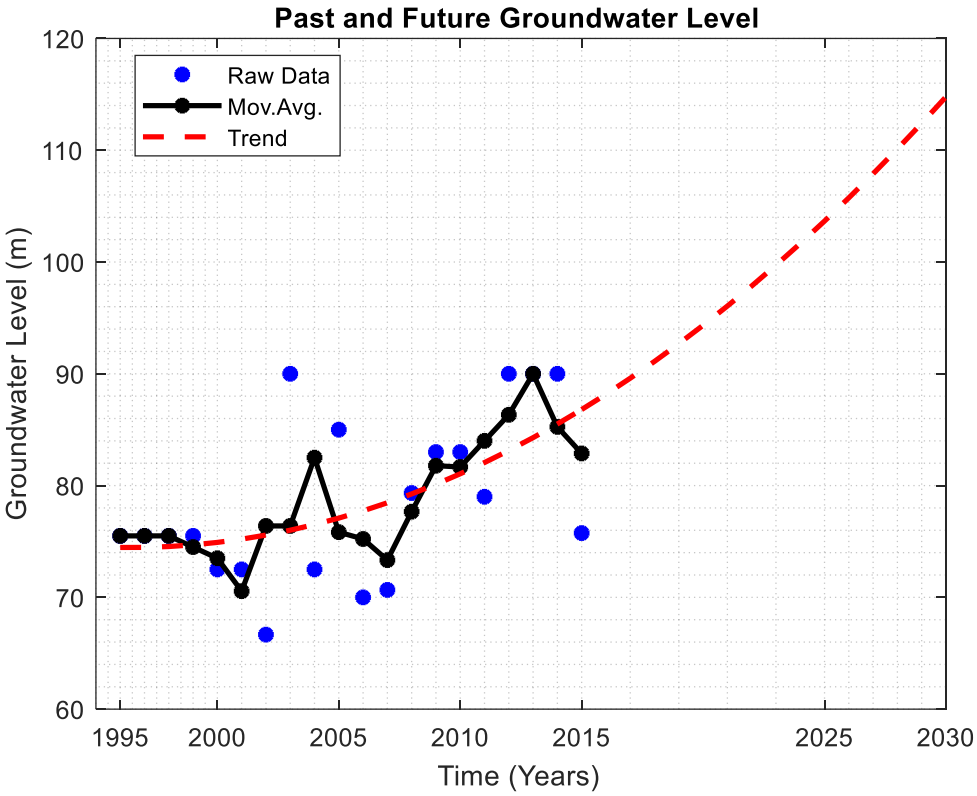

Figure 4.18 Groundwater level data, 1995-2015

A simple difference between the static and dynamic groundwater levels during pumping of water from wells is depicted in Figure 4.18.

The number of urban wells in Tabuk city increased considerably from 1995 (4 wells) to 2015 (28 wells), with four new urban wells added between 2011 and 2015. Wells that opened more recently did not necessarily produce a greater volume of well discharge. For example, well 11 (Sultana-1) produced the highest amount of daily water abstraction of 11,616 m^3/day since opening in 1999 compared to well 18 (Alrayan) which opened in 2014 and discharged 2,016 m^3/day (Figure 4.19).

Photographic evidence (Figure 4.21) showed the high soil salinization around well 11 (Sultana-1).

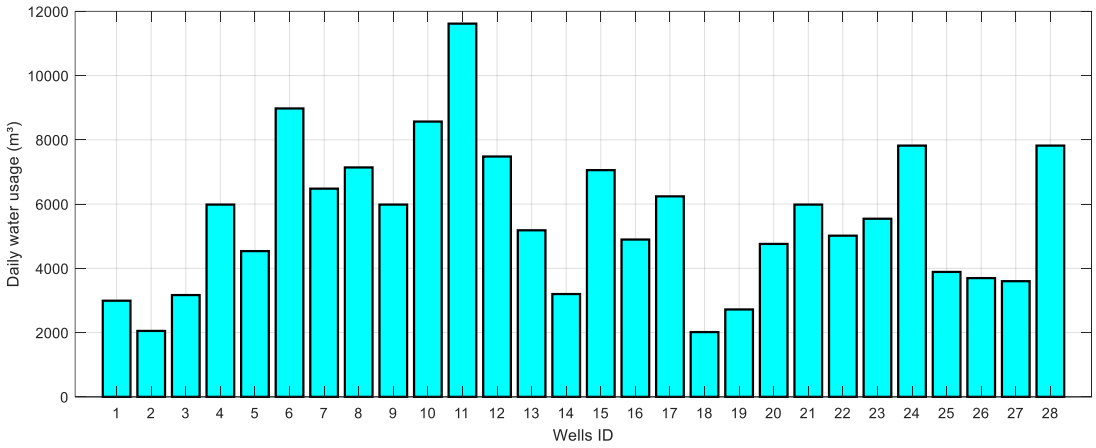

Figure 4.19 Estimated daily urban water usage (m^3) per well in 2015 based on discharge and pump run time (see Table 3.6 for well information)

Figure 4.20 Soil salinization near urban well 11 (sabkhat, east of Tabuk city) caused by high rates of evaporation and excessive groundwater pumping

4. 4 Chapter summary

This chapter presented the results for this study, a short summary of which is provided in this section. The first part of this chapter analysed the LULC change in the agricultural centre of Tabuk using object-based image analysis (OBIA) of Landsat images for seven years (1985, 1990, 1995, 2000, 2005, 2009, and 2015). The LULC change detection results showed a total increase of 556% in urban areas in Tabuk from 48 km^2 in 1985 to 315 km^2 in 2015, compared to an increase of 414% in agricultural land (112 km^2 to 577 km^2) over the same period. Expansion of urban and agricultural areas occurred at the expense of barren land which reduced by 731km^2 between 1985 to 2015. Analysis of LULC change revealed that Tabuk was subject to continuous change during the study period 1985-2015. The temporal trend over the 30-year period showed that the most rapid increase in urban area expansion occurred between 2009 and 2015. Overall classification accuracy ranged from 90% to 97% across the images analysed. 72% of the urban growth type for Tabuk was identified as extension-type, with urban areas expanding toward the northwest and west of Tabuk city.

In the second section, land use satellite imagery from 1985, 1995, 2005 and 2015 was used to predict future land use growth and patterns. The MCCA model was used to create a model based on historical LULC data for factors affecting agricultural and urban growth, including biophysical and proximity factors. Results for 2015 indicated that the prediction capability of the model, when comparing the predicted and reference data, was 98% (i.e., almost total agreement). The future transition for the study area predicted an increase in agricultural land of 125 km^2 and urban areas of 138 km^2 between 2015-2035. The results predicted a clear encroachment on agricultural and urban lands if current trends continue. This can help to explain the negative effect of agricultural and urban land expansion on Tabuk and the need for sustainable water resource management practices in Tabuk

In the third section, water demand estimation results were presented for both agricultural land and urban areas in Tabuk city. The CWR was calculated based on ET_c, and NIR was estimated by computing irrigation demand volumes for varying

portions of ET_c and irrigated area. Overall estimated ET, CWR and NIR values during 1985-2015 were then explained. Urban water demand from 1995 to 2015 was estimated using urban tube wells and available water discharge (abstraction) data.

In the last section of the chapter, haphazard placement of wells, large urban well discharge volumes, and irrigation of agricultural land, were highlighted as the major cause of groundwater depletion from Saq Aquifer. Lack of historical data on agricultural wells and their irrigation use made it difficult to model optimal well drawdown factors (e.g., flow times, well placements and discharge rates) that would reduce well depletion. However, water quantity as the total daily volume extracted from 28 urban wells was estimated to be $2x10^5 m^3$/day. It is strongly recommended that a detailed groundwater management plan is developed with groundwater flow modelling where different scenarios for groundwater exploitation are applied and the resulting drop in groundwater levels can be predicted.

5 Discussion

Remote sensing data provide useful information for research purposes, especially in developing countries where other data is scarce, inaccurate, or difficult to obtain. Several techniques have been developed, however, not all can be applied successfully in arid and semi-arid environments. The object based-image analysis (OBIA) approach used in this study produced useful classification results without the effect of mixed pixels. Using image objects (spatial, spectral, and textural) as individual segments rather than pixels with the OBIA method was effective, especially in agricultural urban classes. This approach aided in accurately assessing the LULC change over time. The results of this study support the view of Galletti and Myint (2014) that OBIA is suitable for assessing areas under mixed urban agriculture classes in arid regions.

The accuracy of results and a visual interpretation of the images show the limitations of OBIA when using Landsat imagery to target the water class (less than 1% of the study area). This is due to the spatial image resolution (30m) and the low percentage of water class represented in the study area (i.e., the size of the objects). For example, the small size of the water class areas within surrounding barren areas in this study resulted in such regions being merged into a single polygon. In general, OBIA classification techniques perform best when using high spatial resolution images and so errors can be expected when using the lower resolution images (Wang et al. 2018). The post-classification technique used in this study provided ‘from-to’ change information of the LULC nature, rate, and location between two dates and produced robust change-detection results. Agricultural land and urban areas in the study area were primarily converted from barren land. Due to the typical arid environment of Tabuk city, agricultural and urban land use types were the main features in the study area.

The expansion of agricultural land was observed, particularly in the northwest, west and southeast of Tabuk city (visible on the LULC maps) due to current good water flow from regional hydrogeology features and ease of access to water extraction.

In the south and southwest areas of Tabuk, agricultural expansion was noticed to be limited due to the existence of the current city. Broadly, Tabuk city's expansion has occurred in most directions, however, the northwest west and south-west of the city appear to be the dominant directions of urban expansion. Availability of flat land (i.e., the slope of 2–5%) has encouraged urban area expansion in the northwest and western directions. Areas east of Tabuk, where slopes can exceed 15%, are mostly vacant since such topography is not as conducive to urban dwellings due to steeper inclines. This agrees with a study from Wu et al. (2015) where the slope was the main factor in determining the distribution of urban areas in three cities of China. The presence of educational facilities (e.g., Tabuk University) and industrial centres in the northwest and west also correlate to co-location of urban areas. The Prince Sultan Charitable Housing project which opened in 2010 saw the construction of 1,000 units resulting in an expansion of urban dwellers in the southwest of Tabuk city where the housing project was located (Alatawi 2015).

Over the 30-year period between 1985 and 2015, Tabuk city has experienced intensive agricultural (414%) and urban development (556%). This development correlates to the Saudi Arabian government's plans and programs (introduced in the 1980s) to increase food self-sufficiency and encourage economic development by increasing population migration to urban areas. Increasing oil revenues and the country's wealth contributed to its developmental policies and direction. The high standard of living and the aspirations of the Saudi population towards independent housing have also had an impact. Urban development was the predominant extension type (72%), notably around the edges of existing urban areas during the entire study period 1985-2015.

The period 1990-1995 can be regarded as the most substantial period of the study as many significant changes occurred after the country's 'oil-boom' and more so when wheat cultivation was introduced to the Saudi agriculture system. Saudi Arabia became a wheat producer and exporter during the 1990s and succeeded in achieving self-sufficiency in wheat production. This placed Tabuk second in the top five regions of the country producing wheat and vegetables at the time and allowed the region to meet a large part of the market needs of Tabuk, as well as other regions of

Saudi Arabia (Al-Harbi 2010; Alzahrani et al. 2012). As a result, Tabuk's agricultural land area increased dramatically during this time (52%) as a response to government support through agricultural subsidies, free land distribution, technology transformation, promotion of modern farming practices, rural road development, low-cost well drilling, and improved irrigation infrastructure to increase productivity (Ouda 2014).

At the same time, government urban planning policies played a key role in driving the growth of the Tabuk city (an increase of 11%) in the period 1990-1995. The implementation of ambitious development programs including interest-free loans, the distribution of residential land plots free of charge, the provision of housing for citizens, and the establishment of the Saudi Industrial Development Fund (SIDF) and a Real Estate Development Fund (REDF) (Chaudhry 1997), all resulted in a notable increase in the population of urbanised areas around the country, including Tabuk. More specifically, the implementation of the Fourth Urban Master Plan. This plan focused on providing basic facilities and municipal services for cities in provincial areas to redirect migration away from the capital city, Al-Riyadh, and holy cities such as Makkah and Al-Madinah which were already densely populated. An increase in urban growth was observed in the study area and in various other Saudi cities, a factor which decreased population pressures in these other cities. For example, Al-Ahsa Province in the eastern region of Saudi Arabia experienced urban growth during the same period thereby alleviating population pressures in other major cities (Abdelatti et al. 2017). As a consequence, the infill growth type was more pronounced in Tabuk city during this period (as depicted in Figure 4.3).

Between 1995 and 2000, there was an increase in the spatial changes of the urban area due to high waves of internal migration to Tabuk which accelerated urban expansion with a total urban area gain of 34 km². Tabuk is one of the most important military cities in the northern border areas of Saudi Arabia and is the site of the King Faisal Air Force which is the second largest airbase in the world. Military townships attract people from other parts of the country, creating settlement pressures and increased demand for housing.

This led to issues with affordable housing, housing shortages, water supply, and pressure on health and education facilities (Abdulsalam et al. 2014). New urban areas in Tabuk sprawled away (i.e., leapfrogged) from Tabuk's central area between 1995 and 2000 which coincided with increased rents and the shortage of affordable housing. During the same period, total agricultural land also increased by 131 km^2 due to population growth and government support.

For the period between 2000 and 2005, agricultural land expansion in Tabuk reached its peak (60%). The map representing agricultural distribution (as seen in Figure 4.3), showed agricultural areas increasing in size by 171 km^2. Population growth was the leading cause of agricultural expansion. The Tabuk population increased by 31% between 2000 and 2005. The people coming to Tabuk were eager to take advantage of agriculture government subsidies, infrastructural development, services, and employment opportunities available at the time. The increase in the population rate also triggered the growth of agricultural land to meet food demand in the study area. This is supported by the findings of Al-Ahmadi (2009) that the number of irrigation wells in production in the region increased significantly between 1989 and 2004 (from 136 to 260 wells) to meet the water demand for agricultural production. This agricultural expansion may have resulted in the irreversible environmental impacts identified such as land degradation from high soil salinity. Other serious environmental problems were groundwater depletion and groundwater contamination risks in Tabuk and other agriculturally important regions in Saudi Arabia (Hassoun 2009; Al-Harbi 2010; Hussain et al. 2010; Zumlot et al. 2013; Nazzal et al. 2014; Zaidi et al. 2015). In terms of urban area expansion, the urban area size has also increased by 23 km^2 over the same period (2000-2005) but, not much as compared to the period between 1995 and 2000.

During the period 2005-2009, a slight reduction was observed in the spatial changes of agricultural land due to the high demand for water and associated environmental impacts, resulting from the government restricting groundwater use after the 2000s. Although restrictions were applied to random well drilling and water meters were implemented for private wells, the amount of agricultural land only decreased by approximately 4 km^2 in the study area.

At the same time, the total urban area increased by 59 km^2 due to the good road networks within and outside the city of Tabuk during this period (2005-2009). There was a large amount of new construction in areas outside of the city boundary for housing and transport infrastructure to accommodate the growing population and improve accessibility. This shows, as suggested by Aljoufie et al. (2013) in Jeddah, Saudi Arabia and by Peng et al. (2015) in Chengdu district in China, that an effective transport network was a direct driving force of urban land expansion and residential growth.

Looking at the period between 2009 and 2015, most of the rapid urban expansion in Tabuk city occurred in this period (total gain of 111 km^2) due to largescale urban development projects and population growth. The Municipality of Tabuk developed and promoted regional investment plans, in line with developments occurring in other parts of the region. This included the asphalting of roads linking villages to the city, and to the provinces to provide faster and easier access to surrounding regions. Similar growth was observed in a previous study of Dammam city, Saudi Arabia, where the urban area doubled due to the government's urban policy and resulting population growth (Alhowaish 2015). The massive urban area expansion during this period created numerous challenges such as unplanned housing and flash flooding due to poor drainage (Al-Ahmadi and Hames 2009; Al-Harbi 2010). Al-Momani and Shawaqfah (2013) also indicated that severe urban hydrology problems (e.g., flood hazards) occurred due to random expansion. Flash flooding hazards have become a serious concern and have caused a loss of life and damage to Tabuk’s urban infrastructure due to unplanned houses in vulnerable areas (Abdelkarim et al. 2019).

In addition, expansion of the urban area (due to population growth) placed additional pressure on limited natural resources such as groundwater contributing to water insecurity. The number of urban wells more than doubled during the study period to meet the increased demand for water as noted by this study. To satisfy the water demand in Tabuk city, the Ministry of Water added about two wells per year to cover domestic urban use. If the current population growth trend continues, Tabuk city is expected to reach to about one million people in 2030, as projected by the UN (2020).

Construction in new urban areas will likely increase to accommodate the influx of people. Understandably, this population will exert further pressure on the already stressed groundwater resources. Land and water deterioration are expected most in fast-growing regions such as Tabuk. There is a clear need for planning to minimise these issues to safeguard livelihoods for the future (Allen et al. 2013).

During the period 2009-2015, a considerable encroachment of urban areas into agricultural land was also observed due to the close proximity of the two land classes. At the same time, agricultural development occurred extensively in Tabuk despite the water regulations in place. Often urban expansion increases at the expense of agricultural land as seen in China (Li et al. 2017), and Al-Kharj in Saudi Arabia (Algahtani et al. 2015). In the case of Tabuk city, expansion of both urban and agricultural areas has put extreme pressure on the fragile natural environment.

Agricultural development and increasing urban areas in the Tabuk city due to population growth was encouraged by the government which had the effect of jeopardising valuable non-renewable groundwater resources. A similar situation was seen in Spain in 2013, where inadequate government policy and land use mismanagement was accompanied by exploitation of water resources in the country (Barbero-Sierra et al. 2013; Stellmes et al. 2013). Significant depletion of groundwater resources was also observed in other cities around the world for the same reasons (Dalin et al. 2017; Naboureh et al. 2017). Better strategies and policies are required to balance the demands of a growing population against the need to conserve natural resources.

Historical LULC maps provide an indication of changes which have occurred in the past and can be useful in determining how and where patterns of LULC will change in the future if LULC change continues at the same rate. LULC prediction is, therefore, an important task for urban planners and policymakers to design policies for more sustainable development. Land use modelling can provide useful information about future land demands and expected changes in the landscape.

The integration MCCA model used in this study has shown it can successfully predict future trends and patterns of LULC change. Cellular automata aided Markov chain modelling has proven to be an effective means for LULC prediction.

The results demonstrate the advantage of the Markov chain, which provides transition matrices by which the land use and land cover system can be modelled dynamically based on historical data. The transition matrix results show differences in the conversion from different land cover classes, with water being the most highly converted class of land (as seen in Table 4.6). This transition is not unexpected in arid environments such as Tabuk because surface water is not permanent (e.g., ponds) and often converts to other land classes or dries up due to arid conditions.

The second highest land class transition was from agricultural land to barren land. The results suggested that some irrigated areas were unsuitable for agriculture and after a while reverted back to the barren land. This conversion of agricultural land back to barren land was due to land degradation which dried the wells resulting in farmers abandoning their agricultural land in favour of other areas, leaving abandoned land exposed. The third highest land conversion was from barren to agricultural land. This conversion can be related to land reclamation projects in the early stages of wheat production in Tabuk. The dynamic Markov chain model only has a temporal dimension and does not consider the spatial dimension. A spatial context (to include neighbourhood effects) was incorporated using the cellular automata model.

The analysis in this study suggested that agricultural land and urban area will experience further growth if current trends continue due to population growth and increased demand for food. Agricultural areas could increase by 125 km^2 in 2035 from the 2015 area. The increase in agricultural land may result in further environmental problems, particularly due to groundwater extraction for irrigation. It has been noted that further development of Tabuk's agricultural lands will see more land transition to environmentally fragile areas.

Such a scenario indicates that unsustainable groundwater extraction will continue if current agricultural land use trends persist. According to Karimi et al. (2018) and Palmate et al. (2017), increased unsustainable human activities (e.g., agriculture expansion that relies solely on groundwater) could result in severe implications for water deterioration and adverse impact livelihoods.

Tabuk City is predicted to undergo further urban growth in the future (i.e., an increase of 9% by 2025 and 11% by 2035 based on the total study area). The predicted future urban growth is likely to take place near road networks in existing urban areas and fringe locations. The proximity to roads and other urban facilities strongly influences growth in such areas. This is consistent with previous studies (Chen et al. 2016; Vaz et al. 2015), where new urban developments occurred in areas where there was the ease of transport and accessibility to places of work and public services.

Modelling exercises also indicated that Tabuk's urban growth will encroach more onto agricultural land in the north-east and southeast of the city due to the close proximity of agricultural areas to existing urban area boundaries in these locations. If the current urban and agricultural land increases continue, maintaining groundwater resources to support that growth will be a challenge in the coming years and will have significant detrimental effects on regional ecosystems. In Jordan, the capital city of Amman experienced similar issues when high population growth and unplanned housing developments substantially increased the cost of agricultural land, resulting in planning and environmental problems (Khawaldah 2016).

Issues that may arise from development activities in a fragile arid environment suggest that careful planning is needed. The use of modelling, particularly using methods which have been assessed in this study, may be beneficial. The MCCA model showed its value by allowing simulations to be conducted even when data was scarce; an issue that is common in many areas of the world (Eastman and Toledano 2018). This study clarified the main drivers of land use change by identifying and using the factors that are influencing agricultural and urban growth in Tabuk. The

model was customised to local conditions using selected biophysical and proximity factors.

The model achieved strong agreement between predicted and actual (reference map) in 2015, providing confidence in the results modelled for the years 2025 and 2035. However, for an even better understanding of the complex agricultural and urban system other factors, including environmental and socio-economic factors, can be incorporated to assess the dynamics of agricultural and urban change and predict future growth (Guan et al. 2011).

The evapotranspiration (ET) trend using the Ivanov model in this study was found to increase over time between 1985 and 2015 due to the climatic fluctuations and an increase in cultivation areas. This agrees with the previous finding from Vijayan and Altalhi (2015), that reported an increasing ET trend in Tabuk from 2002-2011. Climate change is also expected to increase temperature and decrease rainfall in the north of Saudi Arabia, including Tabuk (Almazroui et al. 2012), which could accelerate the depletion of groundwater resources. An imbalance between groundwater discharge and groundwater recharge due to irregular and insufficient rainfall to recharge underground aquifers has already been an issue in Tabuk (MEWA 2015). Heavy reliance on irrigation through pumping of groundwater resources in the arid environment of Tabuk has also deteriorated soil through increased salinity as seen in this study. Uneven water distribution was reported by Zhou et al. (2010) in many regions of the world due to increasing irrigation requirements causing salt accumulation in the soil, groundwater contamination and health risks.

The NIR for Tabuk constantly increased from 1985-2015. A significant increase of approximately 4.2 x 10^{10} m^3 was noted due to increased cropland sized and increased CWR. The result of NIR suggested that maize consumes more water followed by potato than the other crops (i.e., clover and wheat). This was supported by Chowdhury et al. (2013) who reported that maize and potato crops had higher CWR and NIR in the semi-arid environment of Al-Jouf, Saudi Arabia. Agricultural water consumption in Tabuk city accounted for more than 99% in 2015 (Table 4.6) of the total water use from a non-renewable water supply, namely, Saq Aquifer.

In addition, field observation confirmed that there is a massive number of agricultural wells distributed in Tabuk, where many individuals unconsciously drilled several wells where fewer may have been necessary. Most wells are not regulated or monitored leading to increasing groundwater depletion (MEWA 2015). Alarmingly, most of the actual discharge from agricultural wells in Tabuk have exceeded maximum allowable discharge since the 1990s as reported by Sen and Al-Somayien (1991).

Although the Saudi Arabian Ministry of Environment, Water and Agriculture and other authorities-imposed restrictions and permits for drilling irrigation wells to improve water use conservation, farmers were unaware of the groundwater depletion risk. Haphazard agricultural land expansion has impacted groundwater levels and will eventually cause water shortages for urban areas. At the same time, expansion in urban areas and increasing demand for water compounds the problem. Heavy pumping of groundwater in the study area since 1995 has caused a continuous drop of the well water volume with an average yearly rate of 2.7 m^3/year. This is similar to a figure found by Al-Ahmadi (2009) who notes a decrease in the groundwater level between 2.3-10.5 m^3/year. Since the 2000s, several governmental policies to reduce groundwater drawdown were reviewed without any reductions in irrigated land area, water extraction volume, or crop productivity. A deliberate policy should be made by Tabuk's local government to curb the massive agricultural changes because if the trend continues unchecked it will lead to a problem with groundwater shortage, food insecurity and an imbalanced urban ecosystem. Options to consider conserving Tabuk's groundwater include shifting agricultural cultivation to more suitable regions (e.g., southern regions), planting different crops, and optimising irrigation schemes (e.g., drip irrigation).

A key management goal is to minimise the impact of water pumping on availability whilst meeting urban water demands and irrigation needs. Withdrawing water from aquifer storage affects static groundwater levels in the aquifer. If the aquifer is over pumped it may eventually be unable to provide the required volume of water to meet increasing demand.

Ensuring the sustainability of groundwater resources while meeting water demands is possible by replenishing the extracted volume of groundwater in the aquifer to keep static groundwater levels steady. In principle, this process may be carried out through: (a) aquifer storage and recovery (ASR), where each operating well has a pump able to extract water during periods of water demand for urban use and agricultural irrigation and then when surface water is available for storage to allow it to naturally recharge the aquifer, and (b) aquifer pumping and artificial recharge (APR), where after pumping, the aquifer is recharged with surface water at prescribed locations. Both ASR and APR can be modelled in a mathematical framework as an optimisation problem to balance the depletion/increase of the water level caused by both pumping (extraction) and recharging (injection). Such a mathematical model considers the requirements of water demand from urban areas and agricultural land, the availability of water to inject into the aquifer, the maximum and minimum allowable aquifer surface head levels, and the maximum and minimum well operation rates based on well capacities.

Previous governmental policies in place for agricultural land and urban area management has had an adverse impact on water supplies in the fragile environment of Tabuk. Assessing groundwater back to the 1980s poses challenges due to limitations on availability and quality of data. To overcome the limitations, the evapotranspiration method was used as a proxy model to estimate net irrigation requirements based on historical climate data. The methodologies used in this research provided an approximate estimation of agricultural water use. Although there was a lack of comprehensive groundwater data available for more detailed analysis of the past and current groundwater status in Tabuk, the modelled results estimated water demand with a good level of confidence. The study focused closely on the available data, collection and synthesis of field data, and expert knowledge in all phases of application of the methodology to estimate water demand.

Changes in agricultural land and urban areas in the arid landscape of Tabuk combined with estimates of water use, provided evidence for the urgent need to implement rigorous water monitoring and data collection to inform future actions.
An integrated assessment of LULC changes in this study for Tabuk clearly indicated that the current demands for non-renewable groundwater resources in Tabuk are at high risk of depletion. Future urban growth in Tabuk city may also seriously impact the environment unless plans are put in place to mitigate forecasted impacts.

Despite the efforts of the Saudi Arabian government to assess the environment and limited natural resources and understand how to cope with increasing demand, Saudi Arabia is still in need of implementing successful sustainable development strategies. Further commitment and action are required from local, regional, and national actors to develop and enact sustainable policies. Some of this is already captured in Saudi Vision 2030. Saudi Vision 2030 is a roadmap set out by the government for the future of the country up to 2030. The Vision 2030 articulates a commitment to "achieving environmental sustainability" and specifically with regards to water it states, "we will also promote the optimal use of our water resources by reducing consumption and utilizing treated and renewable water" (Saudi Vision 2030 2017).

Two important projects have been flagged in the Saudi Vision 2030 roadmap for the Tabuk region. The first is the NEOM Project on the Egyptian and Jordanian border zone with Saudi Arabia. NEOM is marketed as the first independent smart city powered solely by wind and solar energy (Aboneama 2018). The new economic zone to be developed is touted to be the most important global hub for world trade. The second project is the King Salman Bridge project which will connect Saudi Arabia and Egypt. Both projects will increase the number of pilgrims, boost the tourism sector, attract national and global investment thus contributing positively to Saudi Arabia's gross domestic product (GDP) and Tabuk's future economic growth and development. Again, these large projects will contribute to demand on resources to support industrial activity and expanding populations. Futuristic government policy approaches are required to optimise and ensure sustainable urban and agricultural land expansion and achieve the goals envisioned in Saudi Vision 2030.

The outcomes of this study can be used as a practical reference to support government decision-makers, environmental engineers, and urban planners to define policies that support sustainable urban and agricultural development in Tabuk and beyond.

6 Conclusion

There has been an increasing interest in the study of LULC in arid and semi-arid regions as many developing nations work to improve conditions for their people by securing reliable water and food sources and by providing the infrastructure to accommodate the increasing urban populations. Information regarding LULC in these areas is vital for providing background knowledge to allow the development of sustainable policies and successfully manage finite country resources.

In this study, Tabuk has been used as an example of a rapidly expanding Saudi Arabian city which has been experiencing rapid urbanisation and associated agricultural growth. The primary purpose of the study was to assess the impact of LULC change on non-renewable groundwater resources in an arid environment. Various geospatial techniques, including GIS applications and remotely sensed data, were used in assessing the dynamic interaction on LULC over the last three decades (1985-2015) in the arid areas of Tabuk. Multi-temporal Landsat images from 1985, 1990, 1995, 2000, 2005, 2009 and 2015 were used to quantify these land use changes. The study then predicted LULC change for the years 2025 and 2035. The main study objectives have been achieved by measuring current and historical LULC changes quantitatively and combining the changes with biophysical and socioeconomic driving forces, using different geospatial techniques, spatial analysis, and modelling. The study also examined groundwater demand in Tabuk based on changes in LULC, available data and suitable modelling techniques. This study makes an important contribution to the knowledge about past, present, and likely future LULC changes in Tabuk.

The use of multi-temporal satellite images over a 30-year period was crucial to fill knowledge gaps due to lack of other suitable data. The findings of this study can be used to inform water management decisionmakers and strengthen water security in the region and country more broadly. Policies to collect and record water data and assess LULC change to inform strong environmental policies, effective management, and planning of natural resources are of great importance. Despite the ongoing efforts of the Saudi Arabian government to minimise impacts on existing resources

and achieve urban and economic sustainability, challenges remain. The challenges stem from the fragile environmental conditions of the region, limited natural resources, and predicted climate change impacts. There is an urgent need for more sustainable water management practices and efficient use of water to make sure this vital resource remains available in the future.

The specific research objectives set out in section 1.3 of this thesis have been addressed and summarised in the following sections.

6. 1 Determine the historical pattern of LULC change between 1985-2015 in Tabuk

The LULC change maps provided LULC information with a high degree of accuracy, demonstrating the effectiveness of OBIA in deriving LULC classification. This kind of information is essential to determine past and current levels of LULC, as well as to monitor the change rate for LULC. The main LULC changes noted were related to agricultural land expansion and urban development. Substantial changes in LULC took place in the early 1980s when, backed by increasing oil revenues, many government policies were implemented to boost the country's standard of living. Agricultural areas have expanded by 414% and urban areas by 556% between 1985 and 2015.

The trend toward agricultural land expansion in the northwest and west of Tabuk city was due to the orientation of the Saq Aquifer sub-surface which provided lower cost and easier well drilling for groundwater extraction for irrigation. This study has also quantified the urban growth direction and growth type at various distances from the city centre. The detailed analysis of urban growth in Tabuk revealed that new urban development tended to take place on the periphery of existing urban areas for all time periods examined, mainly exhibiting the extension growth type. Urban development took place predominantly along northwest and west orientations, rather than east west and southeast.

Land degradation, soil salinity, and water stress are environmental issues that have been observed in Tabuk city and around the country due in large part to intensive irrigation for agricultural land and urban expansion.

The results of this study identified several factors that have driven agricultural expansion and urban development in Tabuk, including:

- *Social*: social factors include both internal migration and population growth and is closely associated with the economic growth of the country as a whole. Internal migration from villages and the countryside to the city was a major cause of urban area expansion.
- *Economic:* economic development is linked strongly to urbanisation. Economic activity created new jobs resulting in increased employment opportunities, improved living standards, and increased all forms of production and product demand. Built-up areas are expected to keep expanding with impacts on the overall health of the urban and general environment.
- *Physical (location)*: Tabuk, nicknamed the "North Gate", is a vital trade route and a large number of pilgrims from other countries visit Saudi Arabia's holy sites through Tabuk. The large number of people residing in and passing through the area place a significant demand on the region's resources. Tabuk also hosts large numbers of military personnel associated with Saudi Arabia's Armed Forces based in the region further adding to demands on resources and services. Saudi Arabia's government promoted a plan to make Tabuk a world tourism destination that may attract many investors. It is anticipated that migration to Tabuk will increase encouraged by the Saudi Vision 2030 roadmap aimed at creating a new economic region and improving conditions such as job opportunities and per capita income.

6. 2 Predicting future LULC patterns in 2025 and 2035

This study has demonstrated that the integrated MCCA model was a valuable predictor of LULC pattern in Tabuk city. Such projections make it possible for environmental impacts to be determined and assessed so that government policies can be designed based on scientific analysis. Tabuk's future agricultural and urban area growth was modelled at two points in the future, (2025 and 2035) to assess alignment with the Saudi Vision 2030 roadmap for sustainable land use change and economic development. The modelling and resulting projections were based on historical land use imagery from 1985, 1995, 2005, and 2015. The MCCA technique improved the model by integrating socioeconomic and biophysical factors that influenced agricultural and urban growth. The modelled results revealed that:

- LULC change maps produced using the OBIA classifier provide projections with a high degree of precision
- Tabuk city is predicted to undergo further agricultural and urban growth in the future
- Agricultural and urban areas will continue to grow at the expense of barren land and encroach upon each other. This is further compounded by the already close proximity of agricultural land and urban areas in many parts of the city
- Using biophysical (elevation and slope) and proximity factors (distance from well, road and urban/agricultural area) improved the precision of the prediction
- Urban expansion is most likely to occur near transport networks, water sources, educational and health facilities, and existing urban areas.

6. 3 Estimating net irrigation requirements using the ET model

The study area was considered the epicentre of the agricultural sector with a specific emphasis on the production of maize, wheat, clover, and potatoes in Saudi Arabia. Agricultural expansion during the last 30 years has impacted severely on the limited groundwater natural resource in Tabuk. Increasing water demands to support Tabuk's agricultural activities and the environmental impacts of climate change have

great repercussions for water security. Historical water demands in Tabuk were estimated using climate datasets from 1985 to 2015, agricultural land and the evapotranspiration (ET) method. The modelling and analysis showed that:

- The Ivanov evapotranspiration method can be used to successfully estimate net irrigation requirements (NIR)
- The ET value increased over time between 1985 and 2015 due to climatic fluctuations and continued expansion of agricultural land
- The estimation of past irrigation water requirements in Tabuk city indicated that the volume of water required for irrigation increased substantially and steadily from the 1980s corresponding to agricultural land and population growth
- The NIR results suggested that maize consumes more water followed by potato then the other crops, wheat, and clover
- Agricultural irrigation consumes the largest amount of water supply (99%) of the total water demand in Tabuk
- Expansion of agricultural areas put Tabuk at high risk of water depletion because irrigation was fulfilled by pumping from a non-renewable groundwater source i.e. Saq Aquifer
- The increase in agricultural land may also result in urban environmental problems, particularly urban water shortages, resulting in an imbalance of the urban ecosystem.

6. 4 Estimating urban water usage based on well discharge data

Understanding groundwater levels back to the 1980s poses requires good data availability and quality. Although the Ministry of Water in Tabuk started to monitor groundwater for urban areas since 1995, not all urban wells were regulated or monitored. More commitment is required to regularly collect and record urban well data and implement conservation policies for urban water use that translate into measurable action. The modelling and assessment in this study revealed that:

- The total annual urban water consumption in the study area rapidly increased due to the continuing increase in population
- The heavy pumping of groundwater in the study area since 1995 has caused a continuous drop of the well water volume with an average yearly rate of 2.7 m^3/year.
- The number of urban wells in Tabuk city increased considerably between 1995-2015
- Some wells within urban areas appear salt affected due to excessive groundwater withdrawal from over-pumping.

7 Recommendations and limitations

This chapter presents a set of recommendations informed by the findings of this research study, followed by limitations of the current study.

7. 1 Study recommendations

- Implement strong and focused policies to reduce issues of degradation in Tabuk due to agricultural and urban expansion. New governmental policies based on scientific data are required as a matter of priority.
- Develop new strategies including arid area ecological protection and restoration programs to promote sustainable use of natural resources and highlight the finite availability of water in Tabuk.
- Monitor urban expansion and preserve the remaining biodiversity and groundwater in the arid ecosystem of Tabuk. For sustainable urban development, plans should consider limiting urban development to within the boundaries of existing urban areas and focusing on infrastructure restoration and regeneration programs.
- Encourage movement of people towards other governorates in the Tabuk region to alleviate demands on resources in Tabuk city. There is currently a high wave of migration from many governorates within Tabuk region to the city of Tabuk to benefit from the services available in the city.
- Support farmers to stop damaging farming practices to enhance and sustain land and natural resources. Education of farmers and residents about the environmental problems affecting their region and providing technical assistance would help to improve agricultural practices.
- Improve the efficiency of water use in agricultural areas. Use of modern irrigation methods and optimal selection of crops to minimise excessive irrigation would go a long way conserving limited water resources in Tabuk city.

- Define and implement policies at the local and national government levels that specifically address sustainable groundwater management in response to the rising water insecurity concerns highlighted by this research. Such policies will protect groundwater resources for present and future generations.
- Empower MEWA with the authority to enforce compulsory monitoring and reporting of metrics required for effective groundwater management. This should include reporting on groundwater drawdown, groundwater use, and groundwater elevation. It is recommended that monitoring programs be integrated between different governorates to allow for comparison.
- Conduct further research on the connection between remote sensing, modelling, and in-situ observations of LULC to address land degradation and salinization problems which the main environmental problems identified in the study area.
- Educate local and regional actors about the negative environmental impacts of unsustainable agricultural practices such as inappropriate crop selection and groundwater wastage.
- Establish a government-funded environmental research centre in the Tabuk region that contributes to the scientific body of knowledge of the area and increases awareness of the importance of environmental conservation and the need to mitigate the negative ecological impacts.
- Shift agricultural activities to the southern cities of Saudi Arabia where there are better arable land and higher rainfall. This could help to meet the increasing demand for agricultural products, improve efficiency of land use, and relieve the pressure on Tabuk's ecological fragile areas.
- Integrate geospatial techniques to gain a better understanding of changes in LULC and integrate LULC change in the decision-making of urban planners and policymakers.
- Conduct further research to assess whether urban land use has changed in Tabuk city in response to land use policies in other Tabuk governorates and compare the results. Such a study would support revision of ineffective local

government programs to promote sustainable land use and minimise the negative impacts of urbanisation.

- Incorporate socio-economic, demographic, and environmental factors in future studies that use the MCCA model prediction to gain a more detailed interpretation of the future patterns of land use growth.
- Investigate the relationship between human activity and urban growth in arid and semi-arid cities through the prism of sustainable development to better understand the impacts and inform policymakers.
- Extend this research by assessing the impact of water demand from other sectors (e.g., industry and tourism) to complement the work already done for the agricultural and urban sectors.
- Future research could be done based on the coupling between remote sensing e.g., Gravity Recovery and Climate Experiment (GRACE) satellite gravity data and in-situ observations to monitor groundwater variation and availability.

7. 2 Study limitations

This study used remote satellite data, real-time climate data, and water data to assess the impact of LULC changes on groundwater. Although the Ministry of Water in Tabuk started to monitor groundwater for urban areas since 1995, not all urban wells were regulated or monitored. Most of the groundwater data found was retrieved from an archive and provided in hard copy. Much was incomplete and/or inconsistent.

The following, therefore, have been considered in the research analysis:

- Data availability, quality, and reliability
- Modelling techniques and applicability.

There were no records for agricultural wells or monitoring of water data for irrigated agricultural land. Therefore, interpreting water use in this study was constrained by

available data. As a result, alternative methods were required to estimate water use for agriculture, specifically, for crop irrigation.

The analysis provided thorough LULC data and information on groundwater status and related environmental issues in the study area. Including exact agricultural groundwater withdrawal data, could provide more accurate results and further useful information. The study only considered the available groundwater data so there is room to improve this work with additional data in future.

In terms of groundwater, there was uncertainty in calculating crop water requirement and urban water demand due to limitations in the availability of water data. As such, water requirements for 2025 and 2035 could not be modelled because historical water withdrawal data was not accurate or was inadequate.

References

Abburu, S., & Golla, S. B. (2015). Satellite image classification methods and techniques: A review. International journal of computer applications, 119(8).

Abdelatti, H., Elhadary, Y., & Babiker, A. A. (2017). Nature and Trend of Urban Growth in Saudi Arabia: The Case of Al-Ahsa Province–Eastern Region. Resources and Environment, 7(3), 69-80.

Abderrahman, W. (2003). Should intensive use of non-renewable groundwater resources always be rejected? Intensive Use of Groundwater: Challenges and Opportunities, 191-203.

Abdul Salam, A., Elsegaey, I., Khraif, R., & Al-Mutairi, A. (2014). Population distribution and household conditions in Saudi Arabia: reflections from the 2010 Census. SpringerPlus, 3(1), 530.

Abdullahi, S., Pradhan, B., & Mojaddadi, H. (2018). City compactness: Assessing the influence of the growth of residential land use. Journal of Urban Technology, 25(1), 21-46.

Aboneama, W. A. (2018). Creating a Unique Sustainable Rating System for Saudi Arabia to Achieve Environmental Assessment and 2030 Vision. European Journal of Sustainable Development, 7(4), 269-279.

Afify, H. A. (2011). Evaluation of change detection techniques for monitoring land-cover changes: A case study in new Burg El-Arab area. Alexandria Engineering Journal, 50(2), 187-195.

Aguirre-Gutiérrez, J., Seijmonsbergen, A. C., & Duivenvoorden, J. F. (2012). Optimizing land cover classification accuracy for change detection, a combined pixel-based and object-based approach in a mountainous area in Mexico. Applied geography, 34, 29-37.

Ahmed, B., & Ahmed, R. (2012). Modeling Urban Land Cover Growth Dynamics Using Multi-Temporal Satellite Images: A Case Study of Dhaka, Bangladesh. ISPRS International Journal of Geo-Information, 1(1), 3.

AI-Taher, A. A. (1992). Estimation of potential evapotranspiration in Al-Hassa oasis, Saudi Arabia. GeoJournal, 26(3), 371-379.

Aina, Y. A., Wafer, A., Ahmed, F., & Alshuwaikhat, H. M. (2019). Top-down sustainable urban development? Urban governance transformation in Saudi Arabia. Cities, 90, 272-281.

Akın, A., Sunar, F., & Berberoğlu, S. (2015). Urban change analysis and future growth of Istanbul. Environmental monitoring and assessment, 187(8), 506.

Al-Ahmadi, & Hames, A. (2009). Comparison of four classification methods to extract land use and land cover from raw satellite images for some remote arid areas, kingdom of Saudi Arabia. Earth, 20(1), 167-191.

Al-Ahmadi, M. E. (2009). Hydrogeology of the Saq Aquifer Northwest of Tabuk, Northern Saudi Arabia. Journal of King Abdulaziz University: Earth Sciences, 20, 51-66.

Al-Bakri, J. T., Salahat, M., Suleiman, A., Suifan, M., Hamdan, M. R., Khresat, S., & Kandakji, T. (2013). Impact of climate and land use changes on water and food security in jordan: Implications for transcending “the tragedy of the commons”. Sustainability, 5(2), 724-748.

Al-Bilbisi, H. H., & Makhamreh, Z. M. (2010). A Comparison of Pixel-Based and Object-Based Classification Approaches in Arid and Semi-Arid Areas of Dead Sea Region Using Landsat Imagery. Dirasat: Human & Social Sciences, 37(3).

Al-Filali, I. Y., & Gallarotti, G. M. (2012). Smart development: Saudi Arabia's quest for a knowledge economy. International Studies, 49(1-2), 47-76.

Al-Ghobari, H. M. (2000). Estimation of reference evapotranspiration for southern region of Saudi Arabia. Irrigation Science, 19(2), 81-86.

Al-Harbi, K. (2010). Monitoring of agricultural area trend in Tabuk region–Saudi Arabia using Landsat TM and SPOT data. The Egyptian Journal of Remote Sensing and Space Science, 13(1), 37-42.

Al-Ibrahim, A. A. (1991). Excessive use of groundwater resources in Saudi Arabia: Impacts and policy options. Ambio, 34-37.

Al-Khalifeh, A. H. (1993). "Population spatial distribution policies in Saudi Arabia." In Economic. United Nations (Ed.), Population Spatial Distribution.

Al-Momani, A., & Shawaqfah, M. a. (2013). Assessment and management of flood risks at the city of Tabuk, Saudi Arabia. The Holistic Approach to Environment, 3(1), 15-31.

Al-Naeem, A. A. (2014). Effect of Excess Pumping on Groundwater Salinity and Water Level in Hail Region of Saudi Arabia. Research Journal of Environmental Toxicology, 8(3), 124.

Al-Salamah, I. S., Ghazaw, Y. M., & Ghumman, A. R. (2011). Groundwater modeling of Saq Aquifer Buraydah Al Qassim for better water management strategies. Environmental monitoring and assessment, 173(1-4), 851-860.

Al-sharif, A. A., & Pradhan, B. (2014). Monitoring and predicting land use change in Tripoli Metropolitan City using an integrated Markov chain and cellular automata models in GIS. Arabian Journal of Geosciences, 7(10), 4291-4301.

Al-Shayaa, M. S., Baig, M. B., & Straquadine, G. S. (2012). Agricultural extension in the Kingdom of Saudi Arabia: Difficult present and demanding future. J. Anim. Plant Sci, 22(1), 239-246.

Al-Sheikh, H. M. (1997). Appendix 8: Country case study–water policy reform in Saudi Arabia. Proceedings of the second expert consultation on national water policy reform in the Near East, 24-25.

Al Harbi, K. (2003). Discovering and detecting agricultural change in Eastern Tabuk -Saudi Arabia, using remote sensing technique. Kuwaiti Geographic Society, 283.

Al Humaidi, I. A. (2004). Internal Migration in Saudi Arabia: Its Magnitude and Trends. Journal of King Saud University, 16(1).

Al Rajhi, A., Al Salamah, A., Malik, M., & Wilson, R. (2012). Economic Development in Saudi Arabia: Routledge.

Alamri, Y., & Al-Duwais, A. (2019). Food Security in Saudi Arabia (Case Study: Wheat, Barley, and Poultry). Journal of Food Security, 7(2), 36-39.

Alatawi. Nasser. (2015). Tabuk Dictionary (Second ed.).

Albalawi, E., Dewan, A., & Corner, R. (2018). Spatio-temporal analysis of land use and land cover changes in arid region of Saudi Arabia. International Journal of Geomate, 14(44), 73-81.

Albassam, B. A. (2015). Economic diversification in Saudi Arabia: Myth or reality? Resources Policy, 44, 112-117.

Albhaisi, M., Brendonck, L., & Batelaan, O. (2013). Predicted impacts of land use change on groundwater recharge of the upper Berg catchment, South Africa. Water SA, 39(2), 211-220.

Alexakis, D., Grillakis, M., Koutroulis, A., Agapiou, A., Themistocleous, K., Tsanis, I., Aristeidou, K. (2014). GIS and remote sensing techniques for the assessment of land use change impact on flood hydrology: the case study of Yialias basin in Cyprus. Natural Hazards and Earth System Science, 14(2), 413-426.

Algahtani, O. S., Salama, A. S., Iliyasu, A. M., Selim, B. A., & Kheder, K. (2015). Monitoring Urban and Land Use Changes in Al-Kharj Saudi Arabia using Remote Sensing Techniques. In Progress in Systems Engineering (pp. 515-523): Springer.

Alhowaish, A. K. (2015). Eighty years of urban growth and socioeconomic trends in Dammam Metropolitan Area, Saudi Arabia. Habitat International, 50, 90-98.

Aljoufie, M., Zuidgeest, M., Brussel, M., & van Maarseveen, M. (2013). Spatial–temporal analysis of urban growth and transportation in Jeddah City, Saudi Arabia. Cities, 31, 57-68.

Allam, M., Bakr, N., & Elbably, W. (2019). Multi-temporal assessment of land use/land cover change in arid region based on landsat satellite imagery: Case study in Fayoum Region, Egypt. Remote Sensing Applications: Society and Environment, 14, 8-19.

Allen, R. G., Pereira, L. S., Raes, D., & Smith, M. (1998). Crop evapotranspiration-Guidelines for computing crop water requirements-FAO Irrigation and drainage paper 56. FAO, Rome, 300(9), D05109.

Allen, R. G., & Pruitt, W. O. (1986). Rational use of the FAO Blaney-Criddle formula. Journal of Irrigation and Drainage Engineering, 112(2), 139-155.

Allen, R. R., Bhatti, A. U., Butcher, W. R., Cook, R. J., Day, J. C., Elliott, L. F., Hughes, D. W. (2013). Advances in Soil Science: Dryland Agriculture: Strategies for Sustainability: Springer New York.

Almazroui, M., Nazrul Islam, M., Athar, H., Jones, P., & Rahman, M. A. (2012). Recent climate change in the Arabian Peninsula: annual rainfall and temperature analysis of Saudi Arabia for 1978–2009. International Journal of Climatology, 32(6), 953-966.

Alqurashi, A. F., & Kumar, L. (2014). Land Use and Land Cover Change Detection in the Saudi Arabian Desert Cities of Makkah and Al-Taif Using Satellite Data. Advances in Remote Sensing, 3(03), 106.

Alzahrani, K. H., Muneer, S. E., Taha, A. S., & Baig, M. B. (2012). Appropriate cropping pattern as an approach to enhancing irrigation water efficiency in the Kingdom of Saudi Arabia. J Anim Plant Sci, 22(1), 224-232.

Anderson, J. R. (1976). A land use and land cover classification system for use with remote sensor data (Vol. 964): US Government Printing Office.

Angel, S., Parent, J., & Civco, D. (2007). Urban sprawl metrics: an analysis of global urban expansion using GIS. Paper presented at the Proceedings of ASPRS 2007 Annual Conference, Tampa, Florida May.

Angel, S., Parent, J., & Civco, D. L. (2012). The fragmentation of urban landscapes: global evidence of a key attribute of the spatial structure of cities, 1990–2000. Environment and Urbanization, 24(1), 249-283.

Araya, Y. H., & Cabral, P. (2010). Analysis and modeling of urban land cover change in Setúbal and Sesimbra, Portugal. Remote Sensing, 2(6), 1549-1563.

Arnous, M. O., El-Rayes, A. E., & Helmy, A. M. (2017). Land-use/land-cover change: a key to understanding land degradation and relating environmental impacts in Northwestern Sinai, Egypt. Environmental Earth Sciences, 76(7), 263.

Asif, M. (2016). Growth and sustainability trends in the buildings sector in the GCC region with reference to the KSA and UAE. Renewable and Sustainable Energy Reviews, 55, 1267-1273.

Aslami, F., & Ghorbani, A. (2018). Object-based land-use/land-cover change detection using Landsat imagery: a case study of Ardabil, Namin, and Nir counties in northwest Iran. Environmental monitoring and assessment, 190(7), 376.

Azhar, A. H., & Perera, B. (2011). Evaluation of reference evapotranspiration estimation methods under southeast Australian conditions. Journal of Irrigation and Drainage Engineering, 137(5), 268-279.

Bai, Y., Ochuodho, T. O., & Yang, J. (2019). Impact of land use and climate change on water-related ecosystem services in Kentucky, USA. Ecological indicators, 102, 51-64.

Baier, W., & Robertson, G. W. (1965). Estimation of latent evaporation from simple weather observations. Canadian journal of plant science, 45(3), 276-284.

Baig, M. B., & Straquadine, G. S. (2014). Sustainable agriculture and rural development in the Kingdom of Saudi Arabia: implications for agricultural extension and education. In Vulnerability of agriculture, water and fisheries to climate change (pp. 101-116): Springer.

Banskota, A., Kayastha, N., Falkowski, M. J., Wulder, M. A., Froese, R. E., & White, J. C. (2014). Forest monitoring using Landsat time series data: A review. Canadian Journal of Remote Sensing, 40(5), 362-384.

Barakat, A., Ouargaf, Z., Khellouk, R., El Jazouli, A., & Touhami, F. (2019). Land Use/Land Cover Change and Environmental Impact Assessment in Béni-Mellal District (Morocco) Using Remote Sensing and GIS. Earth Systems and Environment, 3(1), 113-125.

Barati, S., Rayegani, B., Saati, M., Sharifi, A., & Nasri, M. (2011). Comparison the accuracies of different spectral indices for estimation of vegetation cover fraction in sparse vegetated areas. The Egyptian Journal of Remote Sensing and Space Science, 14(1), 49-56.

Barbero-Sierra, C., Marques, M.-J., & Ruíz-Pérez, M. (2013). The case of urban sprawl in Spain as an active and irreversible driving force for desertification. Journal of Arid Environments, 90, 95-102.

Barona, P. C., & Mena, C. (2014). Using Remote Sensing and a Cellular Automata-Markov chains-GEOMOD model for the quantification of the future spread of an invasive plant: a case study of Psidium guajava in Isabela Island, Galapagos.

Batty, M. (2008). Cities as complex systems: scaling, interactions, networks, dynamics, and urban morphologies.

Batty, M. (2012). Building a science of cities. Cities, 29, Supplement 1, S9-S16.

Batty, M. (2017). Science in planning: theory, methods and models. Planning Research and Knowledge, 241-254.

Bhaskaran, S., Paramananda, S., & Ramnarayan, M. (2010). Per-pixel and object-oriented classification methods for mapping urban features using Ikonos satellite data. Applied geography, 30(4), 650-665.

Borrelli, P., Robinson, D. A., Fleischer, L. R., Lugato, E., Ballabio, C., Alewell, C., Ferro, V. (2017). An assessment of the global impact of 21st century land use change on soil erosion. Nature communications, 8(1), 1-13.

Bozkaya, A. G., Balcik, F. B., Goksel, C., & Esbah, H. (2015). Forecasting land-cover growth using remotely sensed data: a case study of the Igneada protection area in Turkey. Environmental monitoring and assessment, 187(3), 59.

Bürgi, M., Bieling, C., Von Hackwitz, K., Kizos, T., Lieskovský, J., Martín, M. G., Plieninger, T. (2017). Processes and driving forces in changing cultural landscapes across Europe. Landscape Ecology, 32(11), 2097-2112.

Cai, J., Liu, Y., Lei, T., & Pereira, L. S. (2007). Estimating reference evapotranspiration with the FAO Penman–Monteith equation using daily weather forecast messages. Agricultural and Forest Meteorology, 145(1-2), 22-35.

Campbell, & Wynne. (2011). Introduction to remote sensing: Guilford Press.

Campbell, J. B. (2002). Introduction to Remote Sensing. New York: The Guilford Press; 3 edition.

Carley, M., & Christie, I. (2017). Managing sustainable development: Routledge.

Castillejo-González, I. L., Angueira, C., García-Ferrer, A., & Sánchez de la Orden, M. (2019). Combining object-based image analysis with topographic data for landform mapping: a case study in the semi-arid Chaco ecosystem, Argentina. ISPRS International Journal of Geo-Information, 8(3), 132.

CDSI, (2018). Umrah Statistics Bulletin 2018. the Central Department of Statistics and Information Retrieved from www.stats.gov.sa/sites/default/files/umrah_statistics_bulletin_2018_en.pdf

Celio, E., Koellner, T., & Grêt-Regamey, A. (2014). Modeling land use decisions with Bayesian networks: Spatially explicit analysis of driving forces on land use change. Environmental Modelling & Software, 52, 222-233.

Chavez, P. S. (1996). Image-based atmospheric corrections-revisited and improved. Photogrammetric engineering and remote sensing, 62(9), 1025-1035.

Cheeseman, J. (2016). Food security in the face of salinity, drought, climate change, and population growth. In Halophytes for Food Security in Dry Lands (pp. 111-123): Elsevier.

Chen, G., Weng, Q., Hay, G. J., & He, Y. (2018). Geographic object-based image analysis (GEOBIA): emerging trends and future opportunities. GIScience & Remote Sensing, 55(2), 159-182.

Chen, L., Chien, T.-W., Hsu, C.-S., Tan, C.-H., Hsu, H.-Y., & Kou, C.-H. (2019). Water Requirement for Irrigation of Complicated Agricultural Land by Using Classified Airborne Digital Sensor Images. Journal of the Indian Society of Remote Sensing, 47(8), 1307-1314.

Chen, Y., Li, X., Liu, X., Ai, B., & Li, S. (2016). Capturing the varying effects of driving forces over time for the simulation of urban growth by using survival analysis and cellular automata. Landscape and Urban Planning, 152, 59-71.

Chaudhry, K. A. (1997). The Price of Wealth: Economies and Institutions in the Middle East: Cornell University Press.

Chowdhury, S., Al-Zahrani, M., & Abbas, A. (2016). Implications of climate change on crop water requirements in arid region: an example of Al-Jouf, Saudi Arabia. Journal of King Saud University-Engineering Sciences, 28(1), 21-31.

Clarke, Hoppen, & Gaydos. (1997). A self-modifying cellular automaton model of historical urbanization in the San Francisco Bay area. Environment and planning B: Planning and design, 24(2), 247-261.

Cohen, J. (1960). A coefficient of agreement for nominal scales. Educational and psychological measurement, 20(1), 37-46.

Congalton, R. G. (1991). A review of assessing the accuracy of classifications of remotely sensed data. Remote Sensing of Environment, 37(1), 35-46.

Conrad, C., Rudloff, M., Abdullaev, I., Thiel, M., Löw, F., & Lamers, J. (2015). Measuring rural settlement expansion in Uzbekistan using remote sensing to support spatial planning. Applied geography, 62, 29-43.

Coppin, P., Jonckheere, I., Nackaerts, K., Muys, B., & Lambin, E. (2004). Review ArticleDigital change detection methods in ecosystem monitoring: a review. International Journal of Remote Sensing, 25(9), 1565-1596.

Cordesman, A. H. (2003). Saudi Arabia Enters the 21st Century: Praeger.

Corner, R. J., Dewan, A. M., & Chakma, S. (2014). Monitoring and prediction of land-use and land-cover (LULC) change. In Dhaka Megacity (pp. 75-97): Springer.

Costa, H., Foody, G. M., & Boyd, D. S. (2017). Using mixed objects in the training of object-based image classifications. Remote Sensing of Environment, 190, 188-197.

Cuadrado-Quesada, G., & Rayfuse, R. (2020). Towards Sustainability in Groundwater Use: An Exploration of Key Drivers Motivating the Adoption and Implementation of Policy and Regulation. Journal of Environmental Law, 32(1), 111-137.

Dang, A. N., & Kawasaki, A. (2016). A review of methodological integration in land-use change models. International Journal of Agricultural and Environmental Information Systems (IJAEIS), 7(2), 1-25.

Deep, S., & Saklani, A. (2014). Urban sprawl modeling using cellular automata. The Egyptian Journal of Remote Sensing and Space Science, 17(2), 179-187.

Djaman, K., Balde, A. B., Sow, A., Muller, B., Irmak, S., N'Diaye, M. K., Saito, K. (2015). Evaluation of sixteen reference evapotranspiration methods under sahelian conditions in the Senegal River Valley. Journal of Hydrology: Regional Studies, 3, 139-159.

Djaman, K., Irmak, S., & Futakuchi, K. (2017). Daily reference evapotranspiration estimation under limited data in Eastern Africa. Journal of Irrigation and Drainage Engineering, 143(4), 06016015.

Doell, P., Mueller Schmied, H., Schuh, C., Portmann, F. T., & Eicker, A. (2014). Global-scale assessment of groundwater depletion and related groundwater abstractions: Combining hydrological modeling with information from well observations and GRACE satellites. Water Resources Research, 50(7), 5698-5720.

Doorenbos, J., & Pruitt, W. (1977). Crop water requirements. FAO Irrigation and drainage paper No. 24. FAO, Rome, 34-37.

Duro, D. C., Franklin, S. E., & Dubé, M. G. (2012). A comparison of pixel-based and object-based image analysis with selected machine learning algorithms for the classification of agricultural landscapes using SPOT-5 HRG imagery. Remote Sensing of Environment, 118, 259-272.

Eastman, & Toledano, J. (2018). A Short Presentation of CA_MARKOV. In M. T. Camacho Olmedo, M. Paegelow, J.-F. Mas, & F. Escobar (Eds.), Geomatic

Approaches for Modeling Land Change Scenarios (pp. 481-484). Cham: Springer International Publishing.

Eastman, J. (2016). IDRISI Terrset Manual. Clark Labs-Clark University: Worcester, MA, USA.

Eastman, J. R. (2009). IDRISI Taiga guide to GIS and image processing. Clark Labs Clark University, Worcester, MA.

Eckert, S. (2011). Urban expansion and its impact on urban agriculture–remote sensing-based change analysis of Kizinga and Mzinga valley–DAR ES SALAAM, Tanzania. Paper presented at the European Association of Remote Sensing Laboratories, EARSeL Proceedings, Strasbourg, France.

Eerens, H., Haesen, D., Rembold, F., Urbano, F., Tote, C., & Bydekerke, L. (2014). Image time series processing for agriculture monitoring. Environmental Modelling & Software, 53, 154-162.

El-Hattab, M. M. (2016). Applying post classification change detection technique to monitor an Egyptian coastal zone (Abu Qir Bay). The Egyptian Journal of Remote Sensing and Space Science, 19(1), 23-36.

El-Kawy, O. A., Rød, J., Ismail, H., & Suliman, A. (2011). Land use and land cover change detection in the western Nile delta of Egypt using remote sensing data. Applied geography, 31(2), 483-494.

Elhadj, E. (2004). Camels don't fly, deserts don't bloom: An assessment of Saudi Arabia's experiment in desert agriculture. Occasional paper, 48(6).

Erener, A., Düzgün, S., & Yalciner, A. C. (2012). Evaluating land use/cover change with temporal satellite data and information systems. Procedia Technology, 1, 385-389.

Famiglietti, J. S. (2014). The global groundwater crisis. Nature Climate Change, 4(11), 945-948.

Feng, Y., Jia, Y., Cui, N., Zhao, L., Li, C., & Gong, D. (2017). Calibration of Hargreaves model for reference evapotranspiration estimation in Sichuan basin of southwest China. Agricultural Water Management, 181, 1-9.

Feng, Y., Yang, Q., Hong, Z., & Cui, L. (2018). Modelling coastal land use change by incorporating spatial autocorrelation into cellular automata models. Geocarto International, 33(5), 470-488.

Fiaz, S., Noor, M. A., & Aldosri, F. O. (2018). Achieving food security in the Kingdom of Saudi Arabia through innovation: Potential role of agricultural extension. Journal of the Saudi Society of Agricultural Sciences, 17(4), 365-375.

Fishman, R. M., Siegfried, T., Raj, P., Modi, V., & Lall, U. (2011). Over-extraction from shallow bedrock versus deep alluvial aquifers: Reliability versus sustainability considerations for India's groundwater irrigation. Water Resources Research, 47(6).

Foody, G. M. (2002). Status of land cover classification accuracy assessment. Remote Sensing of Environment, 80(1), 185-201.

Franklin, S., & Wulder, M. (2002). Remote sensing methods in medium spatial resolution satellite data land cover classification of large areas. Progress in Physical Geography, 26(2), 173-205.

Fudge, S., Peters, M., Hoffman, S. M., & Wehrmeyer, W. (2013). The Global Challenge of Encouraging Sustainable Living: Opportunities, Barriers, Policy and Practice: Edward Elgar Publishing.

Galletti, C. S., & Myint, S. W. (2014). Land-use mapping in a mixed urban-agricultural arid landscape using object-based image analysis: A case study from Maricopa, Arizona. Remote Sensing, 6(7), 6089-6110.

Gassert, F., Reig, P., Tianyi, l., & Andrew, m. (2013). Aqueduct country and river basin rankings a weighted aggregation of spatially distinct hydrological i. World Resources Institute, Working Paper.

Ghaffar, A. (2015). Use of geospatial techniques in monitoring urban expansion and land use change analysis: a case of Lahore, Pakistan. Journal of Basic & Applied Sciences, 11, 265.

Ghanim, A. (2019). Water Resources Crisis in Saudi Arabia, Challenges and Possible Management Options: An Analytic Review. International Journal of Environmental and Ecological Engineering, 13(2), 51-56.

Ghosh, P., Mukhopadhyay, A., Chanda, A., Mondal, P., Akhand, A., Mukherjee, S., Ghosh, T. (2017). Application of Cellular automata and Markov-chain model in geospatial environmental modeling-A review. Remote Sensing Applications: Society and Environment, 5, 64-77.

Gidey, E., Dikinya, O., Sebego, R., Segosebe, E., & Zenebe, A. (2017). Cellular automata and Markov Chain (CA_Markov) model-based predictions of future land use and land cover scenarios (2015–2033) in Raya, northern Ethiopia. Modeling Earth Systems and Environment, 3(4), 1245-1262.

Giri, C. P. (2016). Remote Sensing of Land Use and Land Cover: Principles and Applications: CRC Press.

Goodin, D. G., Anibas, K. L., & Bezymennyi, M. (2015). Mapping land cover and land use from object-based classification: an example from a complex agricultural landscape. International Journal of Remote Sensing, 36(18), 4702-4723.

Guan, D., Gao, W., Watari, K., & Fukahori, H. (2008). Land use change of Kitakyushu based on landscape ecology and Markov model. Journal of Geographical Sciences, 18(4), 455-468.

Guan, D., Li, H., Inohae, T., Su, W., Nagaie, T., & Hokao, K. (2011). Modeling urban land use change by the integration of cellular automaton and Markov model. Ecological Modelling, 222(20), 3761-3772.

Guidigan, M. L. G., Sanou, C. L., Ragatoa, D. S., Fafa, C. O., & Mishra, V. N. (2019). Assessing Land Use/Land Cover Dynamic and Its Impact in Benin Republic Using Land Change Model and CCI-LC Products. Earth Systems and Environment, 3(1), 127-137.

Halmy, M. W. A., Gessler, P. E., Hicke, J. A., & Salem, B. B. (2015). Land use/land cover change detection and prediction in the northwestern coastal desert of Egypt using Markov-CA. Applied geography, 63, 101-112.

Hamon, W. R. (1963). Computation of direct runoff amounts from storm rainfall. International Association of Scientific Hydrology Publication, 63, 52-62.

Hansen, M. C., & Loveland, T. R. (2012). A review of large area monitoring of land cover change using Landsat data. Remote Sensing of Environment, 122, 66-74.

Hargreaves, G. H., & Samani, Z. A. (1985). Reference crop evapotranspiration from temperature. Applied engineering in agriculture, 1(2), 96-99.

Harrington, L., Harrington Jr, J., & Kettle, N. (2007). Groundwater depletion and agricultural land use change in the high plains: a case study from Wichita County, Kansas. The Professional Geographer, 59(2), 221-235.

Hasanean, H., & Almazroui, M. (2015). Rainfall: features and variations over Saudi Arabia, a review. Climate, 3(3), 578-626.

Hassan, Z., Shabbir, R., Ahmad, S. S., Malik, A. H., Aziz, N., Butt, A., & Erum, S. (2016). Dynamics of land use and land cover change (LULCC) using geospatial techniques: a case study of Islamabad Pakistan. SpringerPlus, 5(1), 812.

He, C., Gao, B., Huang, Q., Ma, Q., & Dou, Y. (2017). Environmental degradation in the urban areas of China: Evidence from multi-source remote sensing data. Remote Sensing of Environment, 193, 65-75.

He, S., Wang, X., Dong, J., Wei, B., Duan, H., Jiao, J., & Xie, Y. (2019). Three-Dimensional Urban Expansion Analysis of Valley-Type Cities: A Case Study of Chengguan District, Lanzhou, China. Sustainability, 11(20), 5663.

Hegazy, I. R., & Kaloop, M. R. (2015). Monitoring urban growth and land use change detection with GIS and remote sensing techniques in Daqahlia governorate Egypt. International Journal of Sustainable Built Environment.

Henriques, C., & Tenedório, J. (2009). Remote sensing, GIS application and simulation of coastal land use changes based on cellular automata: a case study of Maputo, Mozambique. Journal of Coastal Research (56), 1518.

Hereher, M. E., Al-Shammari, A. M., & Allah, S. E. A. (2012). Land Cover Classification of Hail—Saudi Arabia Using Remote Sensing. International Journal of Geosciences, 3(02), 349.

Hussain, G., Alquwaizany, A., & Al-Zarah, A. (2010). Guidelines for irrigation water quality and water management in the Kingdom of Saudi Arabia: An overview. Journal of Applied Sciences, 10(2), 79-96.

Jakeman, A. J., Barreteau, O., Hunt, R. J., Rinaudo, J.-D., & Ross, A. (2016). Integrated groundwater management: Springer Nature.

Jensen. (2004). Digital change detection. Introductory digital image processing: A remote sensing perspective, 467-494

Jin, X. (2018). ENVI Automated Image Registration Solutions. Harris Geospatial Solution Inc.: Broomfield, Colorado, USA.

Jones, J. A. A. (2014). Water sustainability: a global perspective: Routledge.

Joshi, N., Baumann, M., Ehammer, A., Fensholt, R., Grogan, K., Hostert, P., Mitchard, E. T. (2016). A review of the application of optical and radar remote sensing data fusion to land use mapping and monitoring. Remote Sensing, 8(1), 70.

Kantakumar, L. N., & Neelamsetti, P. (2015). Multi-temporal land use classification using hybrid approach. The Egyptian Journal of Remote Sensing and Space Science, 18(2), 289-295.

Karimi, H., Jafarnezhad, J., Khaledi, J., & Ahmadi, P. (2018). Monitoring and prediction of land use/land cover changes using CA-Markov model: a case study of Ravansar County in Iran. Arabian Journal of Geosciences, 11(19), 592.

Kaur, S., & Vatta, K. (2015). Groundwater depletion in Central Punjab: pattern, access and adaptations. Current Science, 485-490.

Kazak, J. K. (2018). The use of a decision support system for sustainable urbanization and thermal comfort in adaptation to climate change actions—The case of the Wrocław larger urban zone (Poland). Sustainability, 10(4), 1083.

Khan, M. (2016). Saudi Arabia's vision 2030. Defence Journal, 119(11), 36-42.

Kharrufa, N. S. (1985). Simplified equation for evapotranspiration in arid regions. Beiträge zur Hydrologie Sonderheft, 5(1), 39-47.

Khawaldah, H. A. (2016). A prediction of future land use/land cover in Amman area using GIS-based Markov Model and remote sensing. Journal of Geographic Information System, 8(3), 412-427.

Khraif, R. M., Salam, A. A., Nair, P., & Elsegaey, I. (2019). Migration in Saudi Arabia: Present and Prospects. In India's Low-Skilled Migration to the Middle East (pp. 99-123): Springer.

Kong, F., Yin, H., Nakagoshi, N., & James, P. (2012). Simulating urban growth processes incorporating a potential model with spatial metrics. Ecological indicators, 20, 82-91.

Kramm, T., Hoffmeister, D., Curdt, C., Maleki, S., Khormali, F., & Kehl, M. (2017). Accuracy assessment of landform classification approaches on different spatial scales for the Iranian loess plateau. ISPRS International Journal of Geo-Information, 6(11), 366.

Kumar, S., Radhakrishnan, N., & Mathew, S. (2014). Land use change modelling using a Markov model and remote sensing. Geomatics, Natural Hazards and Risk, 5(2), 145-156.

Kux, H., & Souza, U. D. (2012). Object-based image analysis of WORLDVIEW-2 satellite data for the classification of mangrove areas in the city of São Luís, Maranhão State, Brazil. ISPRS Annals of Photogrammetry, Remote Sensing and Spatial Information Sciences, 1, 95-100.

Lambin, E. F., & Meyfroidt, P. (2011). Global land use change, economic globalization, and the looming land scarcity. Proceedings of the National Academy of Sciences, 108(9), 3465-3472.

Lamqadem, A. A., Saber, H., & Pradhan, B. (2019). Long-Term Monitoring of Transformation from Pastoral to Agricultural Land Use Using Time-Series Landsat Data in the Feija Basin (Southeast Morocco). Earth Systems and Environment, 3(3), 525-538.

Lebourgeois, V., Dupuy, S., Vintrou, É., Ameline, M., Butler, S., & Bégué, A. (2017). A combined random forest and OBIA classification scheme for mapping smallholder agriculture at different nomenclature levels using multisource data (simulated Sentinel-2 time series, VHRS and DEM). Remote Sensing, 9(3), 259.

Leeson, G. W. (2018). The growth, ageing and urbanisation of our world. Journal of Population Ageing, 11(2), 107-115.

Li, M., Zang, S., Zhang, B., Li, S., & Wu, C. (2014). A review of remote sensing image classification techniques: The role of spatio-contextual information. European Journal of Remote Sensing, 47, 389-411.

Lillesand, T., Kiefer, R. W., & Chipman, J. (2014). Remote sensing and image interpretation. New York: John Wiley & Sons.

Lin, X., Xu, M., Cao, C., P Singh, R., Chen, W., & Ju, H. (2018). Land-Use/Land-Cover changes and their influence on the ecosystem in Chengdu City, China during the Period of 1992–2018. Sustainability, 10(10), 3580.

Linacre, E. T. (1977). A simple formula for estimating evaporation rates in various climates, using temperature data alone. Agricultural meteorology, 18(6), 409-424.

Liping, C., Yujun, S., & Saeed, S. (2018). Monitoring and predicting land use and land cover changes using remote sensing and GIS techniques—A case study of a hilly area, Jiangle, China. PloS one, 13(7).

Louca, M., Vogiatzakis, I. N., & Moustakas, A. (2015). Modelling the combined effects of land use and climatic changes: Coupling bioclimatic modelling with Markov-chain Cellular Automata in a case study in Cyprus. Ecological Informatics, 30, 241-249.

Loures, L. C. (2019). Introductory chapter: land-use planning, and land-use change as catalysts of sustainable development. In Land Use-Assessing the Past, Envisioning the Future: IntechOpen.

Löw, F., Fliemann, E., Abdullaev, I., Conrad, C., & Lamers, J. P. A. (2015). Mapping abandoned agricultural land in Kyzyl-Orda, Kazakhstan using satellite remote sensing. Applied geography, 62, 377-390.

Lu, D., Hetrick, S., Moran, E., & Li, G. (2010). Detection of urban expansion in an urban-rural landscape with multitemporal QuickBird images. Journal of applied remote sensing, 4(041880), 041880.

Lu, D., Mausel, P., Brondizio, E., & Moran, E. (2004). Change detection techniques. International Journal of Remote Sensing, 25(12), 2365-2401.

Lu, D., & Weng, Q. (2007). A survey of image classification methods and techniques for improving classification performance. International Journal of Remote Sensing, 28(5), 823-870.

Lu, D., Weng, Q., Moran, E., Li, G., & Hetrick, S. (2011). Remote sensing image classification: CRC Press/Taylor and Francis: Boca Raton, FL, USA.

Luo, T., Young, R., & Reig, P. (2015). Aqueduct projected water stress country rankings. Technical Note. Retrieved from www.wri.org/publication/aqueduct-projected-water-stresscountry-rankings

Lyu, R., Zhang, J., & Xu, M. (2018). Integrating ecosystem services evaluation and landscape pattern analysis into urban planning based on scenario prediction and regression model. Chinese Journal of Population Resources and Environment, 16(3), 252-266.

Ma, L., Li, M., Ma, X., Cheng, L., Du, P., & Liu, Y. (2017). A review of supervised object-based land-cover image classification. ISPRS Journal of Photogrammetry and Remote Sensing, 130, 277-293.

MacLachlan, A., Biggs, E., Roberts, G., & Boruff, B. (2017). Urban growth dynamics in Perth, Western Australia: using applied remote sensing for sustainable future planning. Land, 6(1), 9.

Macleod, R. D., & Congalton, R. G. (1998). A quantitative comparison of change-detection algorithms for monitoring eelgrass from remotely sensed data. Photogrammetric engineering and remote sensing, 64(3), 207-216.

Madani, A., Niyazi, B., Elfakharani, A., & Osman, H. (2019). The Effects of Structural Elements on Groundwater of Wadi Yalamlam, Saudi Arabia Using Integration of Remote Sensing and Airborne Magnetic Survey. Earth Systems and Environment, 3(2), 301-312.

Maddocks, A., Young, R. S., & Reig, P. (2015). Ranking the world's most water-stressed countries in 2040. World Resources Institute, 26.

Madugundu, R., Al-Gaadi, K., Patil, V., & Tola, E. (2014). Detection of Land Use and Land Cover changes in Dirab region of Saudi Arabia using remotely sensed imageries. American Journal of Environmental Sciences, 10(1).

Mahmoud, M. I., Duker, A., Conrad, C., Thiel, M., & Ahmad, H. S. (2016). Analysis of settlement expansion and urban growth modelling using geoinformation for assessing potential impacts of urbanization on climate in Abuja City, Nigeria. Remote Sensing, 8(3), 220.

Mallampalli, V. R., Mavrommati, G., Thompson, J., Duveneck, M., Meyer, S., Ligmann-Zielinska, A., Kok, K. (2016). Methods for translating narrative scenarios into quantitative assessments of land use change. Environmental Modelling & Software, 82, 7-20.

Mas, J. F. (1999). Monitoring land-cover changes: A comparison of change detection techniques. International Journal of Remote Sensing, 20(1), 139-152.

Masini, E., Tomao, A., Barbati, A., Corona, P., Serra, P., & Salvati, L. (2019). Urban growth, land-use efficiency and local socioeconomic context: a comparative analysis of 417 metropolitan regions in Europe. Environmental management, 63(3), 322-337.

Mattar, M. A., Alazba, A., Alblewi, B., Gharabaghi, B., & Yassin, M. A. (2016). Evaluating and calibrating reference evapotranspiration models using water balance under hyper-arid environment. Water Resources Management, 30(11), 3745-3767.

Megahed, Y., Cabral, P., Silva, J., & Caetano, M. (2015). Land Cover Mapping Analysis and Urban Growth Modelling Using Remote Sensing Techniques in Greater Cairo Region—Egypt. ISPRS International Journal of Geo-Information, 4(3), 1750-1769.

Mendoza-Ponce, A., Corona-Núñez, R., Kraxner, F., Leduc, S., & Patrizio, P. (2018). Identifying effects of land use cover changes and climate change on terrestrial ecosystems and carbon stocks in Mexico. Global environmental change, 53, 12-23.

MEWA. (2015). The Ministry of Environment Water and Agriculture, Agricultural Statistical Report. Retrieved from www.mewa.gov.sa/en/Pages/default.aspx

MEWA. (2018). The Ministry of Environment Water and Agriculture, Agricultural Statistical Report. Retrieved from www.mewa.gov.sa/ar/InformationCenter/DocsCenter/YearlyReport

Minderhoud, P., Erkens, G., Pham, V., Bui, V. T., Erban, L., Kooi, H., & Stouthamer, E. (2017). Impacts of 25 years of groundwater extraction on subsidence in the Mekong delta, Vietnam. Environmental research letters, 12(6), 064006.

Mishra, V. N., & Rai, P. K. (2016). A remote sensing aided multi-layer perceptron-Markov chain analysis for land use and land cover change prediction in Patna district (Bihar), India. Arabian Journal of Geosciences, 9(4), 249.

Mohammady, M., Moradi, H., Zeinivand, H., & Temme, A. (2015). A comparison of supervised, unsupervised and synthetic land use classification methods in the north of Iran. International Journal of Environmental Science and Technology, 12(5), 1515-1526.

Mondal, M. S., Sharma, N., Kappas, M., & Garg, P. (2012). Modeling of spatio-temporal dynamics of land use land cover-a review and assessment.

Mondal, T., Qureshi, S. Q., Jhala, Y., & Basu, P. (2019). An assessment of land use land cover change in Central Highland of Deccan Peninsula and Semi-Arid tracts of India. BioRxiv, 665794.

Mousa, H. (2019). Saudi Arabia Grain and Feed Annual. Retrieved from: agriexchange.apeda.gov.in/MarketReport/Reports/Grain_and_Feed_Annual_Riyadh_Saudi_Arabia_4-4-2019.pdf

Moussa, R. A. (2019). King Abdullah Economic City: The Growth of New Sustainable City in Saudi Arabia. In New Cities and Community Extensions in Egypt and the Middle East (pp. 51-69): Springer.

Mubako, S., Belhaj, O., Heyman, J., Hargrove, W., & Reyes, C. (2018). Monitoring of land use/land-cover changes in the arid transboundary middle Rio Grande Basin using remote sensing. Remote Sensing, 10(12), 2005.

Mubarak, F. A. (2004). Urban growth boundary policy and residential suburbanization: Riyadh, Saudi Arabia. Habitat International, 28(4), 567-591.

Muhammad, M. K. I., Nashwan, M. S., Shahid, S., Ismail, T. b., Song, Y. H., & Chung, E.-S. (2019). Evaluation of empirical reference evapotranspiration models using compromise programming: a case study of Peninsular Malaysia. Sustainability, 11(16), 4267.

Müller, M. F., Müller-Itten, M. C., & Gorelick, S. M. (2017). How J ordan and S audi A rabia are avoiding a tragedy of the commons over shared groundwater. Water Resources Research, 53(7), 5451-5468.

Muller, M. R., & Middleton, J. (1994). A Markov model of land-use change dynamics in the Niagara Region, Ontario, Canada. Landscape Ecology, 9(2), 151-157.

Mundy, M., & Musallam, B. (2000). The transformation of nomadic society in the Arab east (Vol. 58): Cambridge University Press.

Munshi, T., Zuidgeest, M., Brussel, M., & van Maarseveen, M. (2014). Logistic regression and cellular automata-based modelling of retail, commercial and residential development in the city of Ahmedabad, India. Cities, 39, 68-86.

Murayama, Y. (2012). Introduction: Geospatial analysis. In Progress in geospatial analysis (pp. 1-9): Springer.

Muriithi, F. K. (2016). Land use and land cover (LULC) changes in semi-arid sub-watersheds of Laikipia and Athi River basins, Kenya, as influenced by expanding intensive commercial horticulture. Remote Sensing Applications: Society and Environment, 3, 73-88.

Myburgh, G., & Van Niekerk, A. (2013). Effect of feature dimensionality on object-based land cover classification: A comparison of three classifiers. South African Journal of Geomatics, 2(1), 13-27.

Myint, S. W., Gober, P., Brazel, A., Grossman-Clarke, S., & Weng, Q. (2011). Per-pixel vs. object-based classification of urban land cover extraction using high spatial resolution imagery. Remote Sensing of Environment, 115(5), 1145-1161.

Naboureh, A., Moghaddam, M. H. R., Feizizadeh, B., & Blaschke, T. (2017). An integrated object-based image analysis and CA-Markov model approach for modeling land use/land cover trends in the Sarab plain. Arabian Journal of Geosciences, 10(12), 259.

Nazzal, Y., Ahmed, I., Al-Arifi, N. S. N., Ghrefat, H., Zaidi, F. K., El-Waheidi, M. M., Zumlot, T. (2014). A pragmatic approach to study the groundwater quality suitability for domestic and agricultural usage, Saq aquifer, northwest of Saudi Arabia. Environmental monitoring and assessment, 186(8), 4655-4667.

Niblock, T. (2015). State, Society and Economy in Saudi Arabia (RLE Saudi Arabia): Routledge.

Okin, G. S., & Roberts, D. A. (2004). Remote sensing in arid regions: challenges and oppurtunities.

Ouda, O. K. (2014). Water demand versus supply in Saudi Arabia: current and future challenges. international Journal of Water resources development, 30(2), 335-344.

Ouda, O. K. M., Shawesh, A., Al-Olabi, T., Younes, F., & Al-Waked, R. (2013). Review of domestic water conservation practices in Saudi Arabia. Applied Water Science, 3(4), 689-699.

Palmate, S. S. (2017). Modelling spatiotemporal land dynamics for a trans-boundary river basin using integrated Cellular Automata and Markov Chain approach. Applied geography, 82, 11-23.

Peiman, R. (2011). Pre-classification and post-classification change-detection techniques to monitor land-cover and land-use change using multi-temporal Landsat imagery: a case study on Pisa Province in Italy. International Journal of Remote Sensing, 32(15), 4365-4381.

Peng, W., Wang, G., Zhou, J., Zhao, J., & Yang, C. (2015). Studies on the temporal and spatial variations of urban expansion in Chengdu, western China, from 1978 to 2010. Sustainable Cities and Society, 17, 141-150.

Petit, C., Scudder, T., & Lambin, E. (2001). Quantifying processes of land-cover change by remote sensing: Resettlement and rapid land-cover changes in southeast ern Zambia. International Journal of Remote Sensing, 22(17), 3435–3456.

Piquer-Rodríguez, M., Butsic, V., Gärtner, P., Macchi, L., Baumann, M., Pizarro, G. G., Kuemmerle, T. (2018). Drivers of agricultural land-use change in the Argentine Pampas and Chaco regions. Applied geography, 91, 111-122.

Pontius. (2000). Quantification error versus location error in comparison of categorical maps. Photogrammetric engineering and remote sensing, 66(8), 1011-1016.

Pontius, & Suedmeyer, B. (2004). Components of agreement between categorical maps at multiple resolutions. Remote sensing and GIS accuracy assessment, 233-251.

Postel, S. (2014). The last oasis: facing water scarcity: Routledge.

Poyen, E. F. B., Ghosh, A. K., & PalashKundu, P. (2016). Review on Different Evapotranspiration Empirical Equations. International Journal of Advanced Engineering, Management and Science, 2(3), 239382.

Pragunanti, T., Nababan, B., Madduppa, H., & Kushardono, D. (2020). Accuracy assessment of several classification algorithms with and without hue saturation intensity input features on object analyses on benthic habitat mapping in the Pajenekang Island Waters, South Sulawesi. Paper presented at the IOP Conference Series: Earth and Environmental Science.

Puertas, O. L., Henríquez, C., & Meza, F. J. (2014). Assessing spatial dynamics of urban growth using an integrated land use model. Application in Santiago Metropolitan Area, 2010–2045. Land use policy, 38, 415-425.

Quej, V. H., Almorox, J., Arnaldo, J. A., & Moratiel, R. (2019). Evaluation of temperature-based methods for the estimation of reference evapotranspiration in the Yucatán peninsula, Mexico. Journal of Hydrologic Engineering, 24(2), 05018029.

Rahman, M. T. (2016). Detection of Land Use/Land Cover Changes and Urban Sprawl in Al-Khobar, Saudi Arabia: An Analysis of Multi-Temporal Remote Sensing Data. ISPRS International Journal of Geo-Information, 5(2), 15.

Raja, R. A., Anand, V., Kumar, A. S., Maithani, S., & Kumar, V. A. (2013). Wavelet based post classification change detection technique for urban growth monitoring. Journal of the Indian Society of Remote Sensing, 41(1), 35-43.

Ram, B., & Kolarkar, A. (1993). Remote sensing application in monitoring land-use changes in arid Rajasthan. International Journal of Remote Sensing, 14(17), 3191-3200.

Rao, Y., Zhou, M., Ou, G., Dai, D., Zhang, L., Zhang, Z., Yang, C. (2018). Integrating ecosystem services value for sustainable land-use management in semi-arid region. Journal of Cleaner Production, 186, 662-672.

Ravazzani, G., Corbari, C., Morella, S., Gianoli, P., & Mancini, M. (2012). Modified Hargreaves-Samani equation for the assessment of reference evapotranspiration in Alpine river basins. Journal of Irrigation and Drainage Engineering, 138(7), 592-599.

Rezaei, M., Valipour, M., & Valipour, M. (2016). Modelling evapotranspiration to increase the accuracy of the estimations based on the climatic parameters. Water Conservation Science and Engineering, 1(3), 197-207.

Rimal, B. (2011). Application of remote sensing and GIS, land use /land cover change in Kathmandu metropolitan city, Nepal. Journal of Theoretical & Applied Information Technology, 23(2).

Rojas, C., Pino, J., Basnou, C., & Vivanco, M. (2013). Assessing land-use and-cover changes in relation to geographic factors and urban planning in the metropolitan area of Concepción (Chile). Implications for biodiversity conservation. Applied geography, 39, 93-103.

Romanenko, V. (1961). Computation of the autumn soil moisture using a universal relationship for a large area. Proc. Ukr. Hydrometeorol. Res. Inst. , 3, 12-25.

Rozenstein, O., & Karnieli, A. (2011). Comparison of methods for land-use classification incorporating remote sensing and GIS inputs. Applied geography, 31(2), 533-544.

Bhagat, V. (2012). Use of remote sensing techniques for robust digital change detection of land: a review. Recent Patents on Space Technology, 2(2), 123-144.

Salih, A. A., Ganawa, E.-T., & Elmahl, A. A. (2017). Spectral mixture analysis (SMA) and change vector analysis (CVA) methods for monitoring and mapping land degradation/desertification in arid and semiarid areas (Sudan), using Landsat imagery. The Egyptian Journal of Remote Sensing and Space Science, 20, S21-S29.

Samin, N. (2019). Of Sand or Soil: Genealogy and Tribal Belonging in Saudi Arabia (Vol. 59): Princeton University Press.

Sang, L., Zhang, C., Yang, J., Zhu, D., & Yun, W. (2011). Simulation of land use spatial pattern of towns and villages based on CA–Markov model. Mathematical and Computer Modelling, 54(3), 938-943.

Santé, I., García, A. M., Miranda, D., & Crecente, R. (2010). Cellular automata models for the simulation of real-world urban processes: A review and analysis. Landscape and Urban Planning, 96(2), 108-122.

Satay, T. (1980). The analytical hierarchy process. And William Rees, 41(11), 1073-1076.

Savva, A. P., & Frenken, K. (2002). Crop water requirements and irrigation scheduling: FAO Sub-Regional Office for East and Southern Africa Harare.

Schendel, U. (1967). Vegetations wasserverbrauch und -wasserbedarf. Habilitation, Kiel, 137.

Sen, Z., & Al-Somayien, M. S. (1991). Some simple management criteria for confined Saq aquifer in Tabuk region, Saudi Arabia. Water Resources Management, 5(2), 161-179.

Senatore, A., Parrello, C., Almorox, J., & Mendicino, G. (2020). Exploring the Potential of Temperature-Based Methods for Regionalization of Daily Reference Evapotranspiration in Two Spanish Regions. Journal of Irrigation and Drainage Engineering, 146(3), 05020001.

Shawul, A. A., & Chakma, S. (2019). Spatiotemporal detection of land use/land cover change in the large basin using integrated approaches of remote sensing and GIS in the Upper Awash basin, Ethiopia. Environmental Earth Sciences, 78(5), 141.

Silver, M., Tiwari, A., & Karnieli, A. (2019). Identifying Vegetation in Arid Regions Using Object-Based Image Analysis with RGB-Only Aerial Imagery. Remote Sensing, 11(19), 2308.

Singh. (1989). Review article digital change detection techniques using remotely sensed data. International Journal of Remote Sensing, 10(6), 989-1003.

Singh, Mustak, Srivastava, Szabó, & Islam. (2015). Predicting spatial and decadal LULC changes through cellular automata Markov chain models using Earth observation datasets and geo-information. Environmental Processes, 2(1), 61-78.

Smith, M. (1992). CROPWAT: A computer program for irrigation planning and management: Food & Agriculture Org.

Soffianian, A., Nadoushan, M. A., Yaghmaei, L., & Falahatkar, S. (2010). Mapping and analyzing urban expansion using remotely sensed imagery in Isfahan, Iran. World applied sciences journal, 9(12), 1370-1378.

Sowers, J., Vengosh, A., & Weinthal, E. (2011). Climate change, water resources, and the politics of adaptation in the Middle East and North Africa. Climatic Change, 104(3), 599-627.

SSYB. (2015). Agricultural Statistical yearbook, Ministry of Economy and Planning. Central Department of Statistics and Information.

Stellmes, M., Röder, A., Udelhoven, T., & Hill, J. (2013). Mapping syndromes of land change in Spain with remote sensing time series, demographic and climatic data. Land use policy, 30(1), 685-702.

Su, Z., Roebeling, R. A., Schulz, J., Holleman, I., Levizzani, V., Timmermans, W. J., Wang, L. (2011). Observation of Hydrological Processes Using Remote Sensing. In Treatise on Water Science (pp. 351-399). Oxford: Elsevier.

Tabari, H., Grismer, M. E., & Trajkovic, S. (2013). Comparative analysis of 31 reference evapotranspiration methods under humid conditions. Irrigation Science, 31(2), 107-117.

Tang, J., Wang, L., & Yao, Z. (2007). Spatio-temporal urban landscape change analysis using the Markov chain model and a modified genetic algorithm. International Journal of Remote Sensing, 28(15), 3255-3271.

Tarawneh, Q. Y., & Chowdhury, S. (2018). Trends of climate change in Saudi Arabia: Implications on water resources. Climate, 6(1), 8.

Tewolde, M., & Cabral, P. (2011). Urban sprawl analysis and modeling in Asmara, Eritrea. Remote Sensing, 3(10), 2148-2165.

Thakkar, A. K., Desai, V. R., Patel, A., & Potdar, M. B. (2017). Post-classification corrections in improving the classification of Land Use/Land Cover of arid region using RS and GIS: The case of Arjuni watershed, Gujarat, India. The Egyptian Journal of Remote Sensing and Space Science, 20(1), 79-89.

The Food and Agriculture Organization. (2016). Saudi Arabia, Country Profiles (http://www.fao.org/faolex/country-profiles/general-profile/en/iso3=SAU).

The General Authority for Statistics. (2015). Population and housing census. https://www.stats.gov.sa/en/13. Retrieved 2015

The World Bank. (2016). World Development Indicators, Saudi Arabia. https://data.worldbank.org/indicator/ SA. Retrieved 2016

Theis, C. V. (1935). The relation between the lowering of the piezometric surface and the rate and duration of discharge of a well using ground-water storage. Eos, Transactions American Geophysical Union, 16(2), 519-524.

Thenkabail, P. (2018). Remote Sensing Handbook-Three Volume Set: CRC Press.

Tsai, Y. H., Stow, D., & Weeks, J. (2011). Comparison of object-based image analysis approaches to mapping new buildings in Accra, Ghana using multi-temporal QuickBird satellite imagery. Remote Sensing, 3(12), 2707-2726.

Thornthwaite, C. W. (1948). An Approach toward a Rational Classification of Climate. Geographical Review, 38(1), 55-94.

Steenbergen, F., Kaisarani, A. B., Khan, N. U., & Gohar, M. S. (2015). A case of groundwater depletion in Balochistan, Pakistan: Enter into the void. Journal of Hydrology: Regional Studies, 4, 36-47.

United Nations. (2016). World Population Prospects. Retrieved from https://population.un.org/wpp/

USGS. (2015). Landsat data. Accessed December 2015 from https://earthexplorer.usgs.gov/

Van Vliet, J., Magliocca, N. R., Büchner, B., Cook, E., Benayas, J. M. R., Ellis, E. C., Liu, J. (2016). Meta-studies in land use science: Current coverage and prospects. Ambio, 45(1), 15-28.

Vapnik, V. N. (1999). An overview of statistical learning theory. Neural Networks, IEEE Transactions on, 10(5), 988-999.

Vaz, E., Arsanjani, J. J., Phillips, L., Johnson, M., Deener, K., Bonanni, C., Lai, Y. (2015). Predicting Urban Growth of the Greater Toronto Area-Coupling a Markov Cellular Automata with Document Meta-Analysis. Journal of Environmental Informatics, 25(2), 71-80.

Verburg, P. H., Schot, P. P., Dijst, M. J., & Veldkamp, A. (2004). Land use change modelling: current practice and research priorities. GeoJournal, 61(4), 309-324.

Verhagen, P. (2007). Case studies in archaeological predictive modelling (Vol. 14): Amsterdam University Press.

Vijayan, L., & AlTalhi, F. A. (2015). Significance of Meteorological Parameters in the Implementation of Agriculture Engineering Practices in and Around Tabuk Region, KSA. International Journal of Applied Science and Technology, 3(5), 53-65.

Vincent, P. (2008). Saudi Arabia: An Environmental Overview: CRC Press.

Vision 2030. (2017). Vision 2030 Kingdom of Saudi Arabia. Retrieved from https://vision2030.gov.sa/sites/default/files/report/Saudi_Vision2030_EN_2017.pdf.

Walter, V. (2004). Object-based classification of remote sensing data for change detection. ISPRS Journal of Photogrammetry and Remote Sensing, 58(3), 225-238.

Wang, L., d'Odorico, P., Evans, J., Eldridge, D., McCabe, M., Caylor, K., & King, E. (2012). Dryland ecohydrology and climate change: critical issues and technical advances.

Wang, L. K., Yang, C. T. & Wang, M. H. (2015). Handbook of Environmental Engineering: Advances in Water Resources Management, (pp. 118-126): Springer.

White, R., & Engelen, G. (2000). High-resolution integrated modelling of the spatial dynamics of urban and regional systems. Computers, Environment and Urban Systems, 24(5), 383-400.

Winowiecki, L. A., Vågen, T.-G., Kinnaird, M. F., & O'Brien, T. G. (2018). Application of systematic monitoring and mapping techniques: Assessing land restoration potential in semi-arid lands of Kenya. Geoderma, 327, 107-118.

Wu, F., Zhan, J., Su, H., Yan, H., & Ma, E. (2015). Scenario-Based Impact Assessment of Land Use. Cover and Climate Changes on Watershed Hydrology in Heihe River Basin of Northwest China, Advances in Meteorology, 2015, 1.

Wu, W., Zhao, S., Zhu, C., & Jiang, J. (2015). A comparative study of urban expansion in Beijing, Tianjin and Shijiazhuang over the past three decades. Landscape and Urban Planning, 134, 93-106.

Wubie, M. A., Assen, M., & Nicolau, M. D. (2016). Patterns, causes and consequences of land use/cover dynamics in the Gumara watershed of lake Tana basin, Northwestern Ethiopia. Environmental Systems Research, 5(1), 8.

Xu, Y., Yu, L., Zhao, Y., Feng, D., Cheng, Y., Cai, X., & Gong, P. (2017). Monitoring cropland changes along the Nile River in Egypt over past three decades (1984–2015) using remote sensing. International Journal of Remote Sensing, 38(15), 4459-4480.

Yagoub, M., & Al Bizreh, A. A. (2014). Prediction of land cover change using Markov and cellular automata models: case of Al-Ain, UAE, 1992-2030. Journal of the Indian Society of Remote Sensing, 42(3), 665-671.

Yanli, Y., Jabbar, M. T., & Zhou, J.-X. (2012). Study of environmental change detection using Remote Sensing and GIS application: A case study of northern Shaanxi Province, China. Pol. J. Environ. Stud, 21(3), 789-790.

Yin, J., Yin, Z., Zhong, H., Xu, S., Hu, X., Wang, J., & Wu, J. (2011). Monitoring urban expansion and land use/land cover changes of Shanghai metropolitan area during the transitional economy (1979–2009) in China. Environmental monitoring and assessment, 177(1-4), 609-621.

Yirsaw, E., Wu, W., Shi, X., Temesgen, H., & Bekele, B. (2017). Land use/land cover change modeling and the prediction of subsequent changes in ecosystem service values in a coastal area of China, the Su-Xi-Chang Region. Sustainability, 9(7), 1204.

Youssef, A. M., & Maerz, N. H. (2013). Overview of some geological hazards in the Saudi Arabia. Environmental Earth Sciences, 70(7), 3115-3130.

Zaidi, F. K., Nazzal, Y., Jafri, M. K., Naeem, M., & Ahmed, I. (2015). Reverse ion exchange as a major process controlling the groundwater chemistry in an arid environment: a case study from northwestern Saudi Arabia. Environmental monitoring and assessment, 187(10), 1-18.

Zewdu, S., Suryabhagavan, K., & Balakrishnan, M. (2016). Land-use/land-cover dynamics in Sego Irrigation Farm, southern Ethiopia: A comparison of temporal soil salinization using geospatial tools. Journal of the Saudi Society of Agricultural Sciences, 15(1), 91-97.

Zhang, J., & Jia, L. (2014). A comparison of pixel-based and object-based land cover classification methods in an arid/semi-arid environment of northwestern China. Paper presented at the 2014 Third International Workshop on Earth Observation and Remote Sensing Applications (EORSA).

Zhang, Q., Ban, Y., Liu, J., & Hu, Y. (2011). Simulation and analysis of urban growth scenarios for the Greater Shanghai Area, China. Computers, Environment and Urban Systems, 35(2), 126-139.

Zhang, X., Zhang, L., He, C., Li, J., Jiang, Y., & Ma, L. (2014). Quantifying the impacts of land use/land cover change on groundwater depletion in Northwestern China – A case study of the Dunhuang oasis. Agricultural Water Management, 146, 270-279.

Zhang, Z., Li, N., Wang, X., Liu, F., & Yang, L. (2016). A comparative study of urban expansion in Beijing, Tianjin and Tangshan from the 1970s to 2013. Remote Sensing, 8(6), 496.

Zhao, R., Chen, Y., Shi, P., Zhang, L., Pan, J., & Zhao, H. (2013). Land use and land cover change and driving mechanism in the arid inland river basin: a case study of Tarim River, Xinjiang, China. Environmental Earth Sciences, 68(2), 591-604.

Zheng, B., Myint, S. W., Thenkabail, P. S., & Aggarwal, R. M. (2015). A support vector machine to identify irrigated crop types using time-series Landsat NDVI data. International Journal of Applied Earth Observation and Geoinformation, 34, 103-112.

Zumlot, T., Batayneh, A., Nazal, Y., Ghrefat, H., Mogren, S., Zaman, H., Qaisy, S. (2013). Using multivariate statistical analyses to evaluate groundwater contamination in the northwestern part of Saudi Arabia. Environmental Earth Sciences, 70(7), 3277-3287.

Appendix A: Seasonal climate analysis

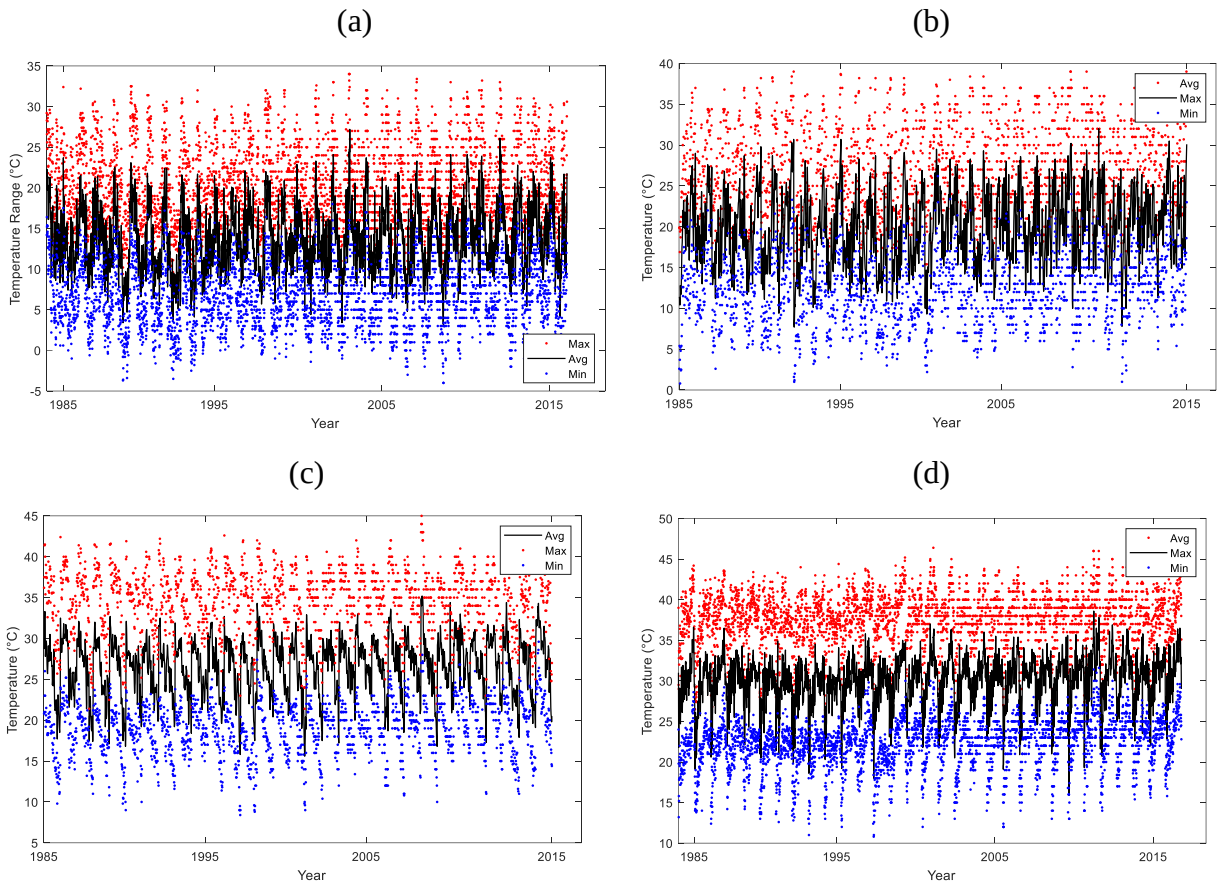

Temperature during the study period 1985-2015: (a) winter (wheat); (b) spring (clover); (c) autumn (potato); and (d) summer (maize)

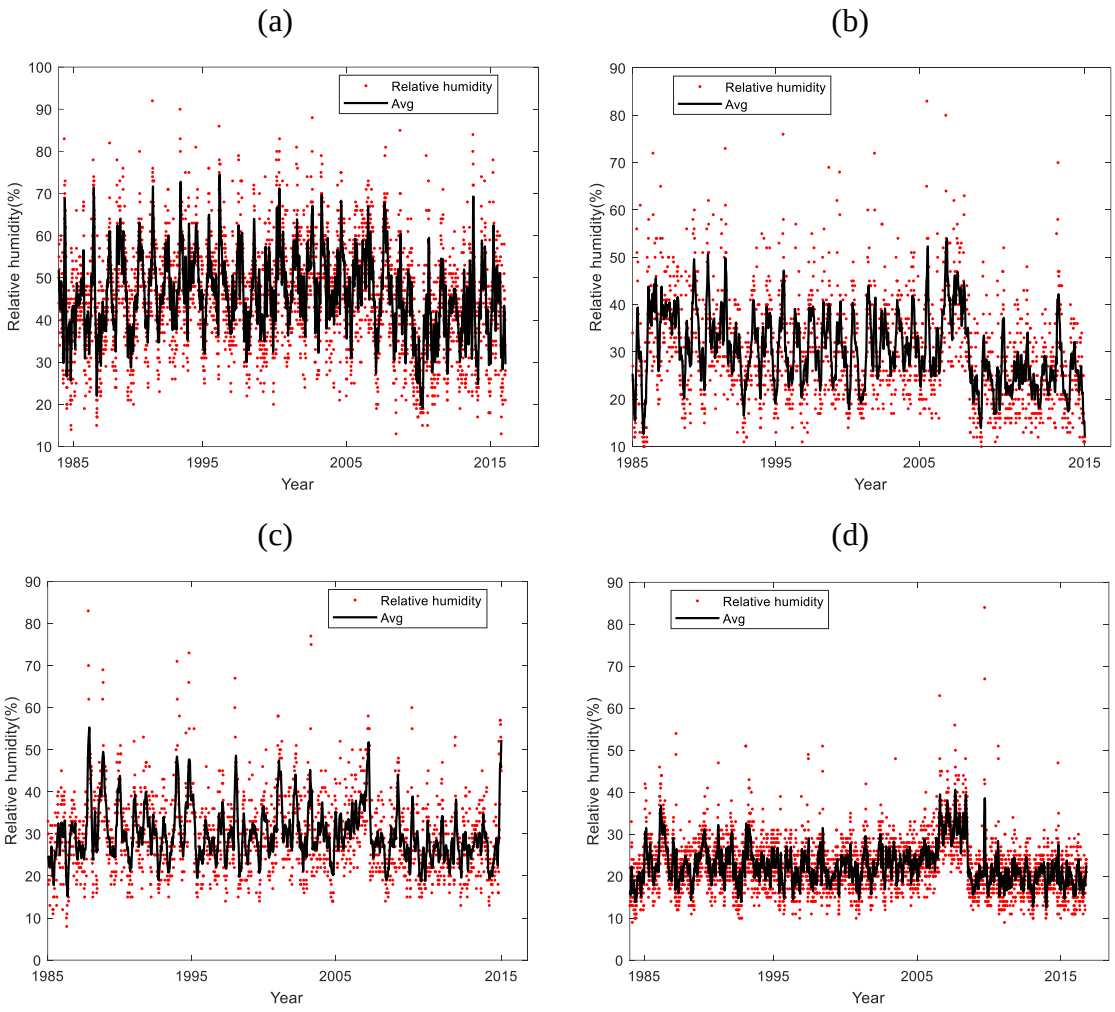

Relative humidity (%) during the study period 1985-2015: (a) winter (wheat); (b) spring (clover); (c) autumn (potato); and (d) summer (maize)

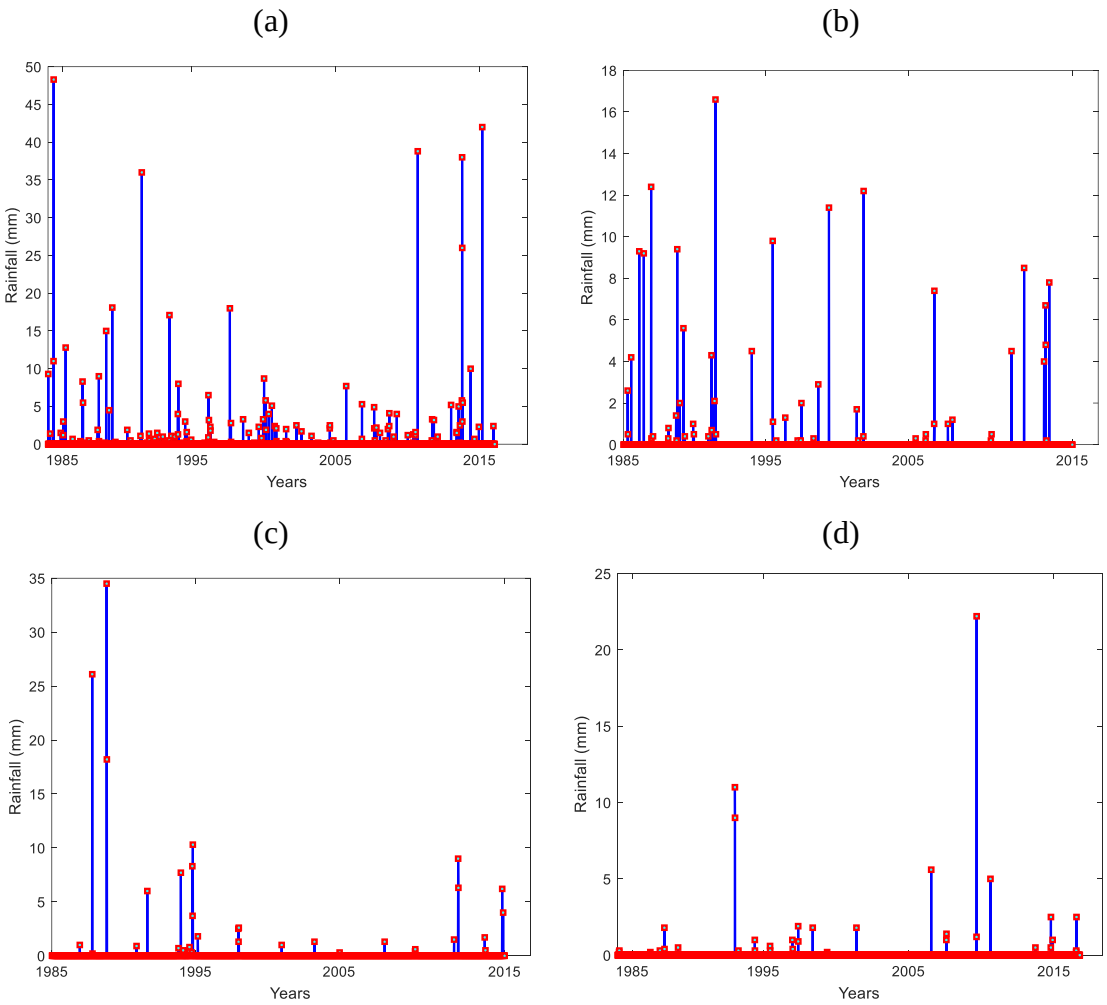

Rainfall (mm) in Tabuk during the period of 1985-2015: (a) winter (wheat); (b) spring (clover); (c) autumn (potato); and (d) summer (maize)

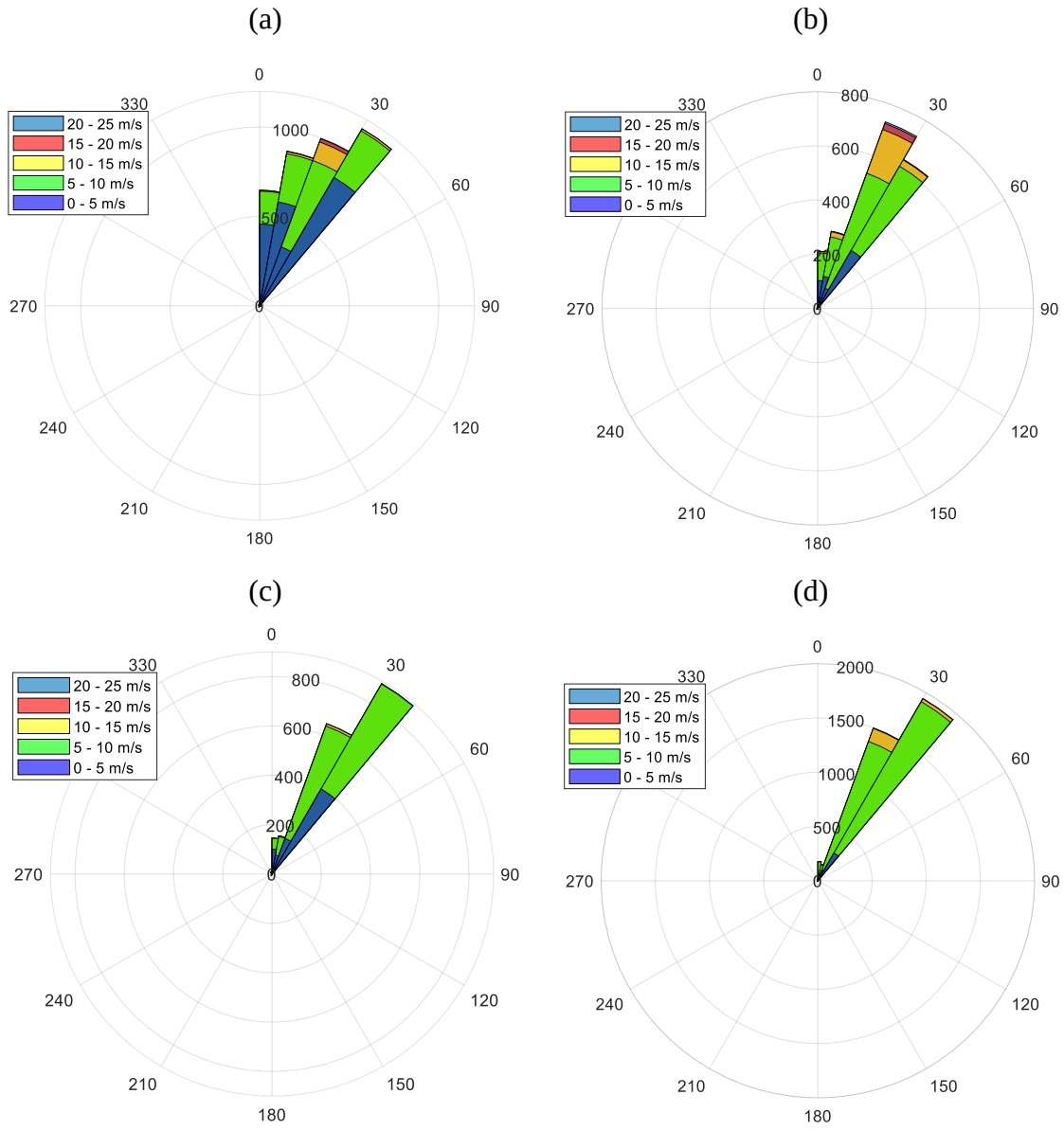

Wind rose diagrams in Tabuk during the period of 1985-2015: (a) winter (wheat); (b) spring (clover); (c) autumn (potato); and (d) summer (maize)

Appendix B: Classification performances using pixel-based (MLC, SVM), and object-based (OBIA) techniques

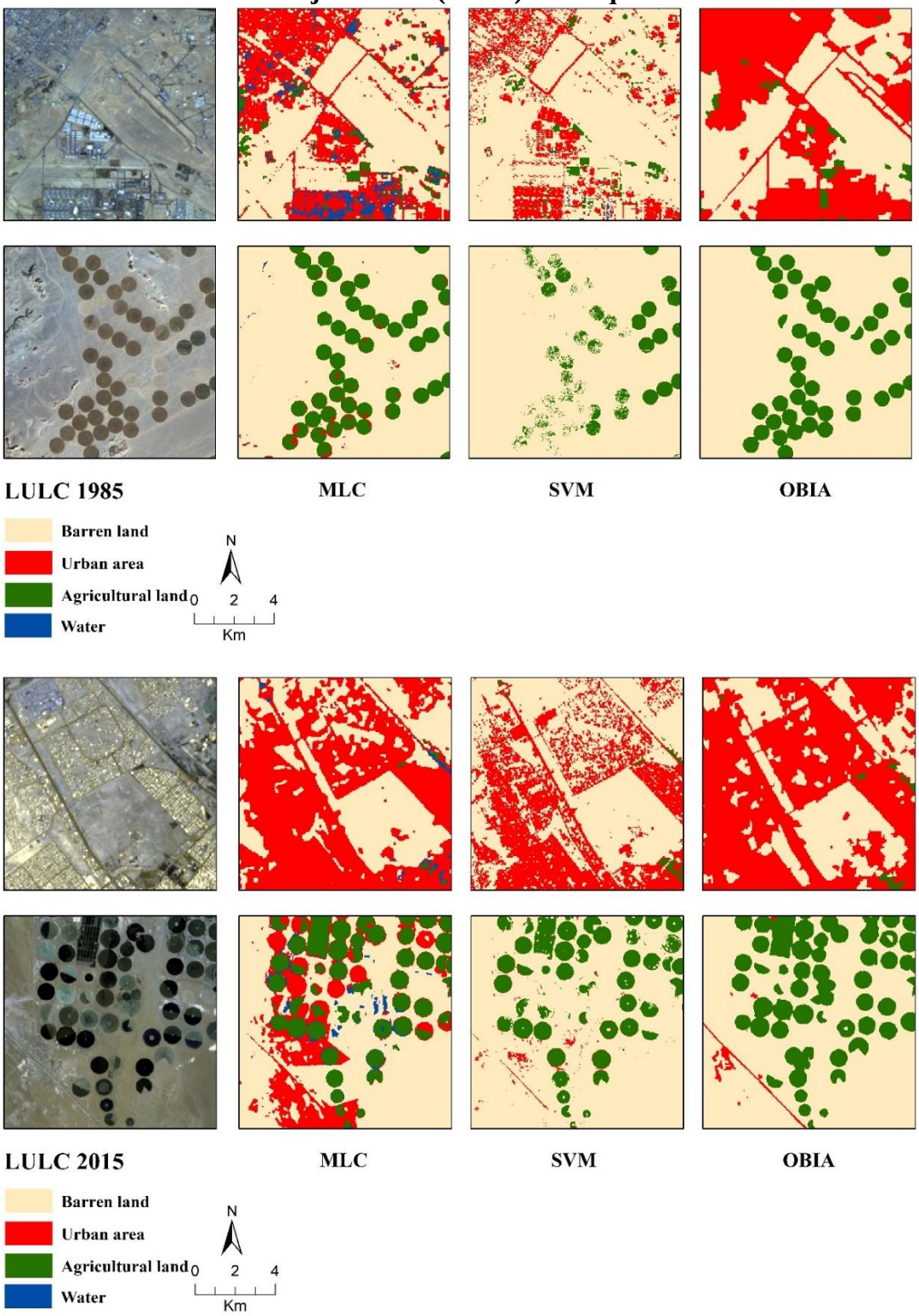

Landsat image showing urban area and agricultural land in the study site in 1985 and 2015, comparison of pixel-based (MLC, SVM), and object-based (OBIA) methods

(a) MLC

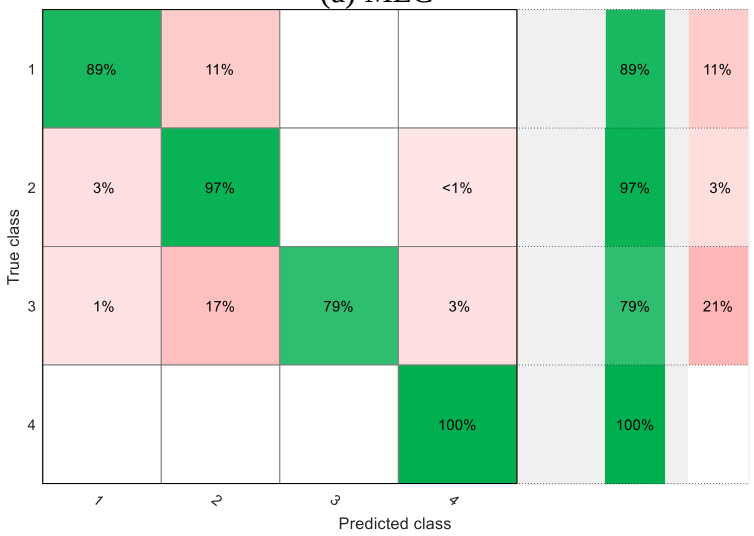

(b) SVM

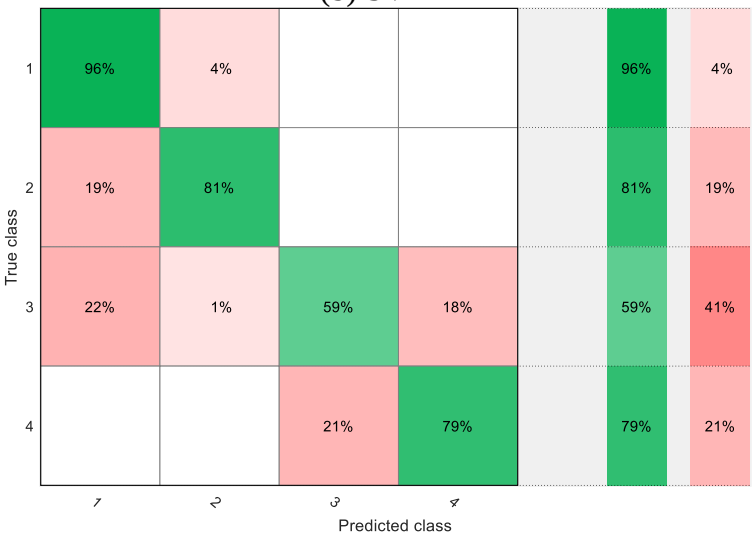

(c) OBIA

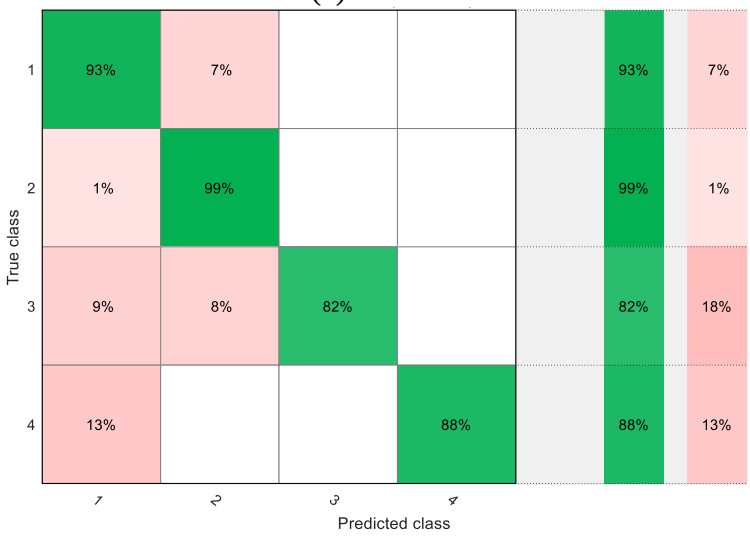

Confusion Matrix example for LULC classification from (a) MLC, (b) SVM, and (c) OBIA using ground truth points (488-points), analysed for 2015 ground truth data. Green indicates a positive predictive value for the correctly predicted points in each class, and red indicates false discovery rates for the incorrectly predicted points in each class

Appendix C: Error matrix

		Reference Data (1985)					
	LULC type	**Barren land**	**Urban**	**Agriculture**	**Water**	**Total**	**Users' accuracy**
Classified Data	**Barren land**	320	9	12	3	344	93
	Urban	0	77	0	0	77	100
	Agriculture	0	9	186	1	196	95
	Water	0	0	1	9	10	90
	Total	320	95	199	13	627	
	Producers' accuracy	100	81	93	69	**Overall accuracy**: 94	
Kappa coefficient: 0.91							

		Reference Data (1990)					
	LULC type	**Barren land**	**Urban**	**Agriculture**	**Water**	**Total**	**Users' accuracy**
Classified Data	**Barren land**	307	7	3	2	319	96
	Urban	0	94	0	2	96	98
	Agriculture	0	1	169	0	170	99
	Water	0	0	0	9	9	100
	Total	307	102	172	13	594	
	Producers' accuracy	100	92	98	69	**Overall accuracy**: 97	
Kappa coefficient: 0.96							

		Reference Data (1995)					
	LULC type	**Barren land**	**Urban**	**Agriculture**	**Water**	**Total**	**Users' accuracy**
Classified Data	**Barren land**	302	15	6	0	323	93
	Urban	2	94	0	0	96	98
	Agriculture	3	2	181	6	192	94
	Water	0	0	0	8	8	100
	Total	307	111	187	14	619	
	Producers' accuracy	98	85	97	57	**Overall accuracy**: 94	
Kappa coefficient: 0.91							

		Reference Data (2000)					
	LULC type	**Barren land**	**Urban**	**Agriculture**	**Water**	**Total**	**Users' accuracy**
Classified Data	**Barren land**	310	1	0	0	311	100
	Urban	1	93	6	4	104	89
	Agriculture	1	5	250	1	257	97
	Water	0	6	9	22	37	59
	Total	312	105	265	27	709	
	Producers' accuracy	99	89	94	54	**Overall accuracy**: 95	
Kappa coefficient: 0.93							

		Reference Data (2005)					
	LULC type	**Barren land**	**Urban**	**Agriculture**	**Water**	**Total**	**Users' accuracy**
Classified Data	**Barren land**	313	14	1	6	334	94
	Urban	1	99	0	0	100	99
	Agriculture	1	1	200	1	203	99
	Water	0	0	0	7	7	100
	Total	315	114	201	14	644	
	Producers' accuracy	99	87	100	50	**Overall accuracy**: 96	
Kappa coefficient: 0.94							

	Reference Data (2009)						
Classified Data	**LULC type**	**Barren land**	**Urban**	**Agriculture**	**Water**	**Total**	**Users' accuracy**
	Barren land	297	1	7	0	305	97
	Urban	2	112	1	0	115	97
	Agriculture	5	1	215	4	225	96
	Water	0	0	0	17	17	100
	Total	304	114	223	21	662	
	Producers' accuracy	98	98	96	81	**Overall accuracy**: 97	
Kappa coefficient: 0.95							

	Reference Data (2015)						
Classified Data	**LULC type**	**Barren land**	**Urban**	**Agriculture**	**Water**	**Total**	**Users' accuracy**
	Barren land	120	1	5	3	125	93
	Urban	2	188	2	0	232	98
	Agriculture	1	0	82	0	89	99
	Water	6	0	12	24	33	54
	Total	125	230	107	24	486	
	Producers' accuracy	94	100	82	88	**Overall accuracy**: 93	
Kappa coefficient: 0.90							